

UvA-DARE (Digital Academic Repository)

Optical coherence tomography (OCT) and irreversible electroporation (IRE) in the diagnosis and treatment of renal masses

Towards a minimally invasive approach

Buijs, M.

Publication date

2021

Document Version

Final published version

[Link to publication](#)

Citation for published version (APA):

Buijs, M. (2021). *Optical coherence tomography (OCT) and irreversible electroporation (IRE) in the diagnosis and treatment of renal masses: Towards a minimally invasive approach*. [Thesis, fully internal, Universiteit van Amsterdam].

General rights

It is not permitted to download or to forward/distribute the text or part of it without the consent of the author(s) and/or copyright holder(s), other than for strictly personal, individual use, unless the work is under an open content license (like Creative Commons).

Disclaimer/Complaints regulations

If you believe that digital publication of certain material infringes any of your rights or (privacy) interests, please let the Library know, stating your reasons. In case of a legitimate complaint, the Library will make the material inaccessible and/or remove it from the website. Please Ask the Library: <https://uba.uva.nl/en/contact>, or a letter to: Library of the University of Amsterdam, Secretariat, Singel 425, 1012 WP Amsterdam, The Netherlands. You will be contacted as soon as possible.

Optical coherence tomography (OCT) and
irreversible electroporation (IRE) in the diagnosis
and treatment of renal masses:
Towards a minimally invasive approach

Mara Buijs



Optical coherence tomography (OCT) and irreversible electroporation (IRE) in the diagnosis and treatment of renal masses

Towards a minimally invasive approach

Mara Buijs

Colofon

Lay-out and printing: ProefschriftMaken II www.proefschriftmaken.nl

ISBN: 978-94-6423-054-3

The research projects in this thesis were performed in collaboration with the following departments:

- Urology department, Academic Medical Center, Amsterdam, the Netherlands
- Radiology department, Academic Medical Center, Amsterdam, the Netherlands
- Biomedical Engineering and Physics, Academic Medical Center, Amsterdam, the Netherlands

The research was supported and funded by the Netherlands Organisation for Health Research and Development (ZonMw).

Publication of this thesis was kindly supported by the Von Hippel-Lindau patient association, Chipsoft, Bayer, the Academic Medical Center, the Radiology Department and the Urology department of the Academic Medical Center.

Optical coherence tomography (OCT) and irreversible electroporation (IRE) in the diagnosis and treatment of renal masses

Towards a minimally invasive approach

ACADEMISCH PROEFSCHRIFT

ter verkrijging van de graad van doctor

aan de Universiteit van Amsterdam

op gezag van de Rector Magnificus

prof. dr. ir. K.I.J. Maex

ten overstaan van een door het College voor Promoties ingestelde
commissie, in het openbaar te verdedigen in de Aula der Universiteit op

vrijdag 28 mei 2021, te 11.00 uur

door Mara Buijs

geboren te Schermer

Promotiecommissie

| | | |
|-----------------------|---------------------------------|---------|
| <i>Promotores:</i> | prof. dr. H.P. Beerlage | AMC-UvA |
| | prof. dr. O.M. van Delden | AMC-UvA |
| <i>Copromotores:</i> | dr. K.P. van Lienden | AMC-UvA |
| | dr. D.M. de Bruin | AMC-UvA |
| <i>Overige leden:</i> | prof. dr. J.T. Annema | AMC-UvA |
| | prof. dr. M.G.H. Besselink | AMC-UvA |
| | prof. dr. F.J. Bemelman | AMC-UvA |
| | prof. dr. ir. M.J.C. van Gemert | AMC-UvA |
| | dr. A. Bex | NKI-AvL |
| | dr. B.W. Lagerveld | OLVG |
| | prof. dr. M.R. Meijerink | VU |

Faculteit der Geneeskunde

Table of contents

Chapter 1

Introduction and aims of thesis 7

Chapter 2

An in-vivo prospective study of the diagnostic yield and accuracy of optical biopsy compared with conventional renal mass biopsy for the diagnosis of renal cell carcinoma: the interim analysis 23

Chapter 3

Available ablation energies to treat cT1 renal cell cancer: emerging technologies 41

Chapter 4

Irreversible electroporation: state of the art 61

Chapter 5

Irreversible electroporation for the ablation of renal cell carcinoma: a prospective, human, in-vivo trial 81

Chapter 6

Feasibility and safety of irreversible electroporation (IRE) in patients with small renal masses: results of a prospective study 101

Chapter 7

MRI and CT in the follow-up after irreversible electroporation (IRE) for the treatment of small renal masses 119

Chapter 8

Concluding remarks and future perspectives 145

Chapter 9

English & Dutch summary 155

Author contributions 163

Curriculum Vitae 167

Dankwoord 169

CHAPTER 1



Introduction and aims of thesis

General Introduction

Rationale

Renal cell carcinoma (RCC) covers the majority of kidney cancers (90%) and is the second most common malignancy diagnosed in the urinary system [1, 2]. Clinical behaviour of RCC varies widely and is mainly inherent to its histopathology: Most common subtypes of RCC are clear cell renal cell carcinoma (75-80%, ccRCC) with the most aggressive behaviour and highest tendency to metastasize, papillary renal cell carcinoma (10-15%, pRCC) and chromophobic renal cell carcinoma (5%, cRCC)[3, 4]. Although the incidence of RCC is rising worldwide, mortality rates appear to be stabilizing in developed countries [2]. A potential explanation for this rise is the increased use of imaging techniques for unrelated disorders, leading to incidentally detected renal masses. A subsequent characteristic associated with incidental detection of renal masses is stage migration to an earlier stage at the time of diagnosis. Over the past decades, the majority of diagnosed renal masses are smaller than 4 cm (small renal mass, SRM) [5, 6].

The median age of a patient with RCC at the time of diagnosis is 64 years [7]. Considering the global increase in the life expectancy of the general population, the number of elderly patients diagnosed with RCC will keep increasing. The preferred treatment for patients with a SRM that appears suspicious for malignancy on imaging has always been surgical resection. The development of ablative therapies however has altered the management of renal masses. A trend is observed towards a more personalized treatment, taking into account not only the oncological outcomes of a treatment but also the age and comorbidity of the patient, as well as histology and localization of the tumour [8]. Moreover, 'shared decision making' plays an increasing role in current practice. Hereby the healthcare practitioner consults the patient regarding the different management options (standard and alternative) with associated risks and benefits. Consequently, the patient will be able to make a fully informed treatment decision regarding his/her choice of treatment [9]. All the above-mentioned factors have driven a tendency towards minimal invasive diagnosis and therapy of renal masses.

State of the art diagnosis of renal cell carcinoma

Incidental detection through cross-sectional imaging, including magnetic resonance imaging (MRI), computed tomography (CT), and ultrasound (US), reveals renal masses that do not exhibit symptoms. Haematuria, flank pain, and an abdominal mass, the 'classic' triad of symptoms due to RCC, currently arise in only 10% of all cases [10]. The increase in asymptomatic SRMs has set the clinician for a dilemma: Cross-sectional imaging techniques are highly accurate in detecting renal masses but fail to reliably distinguish malignant from benign masses. Additionally, cross-sectional imaging cannot assess tumour

grade and therefore cannot predict which SRM will exhibit aggressive behaviour with accompanied poor prognostic factors. To determine an appropriate treatment, the risk of malignancy, and specifically, the risk of high-grade disease and metastatic potential should be assessed.

Certain characteristics can be identified to determine possible malignancy on cross-sectional imaging. One of those features is tumour size: The risk of (high grade) malignancy and the risk of metastasis increases with the size of the renal mass [11, 12]. Another feature is the enhancement of the renal mass on contrast-enhanced CT or MRI: Generally, enhancement of >20 Hounsfield Units (HU) on CT is associated with malignancy. Lastly, a growth rate of more than 0.3 cm per year is also associated with malignancy. Apart from these features, it is known that 25-30% of all SRMs are benign [13, 14]. Another 25% is malignant but appears to exhibit indolent behaviour. Around 30% of SRMs are of intermediate-risk and only 13-20% of SRMs are thought to be high-grade disease [12, 14]. This highlights the fact that not every SRM needs aggressive treatment, in particular not in elderly patients who are likely to die from other comorbidities before their SRM will metastasize or will cause local problems.

Currently, the only way to accurately diagnose RCC is through imaging-guided renal mass biopsy (RMB). Using a core biopsy needle, a suspected lesion can be biopsied percutaneously under image guidance (ultrasound or CT). Accuracy of RMBs is high, with a reported sensitivity and specificity of 98%-99% and 96%-99% respectively [15, 16]. Complications of RMB are not common and include hematomas (4-5%), macroscopic haematuria (1%), and significant pain (1%) [15]. The risk of tumour seeding has been noted in incidental reports, but has never been established in larger series and lacks histopathologic confirmation in the majority of cases [15, 17]. The estimated risk in the literature reported is 0.01%-1.2% and therefore yields low concern in clinical practice, although patients should be informed about this during their consultation.

An important limitation of RMB is the high rate of non-diagnostic results. A non-diagnostic biopsy occurs when there is insufficient tumour tissue harvested or when normal renal parenchyma, predominantly fibrotic tissue or necrotic tissue is found [18]. Non-diagnostic biopsies are reported in up to 22% of RMBs and manifest more often in smaller tumours [15, 16, 19]. This highlights the diagnostic challenge of the growing amount of incidentally detected SRMs, as they give rise to a relatively high percentage of non-diagnostic biopsies compared to larger tumours. The diagnostic yield (the percentage of biopsies that lead to a diagnosis) of RMB is therefore limited and either repeat biopsies are necessary or a treatment plan will be made without histopathological confirmation. Another drawback of RMB is the inability to accurately establish histopathological grade or predict the risk for aggressive malignancy. To establish proper disease management and to estimate cancer-

specific survival, determining the disease grade is of the utmost importance [20]. RMB turns out to underestimate this grade in up to 55% of cases when compared to resected specimen pathology [21]. The clinician prefers not to operate on a benign renal mass since surgery is invasive and may be accompanied by significant complications and side effects. Research has demonstrated that resection without a preoperative histological diagnosis results in benign final pathology in 40% of renal masses smaller than 1 cm, and 20% of renal masses 1 – 4 cm [22]. Nonetheless, routinely performing preoperative RMB's is hampered by a potential non-diagnostic outcome or an underestimation of the nuclear grade, which may direct the treatment in an unwanted direction. Although these considerations should be noted, the increased incidence of SRMs and therefore the relatively high risk of excising a benign renal mass has led towards RMB-guided management. Therefore, there is a need for better and possibly real-time diagnostic tools in the work-up of RCC that combines high diagnostic yield and high accuracy with a minimally invasive method of acquisition.

Optical biopsy to diagnose renal cell carcinoma

Optical biopsy refers to a group of optical technologies that uses light to image and characterise tissue without the need for excision [23]. Optical coherence tomography (OCT) is a high-resolution imaging technology with the potential to operate as an optical biopsy. It uses near-infrared light to establish real-time, cross-sectional imaging of tissue without requiring a contrast-agent. OCT was originally discovered in 1991 with its first application in ophthalmology to assess retinal thickness and morphology. Nowadays, the technique has developed significantly and OCT is a well-established modality that has several clinical uses, such as in the fields of cardiology [24], gastroenterology [25], dermatology [26], gynaecology [27], and urology [28]. OCT may be compared to ultrasound, in which sound waves are used to reconstruct the tissue by measuring the time-delay and amplitude of the returning sound wave. Similarly, OCT detects light that is backscattered by the tissue. OCT is capable of performing fast and high-resolution imaging, with a resolution of 10-15 μm and an imaging depth of 2-3 mm [28–30]. During an OCT scan, the near-infrared light scans circularly and pulls back simultaneously over a trajectory of 54 mm in total. OCT can be performed fiber-optically so that the technique can be applied through an endoscope, catheter, or a needle which allows imaging of internal organs [31]. OCT can be analysed through a qualitative assessment of image features by eye, or quantitative assessment by measuring the backscattered light. Qualitative assessment by eye refers to the ability to recognize micro-architectural changes, in the way a pathologist would do when he analyses tissue under the microscope. A proposed parameter for quantitative assessment is the decay of signal intensity per millimeter tissue penetration, termed the optical attenuation coefficient (μOCT , mm^{-1}) [30]. It has been hypothesized that the μOCT is able to discriminate benign from malignant

tissue, and enables the grading of malignant tissue as well [32]. In tumourigenesis, the cell organelles and the cell structure is altered when compared to normal cells. The mitochondria and nuclei increase in number due to high mitotic activity, and as a result the size and shape of the cell and cell organelles changes. Those changes leads to different optical properties of tissue and therefore alter the backscattering signal measured with OCT [33].

For the diagnosis of RCC, OCT has been investigated in ex-vivo and in-vivo studies [19, 29, 34–39]. In general, the value of qualitative assessment for the diagnosis of RCC appears to be hampered. RCC varies widely in its visual presentation on OCT images, which makes it hard to recognize specific optical features that contribute to an 'OCT diagnosis' for RCC [28]. Only for the qualitative discrimination of angiomyolipoma (AML) and oncocytomas, distinctive visible features on OCT images may be recognized [37, 38]. Fig. 1 illustrates OCT cross-sections (B-scans) with corresponding pathology slides of oncocytoma, RCC, and angiomyolipoma.

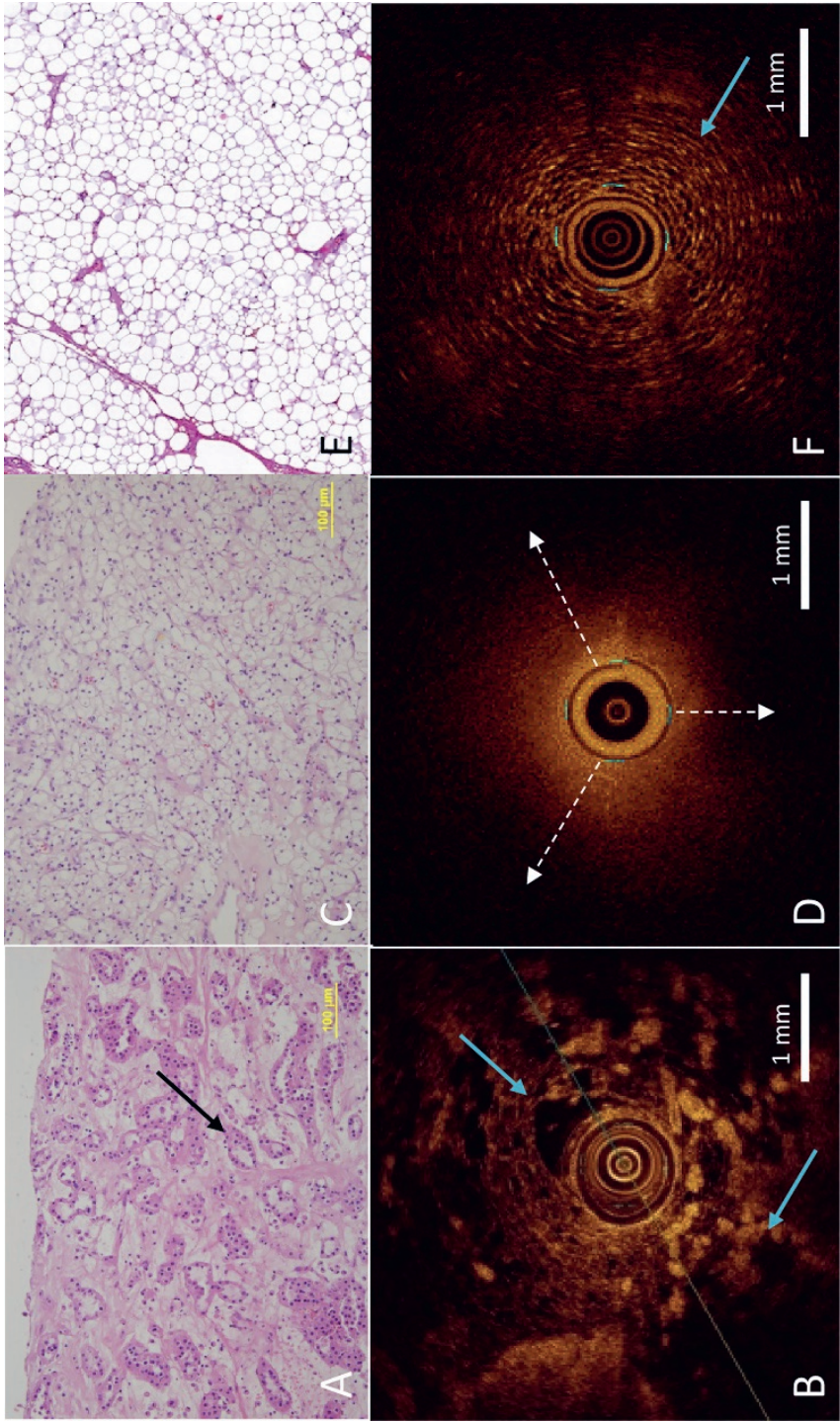


Fig. 1: (A) Oncocytoma pathology slide of RMB with corresponding OCT scan (B). Note the lobulated arrangement (blue arrow) in the OCT scan as well as in the pathology slide (black arrow). (C) A pathology slide of a clear cell renal cell harvested using RMB with a corresponding OCT scan (D). The light decay pattern of RCC exhibits a rapid loss of OCT signal with increasing depth, compared to AML (dotted white arrow). (E) A pathology slide of an angiomyolipoma RMB with a corresponding OCT scan (F). Remarkable is the honeycomb structure, representing the fat of the AML (blue arrow).

The backscattering properties of the renal tumours can also lead to quantitative analysis using the μ OCT. This way of analysing OCT images appeared to be more promising for diagnosing RCC: The μ OCT was significantly higher in RCC compared to benign renal masses and normal renal parenchyma in several in vivo- and ex vivo studies [34–36]. Taking this into consideration, it is hypothesized that by assessing the μ OCT of a renal mass, an objective, fast, and minimally invasive method for RCC-diagnosis might be possible.

Treatment of kidney cancer

According to guidelines, a partial nephrectomy is indicated for localised RCC when technically feasible [40]. A partial nephrectomy is unsuitable for localised RCC in a few situations: tumour involvement of the renal vein, insufficient volume of the remaining parenchyma to maintain a proper renal function, or in case of an unfavourable tumour location (centrally located; adherence to the vessels, ureters, or collecting system) [41]. Even if the tumour is small and located at such an unfavourable spot, a radical nephrectomy is advised with associated consequences for the renal function and comorbidity [41]. Technical advances in partial nephrectomy have led to a maximum nephron-sparing approach accompanied with very low complication rates. Simultaneously, the ablation of SRMs has developed quickly in the last decade and studies have shown significant improvements in both functional outcomes and oncological effectiveness with similar results in recurrences compared to a partial nephrectomy [42].

Renal mass ablation

RCC is increasingly diagnosed at an early stage, requiring a less radical approach since the risk of metastasis is lower in smaller tumours. A challenge in the management of these ‘early diagnosed’ RCCs, that comprises a majority of SRMs, is to find a balance in treating those tumours that will metastasize and display aggressive behaviour, but avoid overtreatment. When there is a chance that the patient will die earlier due to unrelated comorbidities instead of his or her RCC, management options should be carefully weighed in order not to cause the patient further morbidity and consequently a lower quality of life [43]. Image-guided percutaneous ablation has gained popularity in renal mass treatment due to its nephron-sparing properties, fast patient recovery, and low complication rate. The most commonly used ablation techniques are cryoablation (CA), radiofrequency ablation (RFA) and microwave ablation (MWA), all categorized as thermal ablation. According to the European guidelines, the standard of care is partial nephrectomy (PN) for localised RCC [41, 44]. However, recent studies have demonstrated that in terms of oncological outcome, recurrence-free- and metastases free –survival, thermal ablation is comparable to a PN for cT1a tumours (≤ 4 cm and confined to the kidney) [42, 45–48]. These studies also reported lower complications rates, less renal function decrease, and shorter hospital stay for thermal ablation when compared to a PN [45, 46]. Overall survival

(OS) is worse for thermal ablation when compared to PN in most studies [45]. However, in most series, the baseline characteristics of the patient groups reveal a more comorbid and older population in the thermal ablation group when compared to the PN group. Hence, it is thought that the difference in OS is mainly caused by selection bias as thermal ablation is originally a second-line treatment and performed in unfit patients. Other management options such as stereotactic ablative radiotherapy (SABR) are evolving rapidly as a treatment for primary RCC. A recent systematic review demonstrated that SABR has a low toxicity profile and exhibits excellent local tumour control [49, 50]. An additional benefit is that general anaesthesia is not required, and larger tumours (> 4 cm) can be treated as well. Lastly, in elderly patients with a SRM, limited life expectation, high comorbidity, and/or low risk of an aggressive tumour, active surveillance (AS) may be a suitable management option. Early results of a prospective registry demonstrated AS with delayed intervention not to be inferior to active treatment in terms of oncological outcomes [51].

Thermal ablation is considered when the patient is not fit for surgery, has the risk of developing multiple RCCs, has a genetic risk for developing multiple RCCs, and is diagnosed with bilateral tumours or has a solitary kidney and is at risk of complete loss of renal function after resection [52]. The advantages of thermal ablation are low-invasiveness, minimal effect on renal function, and faster recovery for the patient compared to resection. A potential disadvantage is the risk of incomplete ablation due to the so-called heat sink effect: Nearby lying vessels or ureters will drain off heat or cold, and since this is the basis of the mechanism for tissue destruction in thermal ablation this may lead to inconsistent ablation effects. Under-treatment of the tumour side closest to the vessel/ureter might occur and develop into a residual tumour or recurrence. An other potentially harmful consequence is that the vital structure like the ureter, pyelum, or vessels may be damaged by thermal ablation. Especially the urothelial lining of the ureter, pyelum or collecting system is susceptible to extremely high or low temperatures. Hence, thermal ablation is not feasible in a centrally located tumour and the patient is advised to undergo a radical nephrectomy. This will result in a long recovery period and an impairment of the renal function, posing a significant risk for comorbidity for the patient [53]. In patients with a solitary kidney with a centrally located tumour, this results in total loss of renal function and dependency on renal function replacement therapy or kidney transplantation. Especially in this patient group, there is an imperative need for an ablation technique that will not damage the vital structures without decreased effectiveness due to the heat sink. An upcoming ablation technology, hypothesized to fulfill this need, is irreversible electroporation (IRE). IRE is an ablation technique using short, high-voltage electrical pulses to destruct tissue between the placed needles. The mechanism of action behind IRE is not completely understood yet and fuels an ongoing debate to date. IRE is thought to create small holes called nanopores in the cell membrane of tumour cells, which

leads to increased permeability of the membrane [54]. When a sufficient amount of nanopores is reached, the homeostasis of the tumour cell is altered which subsequently causes cell death through apoptosis. Although an increase in temperature is demonstrated in IRE ablated porcine kidneys [55], it is thought that only a minority of the tissue is destroyed by direct thermal ablation [56]. In animal models, preservation of the collecting system and urothelial tissue in renal IRE has suggested that vital structures surrounding kidneys may be less sensitive to the electrical IRE pulses when compared to thermal ablation [57, 58]. Recently, this phenomenon has been reported in humans: Patients that received IRE and 4 weeks later extirpation of their renal tumour showed unaltered normal morphology of the urinary collecting system and urothelial regeneration in the pathology specimen [59]. Therefore, IRE is proposed as a solution for thermal limitations like the heat sink effect and can potentially be used for centrally located tumours [59, 60]. Initial research has demonstrated promising results on renal SRMs, but prospective research should validate those results before IRE can be translated into phase 3 trials and eventually clinical practice.

Aim of the thesis

The first aim of this thesis is to investigate the diagnostic value of needle-based, percutaneous optical coherence tomography (OCT) in the differentiation of renal masses. Secondly, the feasibility and safety of percutaneous, irreversible electroporation (IRE) are assessed for the treatment of SRMs.

Outline of the thesis

Chapter 2 reports on the comparison between OCT and conventional RMB for the differentiation of renal masses. Diagnostic yield (total percentage of biopsies that lead to diagnosis) and accuracy, (sensitivity, specificity, negative predictive value, and positive predictive value) will be assessed for both OCT and RMB in a prospective cohort of 95 patients. In **chapter 3** a literature overview is presented of the novel ablative technologies, including irreversible electroporation (IRE), microwave ablation (MWA), and stereotactic ablative radiation therapy (SABR), for the treatment of localised RCC. They are compared to the currently established ablative techniques, cryoablation and radiofrequency ablation (RFA). In **chapter 4** a literature overview on IRE in several organs is provided including the liver, pancreas, kidney, and prostate. Additionally, the principle and the procedure of IRE is described. **Chapter 5** reports on the study protocol regarding IRE for the ablation of localised RCC in humans. It aims at feasibility and safety, functional outcomes, and clinical efficacy. Additionally, the protocol has a specific focus on several imaging techniques (MRI, CT, and contrast-enhanced ultrasound) used in the follow-up after IRE. **Chapter 6** reports on the feasibility and safety results of the IRE study, as well as the functional outcomes including postoperative pain and renal function. **Chapter 7** describes the imaging

characteristics, enhancement, and the volume of the ablated tumour after renal IRE ablation using contrast-enhanced CT and MRI. **Chapters 8** finalizes this thesis by reporting on a conclusion, summary, and future perspectives. In **chapter 9** an English and Dutch summary is provided per chapter.

References

1. Siegel, R. L., Miller, K. D., & Jemal, A. (2019). Cancer statistics, 2019. *CA: a cancer journal for clinicians*, 69(1), 7–34. <https://doi.org/10.3322/caac.21551>
2. Znaor, A., Lortet-Tieulent, J., Laversanne, M., Jemal, A., & Bray, F. (2015). International variations and trends in renal cell carcinoma incidence and mortality. *European Urology*, 67(3), 519–530.
3. Moch, H., Cubilla, A. L., Humphrey, P. A., Reuter, V. E., & Ulbright, T. M. (2018). The 2016 WHO Classification of Tumours of the Urinary System and Male Genital Organs, Part A: Renal, Penile, and Testicular Tumours. *European Urology*, 70(1), 93–105. <https://doi.org/10.1016/j.eururo.2016.02.029>
4. Avasthi, P., & Marshall, W. F. (2012). NIH Public Access. *International Society of Differentiation*, 83(2), 1–29. <https://doi.org/10.1158/0008-5472.CAN-10-4002.BONE>
5. Kane, C. J., Mallin, K., Ritchey, J., Cooperberg, M. R., & Carroll, P. R. (2008). Renal cell cancer stage migration: Analysis of the National Cancer Data Base. *Cancer*, 113(1), 78–83. <https://doi.org/10.1002/cncr.23518>
6. Huang, W. C., Atoria, C. L., Bjurlin, M., Pinheiro, L. C., Russo, P., Lowrance, W. T., & Elkin, E. B. (2015). Management of Small Kidney Cancers in the New Millennium: Contemporary Trends and Outcomes in a Population-Based Cohort. *JAMA Surg*, 150(7), 664–672. <https://doi.org/10.1001/jamasurg.2015.0294>
7. Bray, F., Ferlay, J., Soerjomataram, I., Siegel, R. L., Torre, L. A., & Jemal, A. (2018). Global cancer statistics 2018: GLOBOCAN estimates of incidence and mortality worldwide for 36 cancers in 185 countries. *CA: a cancer journal for clinicians*, 68(6), 394–424. <https://doi.org/10.3322/caac.21492>
8. Boorjian, S. A., & Uzzo, R. G. (2009). The evolving management of small renal masses. *Current Oncology Reports*, 11(3), 211–217. <https://doi.org/10.1007/s11912-009-0030-6>
9. Fried, T. R. (2016). Shared decision making—finding the sweet spot. *New England Journal of Medicine*, 374(2), 104–106.
10. Motzer, R. J., Bander, N. H., & Nanus, D. M. (1996). Renal-cell carcinoma. *The New England journal of medicine*, 335(12), 865–875. <https://doi.org/10.1056/NEJM199609193351207>
11. Herts, B. R., Silverman, S. G., Hindman, N. M., Uzzo, R. G., Hartman, R. P., Israel, G. M., ... Pandharipande, P. V. (2018). Management of the Incidental Renal Mass on CT: A White Paper of the ACR Incidental Findings Committee. *Journal of the American College of Radiology*, 15(2), 264–273. <https://doi.org/10.1016/j.jacr.2017.04.028>
12. Reuter, V. E., Kurta, J. M., Nogueira, L., Kundu, S., Kaag, M., Russo, P., ... Tickoo, S. K. (2009). Tumour Size is Associated With Malignant Potential in Renal Cell Carcinoma Cases. *Journal of Urology*, 181(5), 2033–2036. <https://doi.org/10.1016/j.juro.2009.01.027>
13. ZINCKE, H., WEAVER, A. L., LOHSE, C. M., FRANK, I., BLUTE, M. L., & CHEVILLE, J. C. (2004). Solid Renal Tumours: An Analysis of Pathological Features Related to Tumour Size. *Journal of Urology*, 170(6), 2217–2220. <https://doi.org/10.1097/01.ju.0000095475.12515.5e>
14. Frank, I., Blute, M. L., Cheville, J. C., Lohse, C. M., Weaver, A. L., & Zincke, H. (2002). An outcome prediction model for patients with clear cell renal cell carcinoma treated with radical nephrectomy based on tumour stage, size, grade and necrosis: The SSIGN score. *Journal of Urology*, 168(6), 2395–2400. [https://doi.org/10.1016/S0022-5347\(05\)64153-5](https://doi.org/10.1016/S0022-5347(05)64153-5)
15. Patel, H. D., Johnson, M. H., Pierorazio, P. M., Sozio, S. M., Sharma, R., Iyoha, E., ... Allaf, M. E. (2016). Diagnostic Accuracy and Risks of Biopsy in the Diagnosis of a Renal Mass Suspicious for Localised Renal Cell Carcinoma: Systematic Review of the Literature. *The Journal of Urology*, 195(February), 1–8.
16. Marconi, L., Dabestani, S., Lam, T. B., Hofmann, F., Stewart, F., Norrie, J., ... Volpe, A. (2015). Systematic Review and Meta-analysis of Diagnostic Accuracy of Percutaneous Renal Tumour Biopsy. *European Urology*, 69(4), 660–673.
17. Macklin, P. S., Sullivan, M. E., Tapping, C. R., Cranston, D. W., Webster, G. M., Roberts, I. S. D., ... Browning, L. (2018). Tumour Seeding in the Tract of Percutaneous Renal Tumour Biopsy: A Report on Seven Cases from a UK Tertiary Referral Centre. *European Urology*. <https://doi.org/10.1016/j.eururo.2018.12.011>
18. Leveridge, M. J., Finelli, A., Kachura, J. R., Evans, A., Chung, H., Shiff, D. A., ... Jewett, M. A. S. S. (2011). Outcomes of small renal mass needle core biopsy, non-diagnostic percutaneous biopsy, and the role of repeat biopsy. *European Urology*, 60(3), 578–584.
19. Buijs, M., Wagstaff, P. G. K., de Bruin, D. M., Zondervan, P. J., Savci-Heijink, C. D., van Delden, O. M., ... Laguna Pes, M. P. (2017). An In-vivo Prospective Study of the Diagnostic Yield and Accuracy of Optical Biopsy Compared with

- Conventional Renal Mass Biopsy for the Diagnosis of Renal Cell Carcinoma: The Interim Analysis. *European Urology Focus*. <https://doi.org/10.1016/j.euf.2017.10.002>
20. Tsui, K. H., Shvarts, O., Smith, R. B., Figlin, R., de Kernion, J. B., & Beldegrun, A. (2000). Renal cell carcinoma: prognostic significance of incidentally detected tumours. *The Journal of urology*, 163(2), 426–430.
 21. Blumenfeld, A. J., Guru, K., Fuchs, G. J., & Kim, H. L. (2010). Percutaneous Biopsy of Renal Cell Carcinoma Underestimates Nuclear Grade. *Urology*, 76(3), 610–613.
 22. Johnson, D. C., Vukina, J., Smith, A. B., Meyer, A. M., Wheeler, S. B., Kuo, T. M., ... Nielsen, M. E. (2015). Preoperatively misclassified, surgically removed benign renal masses: a systematic review of surgical series and United States population level burden estimate. *The Journal of urology*, 193(1), 30–35.
 23. Tearney, G. J., Brezinski, M. E., Bouma, B. E., Boppart, S. A., Pitris, C., Southern, J. F., & Fujimoto, J. G. (1997). In vivo endoscopic optical biopsy with optical coherence tomography. *Science*, 276(5321), 2037–2039.
 24. Jang, I.-K., Bouma, B. E., Kang, D.-H., Park, S.-J., Park, S.-W., Seung, K.-B., ... Pomerantsev, E. (2002). Visualization of coronary atherosclerotic plaques in patients using optical coherence tomography: comparison with intravascular ultrasound. *Journal of the American College of Cardiology*, 39(4), 604–609.
 25. Pitris, C., Jessor, C., Boppart, S. A., Stamper, D., Brezinski, M. E., & Fujimoto, J. G. (2000). Feasibility of optical coherence tomography for high-resolution imaging of human gastrointestinal tract malignancies. *Journal of Gastroenterology*, 35(2), 87–92. <https://doi.org/10.1007/s005350050019>
 26. Welzel, J. (2001). Optical coherence tomography in dermatology: A review. *Skin Research and Technology*, 7(1), 1–9. <https://doi.org/10.1034/j.1600-0846.2001.007001001.x>
 27. Wessels, R., de Bruin, D. M., Faber, D. J., van Boven, H. H., Vincent, A. D., van Leeuwen, T. G., ... Ruers, T. J. M. (2012). Optical coherence tomography in vulvar intraepithelial neoplasia. *Journal of biomedical optics*, 17(11), 116022.
 28. Freund, J. E., Buijs, M., Savci-Heijink, C. D., de Bruin, D. M., de la Rosette, J., van Leeuwen, T. G., & Laguna, M. P. (2019). Optical Coherence Tomography in Urologic Oncology: a Comprehensive Review. *SN Comprehensive Clinical Medicine*, 1(2), 67–84.
 29. Wagstaff, P. G., Ingels, A., De Bruin, D. M., Buijs, M., Zondervan, P. J., Dilara, C., ... Pes, L. (2015). Percutaneous Needle Based Optical Coherence Tomography for the Differentiation of Renal Masses: a Pilot Cohort Percutaneous Needle Based Optical Coherence Tomography for the Differentiation of Renal Masses: a Pilot Cohort. *The Journal of Urology*, 195(February), 1–8.
 30. Faber, D. J., van der Meer, F. J., Aalders, M. C. G., & van Leeuwen, T. G. (2004). Quantitative measurement of attenuation coefficients of weakly scattering media using optical coherence tomography. *Optics Express*, 12(19), 4353. <https://doi.org/10.1364/opex.12.004353>
 31. Yaqoob, Z., Wu, J., McDowell, E. J., Heng, X., & Yang, C. (2006). Methods and application areas of endoscopic optical coherence tomography. *Journal of Biomedical Optics*, 11(6), 1–19.
 32. Wessels, R., De Bruin, D. M., Faber, D. J., Van Leeuwen, T. G., Van Beurden, M., & Ruers, T. J. M. (2014). Optical biopsy of epithelial cancers by optical coherence tomography (OCT). *Lasers in medical science*, 29(3), 1297–1305.
 33. Hielscher, A. H., Shen, D., Johnson, T. M., Mourant, J. R., Eick, A. A., & Freyer, J. P. (2008). Mechanisms of light scattering from biological cells relevant to noninvasive optical-tissue diagnostics. *Applied Optics*, 37(16), 3586. <https://doi.org/10.1364/ao.37.003586>
 34. Barwari, K., Bruin, D. M. De, Faber, D. J., Leeuwen, T. G. Van, Rosette, J. J. De, & Laguna, M. P. (2012). Differentiation between normal renal tissue and renal tumours using functional optical coherence tomography: a phase I, 415–420.
 35. Lee, H.-C., Zhou, C., Cohen, D. W., Mondelblatt, A. E., Wang, Y., Aguirre, A. D., ... Connolly, J. L. (2012). Integrated optical coherence tomography and optical coherence microscopy imaging of ex vivo human renal tissues. *The Journal of urology*, 187(2), 691–699.
 36. de Bruin, D. M., de la Rosette, J., Wijkstra, H., Faber, D. J., Laguna, M. P., van Leeuwen, T. G., ... Cauberg, E. C. C. (2011). Advanced Diagnostics in Renal Mass Using Optical Coherence Tomography: A Preliminary Report. *Journal of Endourology*, 25(2), 311–315. <https://doi.org/10.1089/end.2010.0408>
 37. Linehan, J. A., Bracamonte, E. R., Hariri, L. P., Sokoloff, M. H., Rice, P. S., Barton, J. K., & Nguyen, M. M. (2011). Feasibility of optical coherence tomography imaging to characterise renal neoplasms: limitations in resolution and depth of penetration. *BJU international*, 108(11), 1820–1824.
 38. Jain, M., Robinson, B. D., Salamon, B., Thouvenin, O., Boccara, C., & Mukherjee, S. (2015). Rapid evaluation of fresh ex vivo kidney tissue with full-field optical coherence tomography. *Journal of pathology informatics*, 6.

39. Ludwig, W. W., Wobker, S. E., Ball, M. W., Zysk, A. M., Yemul, K. S., Pierorazio, P. M., ... Allaf, M. E. (2018). Margin assessment in renal surgery using a handheld optical coherence tomography probe. *Urology*, 113, 241–245.
40. Perzyna, B., & Stolzmann, W. (2018). EAU Guidelines on Renal Cell Carcinoma 2018, 29(5), 451–458.
41. Ljungberg, B., Albiges, L., Bensalah, K., Bex, A., Giles, R., Hora, M., ... Tahbaz, R. (2018). EAU Guidelines on Renal Cell Carcinoma 2018. *Euro Urol*, 29(5), 451–458.
42. Rivero, J. R., De La Cerdá, J. 3rd, Wang, H., Liss, M. A., Farrell, A. M., Rodriguez, R., ... Kaushik, D. (2017). Partial Nephrectomy versus Thermal Ablation for Clinical Stage T1 Renal Masses: Systematic Review and Meta-Analysis of More than 3,900 Patients. *Journal of vascular and interventional radiology: JVIR*. <https://doi.org/10.1016/j.jvir.2017.08.013>
43. Weight, C. J., Lane, B. R., Campbell, S. C., Gao, T., Hernandez, A. V., Gill, I. S., ... Kaouk, J. H. (2010). Active treatment of localised renal tumours may not impact overall survival in patients aged 75 years or older. *Cancer*, 116(13), 3119–3126. <https://doi.org/10.1002/cncr.25184>
44. Cadeddu, J. A., Chang, A., Clark, P. E., Davis, J., Derweesh, I. H., Giambarrresi, L., & Debra, A. (2017). American Urological Association (AUA) RENAL MASS AND LOCALISED RENAL CANCER : AUA GUIDELINE American Urological Association (AUA) Renal Mass and Localised Renal Cancer. *American Urological Association*, 1–49.
45. Thompson, R. H., Atwell, T., Schmit, G., Lohse, C. M., Kurup, A. N., Weisbrod, A., ... Leibovich, B. C. (2015). Comparison of partial nephrectomy and percutaneous ablation for cT1 renal masses. *Eur Urol*, 67(2), 252–259. <https://doi.org/10.1016/j.eururo.2014.07.021>
46. Pierorazio, P. M., Johnson, M. H., Patel, H. D., Sozio, S. M., Sharma, R., Iyoha, E., ... Allaf, M. E. (2016). Management of Renal Masses and Localised Renal Cancer: Systematic Review and Meta-Analysis. *Journal of Urology*, 196(4), 989–999. <https://doi.org/10.1016/j.juro.2016.04.081>
47. Van Poppel, H., Da Pozzo, L., Albrecht, W., Matveev, V., Bono, A., Borkowski, A., ... Sylvester, R. (2011). A prospective, randomised EORTC intergroup phase 3 study comparing the oncologic outcome of elective nephron-sparing surgery and radical nephrectomy for low-stage renal cell carcinoma. *European Urology*, 59(4), 543–552. <https://doi.org/10.1016/j.eururo.2010.12.013>
48. Zhou, M., Mills, A., Noda, C., Ramaswamy, R., & Akinwande, O. (2018). SEER study of ablation versus partial nephrectomy in cT1A renal cell carcinoma. *Future Oncology*, 14(17), 1711–1719. <https://doi.org/10.2217/fon-2017-0678>
49. Siva, S., Louie, A. V., & Warner, A. (2018). Pooled Analysis of Stereotactic Ablative Radiotherapy for Primary Renal Cell Carcinoma : A Report From the International Radiosurgery Oncology Consortium for Kidney (IROCK). <https://doi.org/10.1002/cncr.31156>
50. Correa, R. J. M., Louie, A. V., Zaorsky, N. G., Lehrer, E. J., Ellis, R., Ponsky, L., ... Siva, S. (2019). The Emerging Role of Stereotactic Ablative Radiotherapy for Primary Renal Cell Carcinoma: A Systematic Review and Meta-Analysis. *European Urology Focus*, 5(6), 958–969. <https://doi.org/10.1016/j.euf.2019.06.002>
51. Pierorazio, P. M., Johnson, M. H., Ball, M. W., Gorin, M. A., Trock, B. J., Chang, P., Allaf, M. E. (2015). Five-year Analysis of a Multi-institutional Prospective Clinical Trial of Delayed Intervention and Surveillance for Small Renal Masses: The DISSRM Registry. *European Urology*, 68(3), 408–415. <https://doi.org/10.1016/j.eururo.2015.02.001>
52. Ljungberg, B., Bensalah, K., Canfield, S., Dabestani, S., Hofmann, F., Hora, M., ... Bex, A. (2015). EAU Guidelines on Renal Cell Carcinoma: 2014 Update. *European Urology*, 67(5), 913–924.
53. Mir, M. C., Derweesh, I., Porpiglia, F., Zargar, H., Mottrie, A., & Autorino, R. (2017). Partial Nephrectomy Versus Radical Nephrectomy for Clinical T1b and T2 Renal Tumours: A Systematic Review and Meta-analysis of Comparative Studies. *European Urology*, 71(4), 606–617. <https://doi.org/10.1016/j.eururo.2016.08.060>
54. Davalos, R., Mir, L., & Rubinsky, B. (2005). Tissue ablation with irreversible electroporation. *Annals of Biomedical Engineering*, 33(2), 223–231. <https://doi.org/10.1007/s10439-005-8981-8>
55. Wagstaff, P. G. K., de Bruin, D. M., van den Bos, W., Ingels, A., van Gemert, M. J. C., Zondervan, P. J., ... Laguna Pes, M. P. (2014). Irreversible electroporation of the porcine kidney: Temperature development and distribution. *Urologic Oncology: Seminars and Original Investigations*, 33(4), 168.e1–168.e7. <https://doi.org/10.1016/j.urolonc.2014.11.019>
56. Agnass, P., van Veldhuisen, E., van Gemert, M. J. C., van der Geld, C. W. M., van Lienden, K. P., van Gulik, T. M., ... Crezee, J. (2020). Mathematical modeling of the thermal effects of irreversible electroporation for in vitro , in vivo , and clinical use: a systematic review. *International Journal of Hyperthermia*, 37(1), 486–505. <https://doi.org/10.1080/02656736.2020.1753828>

57. Tracy, C. R., Kabbani, W., & Cadeddu, J. A. (2011). Irreversible electroporation (IRE): A novel method for renal tissue ablation. *BJU International*, 107(12), 1982–1987. <https://doi.org/10.1111/j.1464-410X.2010.09797.x>
58. Wendler, J. J., Pech, M., Porsch, M., Janitzky, A., Fischbach, F., Buhtz, P., Strang, C. (2012). Urinary tract effects after multifocal nonthermal irreversible electroporation of the kidney: acute and chronic monitoring by magnetic resonance imaging, intravenous urography and urinary cytology. *Cardiovascular and interventional radiology*, 35(4), 921–926.
59. Wendler, J. J. et al. (2017). Upper-Urinary-Tract Effects After Irreversible Electroporation (IRE) of Human Localised Renal-Cell Carcinoma (RCC) in the IRENE Pilot Phase 2a Ablate-and-Resect Study. *Cardiovasc Intervent Radiol.*, ((Epub ahead of print)). <https://doi.org/10.1007/s00270-017-1795-x>
60. Deodhar, A., Monette, S., Single, G. W., Hamilton, W. C., Thornton, R., Maybody, M., Solomon, S. B. (2011). Renal tissue ablation with irreversible electroporation: Preliminary results in a porcine model. *Urology*, 77(3), 754–760. <https://doi.org/10.1016/j.urology.2010.08.036>

CHAPTER 2

2

An in-vivo prospective study of the diagnostic yield and accuracy of optical biopsy compared with conventional renal mass biopsy for the diagnosis of renal cell carcinoma: The interim analysis

M Buijs, PGK Wagstaff, DM de Bruin, PJ Zondervan, CD Savci-Heijink, OM van Delden, TG van Leeuwen, RJA van Moorselaar, JJMCH de la Rosette, MP Laguna Pes

Abstract

Background: Lack of accuracy in preoperative imaging leads to overtreatment of benign renal masses (RMs) or indolent renal cell carcinomas (RCCs). Optical coherence tomography (OCT) is a real-time and high-resolution optical technique, enabling quantitative analysis through the attenuation coefficient (μOCT , mm^{-1}).

Objective: To determine the accuracy, the sensitivity, specificity, positive predictive value (PPV), and negative predictive value (NPV), and the diagnostic yield, the percentage that leads to a diagnosis, of OCT and renal mass biopsy (RMB) for the differentiation of benign RMs versus RCC, and oncocytoma versus RCC.

Design, setting, and participants: From October 2013 to June 2016, 95 patients with solid enhancing RMs on cross-sectional imaging were prospectively included. All patients underwent subsequent excision or ablation.

Intervention: Percutaneous, image-guided, needle-based OCT followed by a RMB in an outpatient setting under local anaesthesia.

Outcome measurements and statistical analysis: Accuracy and diagnostic yield, μOCT correlated to resection pathology or second biopsy during ablation. Tables (2x2) for RMB and receiver operating characteristic curves for OCT were determined. A Mann-Whitney test was used to differentiate between the μOCT s of the RMs.

Results and limitations: RMB diagnostic yield was 79% with sensitivity, specificity, positive predictive value, and negative predictive value of 100%, 89%, 99%, and 100%, respectively. The diagnostic yield of OCT to differentiate RCC from benign was 99%. A significant difference was observed in the median μOCT between benign RMs (3.2 mm^{-1} , interquartile range [IQR]: 2.65–4.35) and RCCs (4.3 mm^{-1} , IQR: 3.70–5.00), $p = 0.0171$, and oncocytomas (3.38 mm^{-1} , IQR: 2.68–3.95) and RCCs (4.3 mm^{-1} , IQR: 3.70–5.00), $p = 0.0031$. OCT showed sensitivity, specificity, PPV, and NPV of 91%, 56%, 91%, and 56%, respectively, to differentiate benign RMs from RCCs and 92%, 67%, 95%, and 55%, respectively, to differentiate oncocytomas from RCCs. Limitations include two reference standards and the heterogeneity of the benign RMs.

Conclusions: Compared with RMB, OCT has a higher diagnostic yield. OCT accurately distinguishes benign RMs from RCCs, and oncocytoma from RCCs, although specificity and NPV are lower.

Introduction

Recent decades witnessed a significant change in renal cell carcinoma (RCC) stage distribution at diagnosis and a steady rise in clinical small renal masses (SRMs; ≤ 4 cm) [1,2]. Surgery, when possible, remains indicated when RCC suspicion rises on cross-sectional imaging [3–5]. However, 17–40% of resected renal masses (RMs) turn out to be benign suggesting an imbalance between diagnosis and treatment paradigms. The RMs shifted presentation and expanded treatment options provide the foundation to modify the diagnostic approach [6].

Cross-sectional imaging is excellent to detect RMs but cannot reliably differentiate benign from malignant RMs. Renal mass biopsy (RMB) emerges as the most valid tool to preoperatively determine the histological diagnosis. When diagnostic, RMB is highly accurate in differentiating benign from malignant and for subtype determination. However, accuracy is mostly determined after the exclusion of non-diagnostic biopsies (NDB) [7,8]. NDB rates remain variable and are reported in up to 23% in SRMs [20]. Additionally, RMB has a low negative predictive value (NPV) and underestimates the Fuhrman grade in 24–55% of the cases when compared with pathology specimen [10,11].

Optical imaging modalities such as optical coherence tomography (OCT) arise as potential diagnostic tools in urologic cancers to overcome RMB pitfalls [7,8,12,13]. OCT is a real-time imaging technique that allows the visualization of tissue at a cellular level. High-resolution images, with a tissue penetration of 2–3 mm, are obtained within seconds without the need for a contrast agent. Percutaneous, needle-based OCT differentiation between benign and malignant renal tumours using a quantitative parameter (attenuation coefficient, μ OCT) has proven to be safe and feasible [11]. Based on these pilot results, we launched a prospective diagnostic study comparing needle-based OCT with conventional RMB in patients with RMs tributary of active treatment.

The primary objective is an interim analysis assessing the diagnostic accuracy of OCT versus conventional RMB for differentiation between benign and malignant RMs and between RCC and oncocytoma. The secondary objective is to determine the diagnostic yield of both techniques.

Material and methods

Study design

This is a prospective diagnostic study, approved by the Institutional Review Board of our Institute (2012_269). Trial registration was completed by the Dutch Central Committee on Research Involving Human Subjects (NL41985.018.12) and in the clinicaltrials.gov database (NCT02073110) [13]. All patients gave written informed consent. This study conforms to Standards for Reporting Diagnostic Accuracy guidelines [14].

Participants

From October 2013 to July 2016, consecutive patients with a solid enhancing RM seen at the outpatient clinic (tertiary care hospital) were offered a RMB and participation in the study. Inclusion criteria comprised: older than 18 yr, solid enhancing RM on cross-sectional imaging suspicious for RCC, and candidate for active treatment (surgery or ablation). In our center, RMB is included in the diagnostic workup of solid RMs. Nonparticipation in the study did not preclude RMB. Patients who were not candidates for active treatment were excluded from the study.

Test methods

Patients underwent percutaneous needle-based OCT (index test) followed by image-guided RMB (standard test) in the same procedure. The percutaneous tract and RMB were performed by interventional radiologists and the OCT by resident urology. The reference standard was the surgical pathology specimen in patients receiving radical/partial nephrectomy, or a second procedural biopsy in patients receiving ablation. Ablation was recommended to patients with high comorbidity or surgical risk [3,4]. Surgical specimens and RMBs were pre-specified as a positive test when histology/pathology results reported renal malignancy. OCT results tested as positive when the determined cut-off value of μ OCT was reached or exceeded (exploratory). RMB and OCT procedures were performed according to the protocol as previously described to warrant systematic data acquisition [11].

Analysis: histology and pathology

A genitourinary pathologist blinded for OCT results performed the analysis of the RMBs and the surgical specimens. Pathology analysis was performed according to the pathology department-specific protocol [11]. NDBs included those reported by the pathologists as normal renal parenchyma, fibrosis, necrosis, or insufficient tissue for analysis.

Analysis: OCT

As described previously, quantitative analysis consisted of determining the average μ OCT based on five different B-scans [11,15–17]. From one volumetric OCT scan (541 B-scans), five B-scans were randomly selected to determine the average μ OCT values of the corresponding five A-scans (Fig. 1). The μ OCT values were corrected for the point spread function, the system roll-off, and the refractive index $n = 1.4$ [15]. When OCT scans revealed only fluid or perinephric fat tissue, OCT was interpreted as non-diagnostic (ND). The resident urology and the engineer that analysed the OCT scans were blinded for the pathology results.

Statistical analysis

A sample size calculation was performed based on our pilot study [18], resulting in a needed inclusion number of 194 patients [13]. The Institutional Review Board predetermine the interim analysis to be conducted once half of the patients were included. The diagnostic yield for RMB and OCT was calculated by dividing the diagnostic cases by the total number of cases $\times 100$. Diagnostic accuracy (sensitivity, specificity, PPV, and NPV) of RMB was calculated based on histopathology at treatment. The values of μ OCT were unpaired and numeric, and non-normally distributed. The Mann-Whitney U test was used to evaluate the difference in μ OCT value between malignant and benign RMs, and RCCs and oncocytomas. Test results were interpreted as significant if the two-sided p-value was below 0.05. The receiver operating characteristic (ROC) curve was used to investigate different μ OCT cut-off values to determine the optimal trade-off between sensitivity, specificity, PPV, and NPV. The added value of OCT was calculated using the μ OCT optimal cut-off value, the proportion of correctly diagnosed tumours by OCT was calculated among the group of NDBs. The overall added value of OCT was calculated by dividing the correctly identified tumours by the total interim cohort $\times 100$.

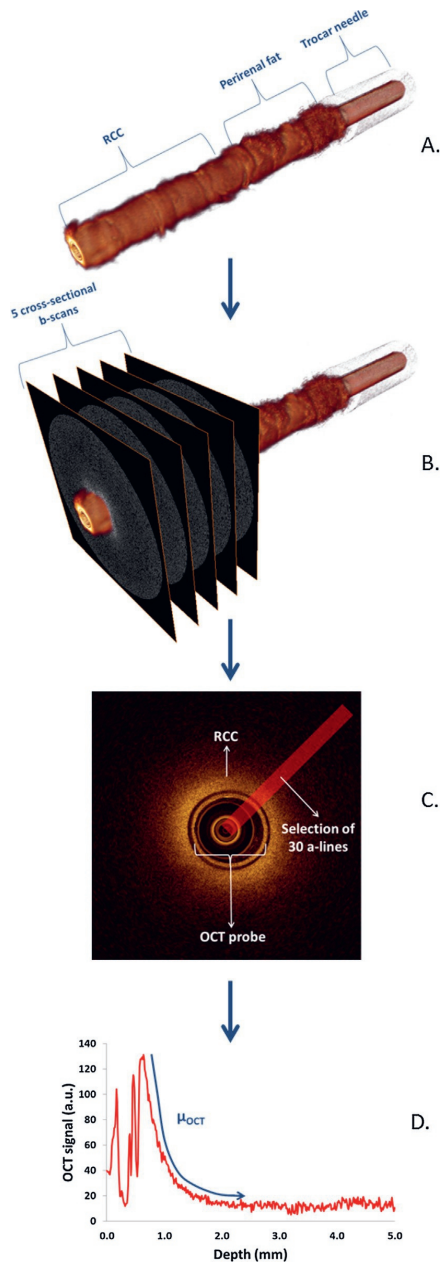


Fig. 1 – Quantitative analysis of optical coherence tomography (OCT) scan. (A) One volumetric OCT scan (54 mm total in length) of renal cell carcinoma tissue and adjacent perirenal fat tissue. (B) One volumetric OCT scan consisted of 541 cross-sectional B-scans. Five cross-sectional B-scans were selected for analysis. (C) In each cross-sectional B-scan 30 parallel A-lines (A-scan) are drawn, radiating outward from the heart of the probe. (D) An average of five A-scans from each selected B-scan is plotted in a graph using Fiji plugin (developed in house). The slope of the graphic represents the μ_{OCT} .

Results

Participants

During the study period, 281 patients presented with a solid-enhancing RM at the outpatient clinic, and 95 patients were included in this interim cohort. The inclusion flowchart is presented in Fig. 2. Patient demographics, tumour characteristics and complexity, and type of treatment of the entire and diagnostic RMB and OCT cohorts are depicted in Table 1.

Diagnostic yield

Overall, RMB was ND in 20 patients (21%) and OCT was non-diagnostic in one patient (1%). The diagnostic yields of RMB and OCT were 79% and 99%, respectively (Table 2).

Diagnostic accuracy

The diagnostic RMB group (75 patients) consisted of nine oncocytomas and 66 RCCs. In differentiating between RCC and oncocytoma, no false-negative and one false positive case were observed. Sensitivity, specificity, PPV, and NPV were 100%, 89%, 99%, and 100%, respectively (Table 2).

The diagnostic OCT group (94 patients) consisted of 78 RCCs, nine oncocytomas, three cysts, one papillary adenoma, one leiomyoma, one case of granulation tissue mass, and one haemangioma. The median μ OCT of benign RMs (3.2 mm^{-1} , interquartile range [IQR]: $2.65\text{--}4.35$) was significantly lower than the median μ OCT of RCCs (4.3 mm^{-1} , IQR: $3.70\text{--}5.00$), $p = 0.0171$ (Fig. 3). ROC analysis showed an optimal μ OCT cut-off value of $>3.2 \text{ mm}^{-1}$ for sensitivity, specificity, PPV, and NPV of 91%, 56%, 91%, and 56%, respectively (Table 2). The area under the curve (AUC) was 0.69 (95% confidence interval [CI]: $0.59\text{--}0.78$). A subset analysis in patients exclusively receiving radical or partial nephrectomy ($N = 84$) demonstrated an AUC of 0.64 (95% CI: $0.53\text{--}0.74$).

For differentiation between oncocytoma ($n = 8$) and RCC ($n = 78$), the median μ OCT of oncocytoma (3.2 mm^{-1} , IQR: $2.68\text{--}3.95$) was significantly lower than the median μ OCT of RCC (4.3 mm^{-1} , IQR: $3.70\text{--}5.00$), $p = 0.0031$ (Fig. 3). ROC curve showed an optimal μ OCT cut-off value of $>3.2 \text{ mm}^{-1}$ for a sensitivity, specificity, PPV, and NPV of 92%, 67%, 95%, and 55%, respectively (Table 2). The AUC was 0.81 (95% CI: $0.73\text{--}0.91$). Subset analysis in patients receiving radical or partial nephrectomy showed an AUC of 0.77 (95% CI: $0.66\text{--}0.86$).

Added-value of OCT

Applying the established μ OCT cut-off value of 3.2 mm^{-1} , OCT was diagnostic in 14 (70%) out of 20 ND-RMBs. This included 11 of 13 malignant masses (85%), and three of seven

benign masses (43%). The added value of the OCT in our interim cohort was 15%. Patient demographics of the ND group are depicted in Table 3. ND-RMBs occurred more frequently in men and in smaller masses.

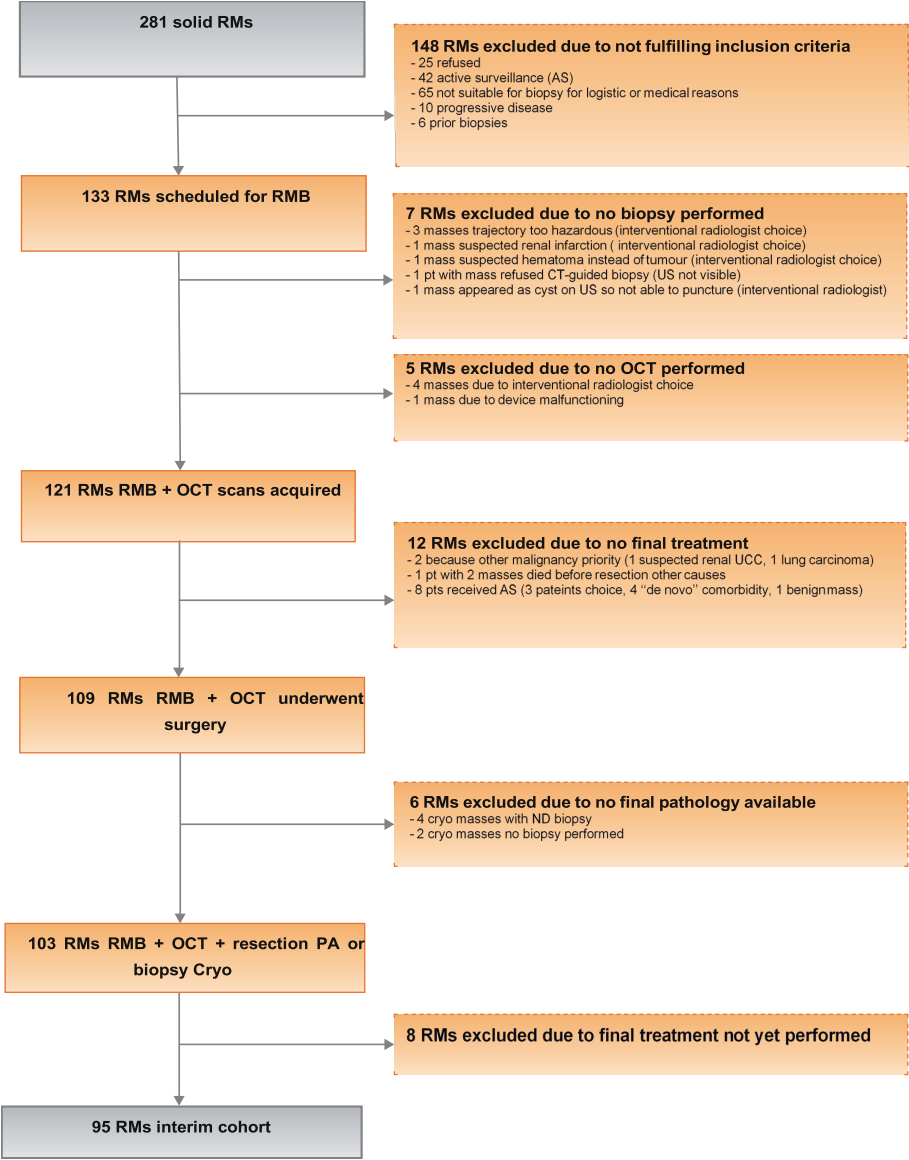


Fig. 2 – Flowchart of inclusion of interim cohort. Surgery includes radical or partial nephrectomy. Cryo = cryoablation; CT = computed tomography; ND = non-diagnostic; OCT = optical coherence tomography; PA = pathology analysis; pt = patient; RM = renal mass; RMB = renal mass biopsy; US = ultrasound.

Adverse events

A total of three patients developed a perinephric haematoma requiring overnight hospital admission for observation. One of them presented with transient macroscopic haematuria (Grade 1 according to Common Terminology Criteria for Adverse Events version 3.0). No patient required a blood transfusion. One patient developed a lung embolism 1 week after OCT/RMB procedure requiring therapeutic nadroparin (Grade 4 according to Common Terminology Criteria for Adverse Events version 3.0). All patients recovered and did not experience any lasting symptoms.

Table 1 – Patient characteristics. In accordance with the PADUA score, tumours were interpreted as low (5–7 points), moderate (8–9 points), or high (10 points). RENAL Nephrometry Scores 4–6 were considered low complexity for resection, 7–9 were considered moderate complexity, and 10–12 were considered high complexity.

| Characteristics | Interim cohort (N = 95) | Diagnostic OCT (N = 94) | Diagnostic RMB (N = 75) |
|-----------------------------|-------------------------|-------------------------|-------------------------|
| Mean age, yr (SD) | 59 (12) | 58 (12) | 47 (12) |
| Median size in cm (range) | 3.3 (1.2–9.1) | 3.3 (1.2–9.1) | 3.6 (1.2–9.1) |
| SRMs (%) | 60 (63) | 59 (63) | 42 (56) |
| Men (%) | 65 (68) | 64 (68) | 50 (67) |
| Mean PADUA (SD) | 9 (2) | 9 (2) | 9 (2) |
| Low 5–7 (%) | 30 (32) | 29 (31) | 23 (31) |
| Moderate 8–9 (%) | 29 (31) | 29 (31) | 24 (32) |
| High >10 (%) | 36 (38) | 36 (38) | 28 (37) |
| Mean RENAL (SD) | 8 (2) | 8 (2) | 8 (2) |
| Low 4–6 (%) | 29 (31) | 28 (30) | 21 (28) |
| Moderate 7–9 (%) | 38 (40) | 38 (40) | 31 (41) |
| High 10–12 (%) | 28 (29) | 28 (29) | 23 (31) |
| Treatment type | | | |
| Open partial nephrectomy | 11 (12) | 11 (12) | 8 (11) |
| Open radical nephrectomy | 4 (4) | 4 (4) | 4 (5) |
| Lap partial nephrectomy | 48 (50) | 48 (50) | 35 (47) |
| Lap radical nephrectomy | 21 (22) | 21 (22) | 18 (24) |
| Cryoablation | 11 (12) | 10 (11) | 10 (13) |
| Resection PA | | | |
| ccRCC (%) | 53 (56) | 53 (56) | 42 (56) |
| pRCC (%) | 18 (19) | 18 (19) | 17 (23) |
| chrRCC (%) | 7 (7) | 6 (6) | 6 (8) |
| RCC (%) | 1 (1) | 1 (1) | 1 (1) |
| Oncocytoma (%) | 9 (10) | 9 (10) | 9 (12) |
| Cyst (%) | 3 (3) | 3 (3) | 0 (0) |
| Other benign pathology (%) | 4 (4) | 4 (4) | 0 (0) |
| Papillary adenoma (%) | 1 (1) | 1 (1) | 0 (0) |
| Leiomyoma (%) | 1 (1) | 1 (1) | 0 (0) |
| Granulation tissue mass (%) | 1 (1) | 1 (1) | 0 (0) |
| Haemangioma (%) | 1 (1) | 1 (1) | 0 (0) |
| CT-guided RMB | 1 (1) | 1 (1) | 1 (1) |
| CEUS-guided RMB | 1 (1) | 1 (1) | 1 (1) |
| US-guided RMB | 93 (98) | 92 (98) | 73 (98) |

ccRCC = clear cell renal cell carcinoma; CEUS = contrast-enhanced ultrasound; chrRCC = chromophobe renal cell carcinoma; CT = computed tomography; Lap = laparoscopic; OCT = optical coherence tomography; PA = pulmonary artery; pRCC = papillary renal cell carcinoma; RCC = mucinous-spindle RCC; RMB = renal mass biopsy; SD = standard deviation; SRM = small renal mass; US = ultrasound.

Table 2 – Comparison of diagnostic yield and accuracy of renal mass biopsy (RMB) and optical coherence tomography (OCT) in the interim cohort. (Only diagnostic RMBs and diagnostic OCT scans are included in the table for accuracy calculations. For OCT, the optimal cut-off value of 3.2 mm⁻¹ is used for accuracy calculation).

| | DY (%) | Sens (%) | Spec (%) | PPV (%) | NPV (%) | AUC | AUC CI |
|---|-----------|-------------|-------------|------------|------------|------|------------|
| 1. Conventional RMB: oncocytomas vs RCCs (N = 75) | 79 | 100 | 89 | 99 | 100 | — | — |
| 2. OCT: benign vs RCCs (N = 94) | 99 | 91 | 56 | 91 | 56 | 0.69 | 0.59–0.769 |
| 3. OCT: oncocytomas vs RCCs (N = 87) | 99 | 92 | 67 | 95 | 55 | 0.81 | 0.71–0.88 |

DY= diagnostic yield; Sens= sensitivity; Spec = specificity; PPV = positive predictive value; NPV = negative predictive value; RCC = renal cell carcinoma; AUC = area under the curve; CI = confidence interval.

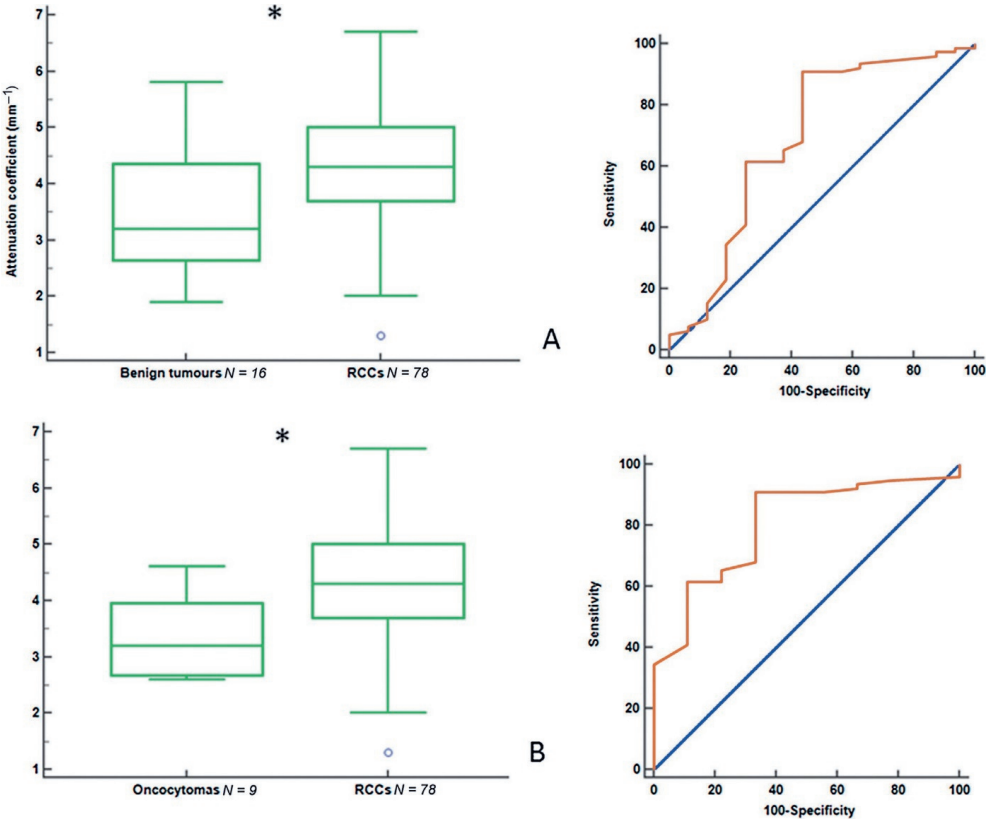


Fig. 3 – (A) Optical coherence tomography boxplot of benign renal masses (N = 16) versus renal cell carcinomas (RCCs; N = 78). Median μ OCT of benign tumours (3.2 mm⁻¹, interquartile range [IQR]: 2.65–4.35) was significantly lower than median μ OCT of malignant tumours (4.3 mm⁻¹, IQR: 3.70–5.00) with p = 0.0171. Statistical analysis was performed using the Mann-Whitney test (* = p < 0.05). Receiver operating characteristic curve of benign renal masses versus RCCs with an area under the curve of 0.69 (95% confidence interval [CI]: 0.59–0.78). Optimal cut-off value of 3.2 mm⁻¹ was determined, yielding a sensitivity, specificity, positive predictive value, and negative predictive value of 91%, 56%, 91%, and 56%, respectively (95% CI: 0.59–0.78). (B) Optical coherence tomography boxplot of oncocytomas (N = 9) versus

RCCs (N = 78). Median μ OCT of oncocytoma (3.2 mm^{-1} , IQR: 2.68–3.95) was significantly lower than median μ OCT of RCC (4.3 mm^{-1} , IQR: 3.90–5.00) with $p = 0.0031$. Statistical analysis was performed using the Mann-Whitney test ($* = p < 0.05$). Receiver operating characteristic curve of oncocytomas versus RCCs with an area under the curve of 0.81 (95% CI: 0.73–0.91). An optimal cut-off value of 3.2 mm^{-1} was determined, yielding a sensitivity, specificity, positive predictive value, and negative predictive value of 91%, 67%, 95%, and 54%, respectively (95% CI: 0.73–0.91).

Table 3 – Patient characteristics of non-diagnostic renal mass biopsy (RMB) group (n = 20). In accordance with the PADUA score, tumours were interpreted as low (5–7 points), moderate (8–9 points), or high (10 points). RENAL Nephrometry Scores 4–6 were considered low complexity for resection, 7–9 were considered moderate complexity, and 10–12 were considered high complexity.

| Characteristics | Value |
|------------------------------|---------------|
| Mean age in yr (SD) | 59 (14) |
| Median size in cm (range) | 2.5 (1.2–7.9) |
| SRMs (%) | 18 (90%) |
| Male (%) | 15 (75%) |
| Mean PADUA (SD) | 9 (2) |
| Low 5–7 (%) | 5 (25%) |
| Moderate 8–9 (%) | 8 (40%) |
| High $10 \geq$ (%) | 7 (35%) |
| Mean RENAL (SD) | 7 (2) |
| Low 4–6 (%) | 7 (35%) |
| Moderate 7–9 (%) | 10 (50%) |
| High 10–12 (%) | 3 (15%) |
| <u>Treatment type</u> | |
| Open partial nephrectomy (%) | 3 (15%) |
| Open radical nephrectomy (%) | 0 (0%) |
| Lap partial nephrectomy (%) | 13 (65%) |
| Lap radical nephrectomy (%) | 3 (15%) |
| Cryoablation (%) | 1 (5%) |
| <u>Resection PA</u> | |
| ccRCC (%) | 11 (55%) |
| pRCC (%) | 1 (5%) |
| chrRCC (%) | 1 (5%) |
| other RCC (%) | 0 (0%) |
| Oncocytoma (%) | 0 (0%) |
| Cyst (%) | 3 (15%) |
| <u>other benign PA (%)</u> | 4 (20%) |
| Papillary adenoma (%) | 1 (5%) |
| Leiomyoma (%) | 1 (5%) |
| Granulation tissue (%) | 1 (5%) |
| Hemangioma (%) | 1 (5%) |
| CT-guided RMB | 0 (0%) |
| CEUS-guided RMB | 0 (0%) |
| US-guided RMB | 20 (100%) |

ccRCC = clear cell renal cell carcinoma; CEUS = contrast-enhanced ultrasound; chrRCC = chromophobe renal cell carcinoma; CT = computed tomography; Lap = laparoscopy; PA = pulmonary artery; other RCC = mucinous-spindle RCC; pRCC: papillary renal cell carcinoma; RMB = renal mass biopsy; SD = standard deviation; SRM = small renal masses; US = ultrasound.

Discussion

Our prospective interim analysis comparing the diagnostic accuracy of OCT and RMB provides evidence that OCT differentiates between benign RMs and RCC with a sensitivity and PPV of 91% (both) similar to RMB (100% and 99%, respectively). These figures are slightly higher in differentiating RCC from oncocytoma. However, OCT has a lower specificity and NPV than RMB in both comparative scenarios. As a counterpart, the diagnostic yield of OCT is higher than of RMB (99% vs 79%, respectively).

Two recent systematic reviews (SR) and meta-analysis on the accuracy of RMB highlighted a very high sensitivity (97.5–99.1%) and specificity (96.2–99.7%) with narrow CIs [9,10]. The sensitivity of the RMB and OCT mimics in our study the SR data. The high risk of selection bias and the use of different reference standards among studies included in the SRs is minimised in our setting by the prospective design and two well predefined standards for comparison, both including a second histological/pathological confirmation. It is recognised that when the reference standard at use is the surgical specimen, specificity may decrease justifying the slightly lower specificity of the RMB in our study.

The lower specificity and NPV of the OCT are justified by the quantitative character of the OCT measurement resulting in overlap (Fig. 3). The manner in which OCT data were analysed is a limitation. In our study, the five B-scans in which the average μ OCT were determined, and were randomly selected within the tumour region. Considering that one volumetric OCT scan pulls back over a trajectory of 54 mm (\sim 541 B-scans), of which approximately 70% is tumour region (\sim 380 B-scans), our analysis omits a large share of data without knowing if this could be of any diagnostic profit. RMs may contain necrosis, inflammation, or cystic areas, all holding very low μ OCT values that may explain our false-negative OCT scans. Oncocytomas may contain calcifications in 40% of the cases [19] leading to high μ OCT values contributing to false-positive results. In the future, optimisation of the technique should include automated OCT analysis comprising all B-scans within the tumour region, in order to detect the lowest μ OCT value and calculate the proportion of μ OCT value $<3.2 \text{ mm}^{-1}$. Automating analysis may improve NPV and specificity, reduce selection bias and interobserver variability, and even overcome the difficulties to determine subtype heterogeneity in a biopsy.

Overall median diagnostic yield of 86–92% is described for RMB in the previously mentioned meta-analysis. The characteristics of our cohort with a clinical median tumour size of 3.3 cm (range: 1.2–9.1 cm) and 63% of SRMs justify the 21% of NDBs. While in the upper range of the literature, these rates are not rare for small tumours RMBs. On the contrary, OCT exhibits an almost perfect diagnostic yield that minimises deceiving diagnostics or repeat biopsies and deserves to be paired with the lower specificity and NPV of the RMB.

When analysing the ND-RMB cohort, a median size of 2.5 cm (range: 1.2–7.9 cm) was noted and 90% were SRMs. Although no statistics were done due to the small sample size (N=20 patients), a trend for a smaller size in the ND-RMB group was evident and consistent with the negative correlation between size and diagnostic RMB [21,22]. Specifically, within the group of ND-RMBs, OCT reduces the ND rate by 70%, suggesting that a future OCT indication may be as an adjunct or first choice test in small or very SRMs to overcome the ND shortcoming related to size.

We acknowledge that the number of biopsy cores, operator expertise, as well as the ultrasound guidance, may have hindered the diagnostic yield of the RMB biopsy. The most recent literature on ultrasound-guided RMB shows ND rates between 13% and 19%, similar to ours [23,24], although no direct comparison exists with computed tomography-guidance. In this sense the gain hereby reported by the superior diagnostic yield of the OCT may not be reproducible in other settings.

ND-RMB rates also increase when strict definitions for a diagnostic RMB are contemplated. The extremely exclusive ND definition used in our study may be partially responsible for the low diagnostic yield of the RMB, responding otherwise to the expectations of physicians and patients in terms of defining an accurate diagnostic technique. Moreover, we cannot rule out that performing OCT before RMB might have increased the number of ND-RMBs by jeopardising the trajectory of the biopsy needle.

The use of two different reference standards (histopathology surgical specimen and histology of second ablation biopsy) may be considered a limitation by some. However, besides the fact that more than one reference standard is allowed in a diagnostic study [15], the concordance rate of tumour histology type between RMB and resection pathology is high, supporting the second RMB as the alternative reference standard.

An interesting observation is that the diagnostic RMB group merely contained RCCs and oncocytomas, while the diagnostic OCT group comprised of seven different types of tumour suggesting that the rarest benign pathology is reported as ND by RMB, resulting in two heterogeneous groups for RMB- and OCT accuracy analysis. The IQR for OCT accuracy analysis is broad, with a larger variability and overlap between benign and malignant masses (Fig. 3A). These findings are mainly due to the numerous different types of tumour and the small sample size per tumour type. Our data support the usefulness of the OCT at least at the same level of conventional RMB, and the balance between accuracy and diagnostic yield provides evidence to further proceed with the study until full sample inclusion. However, conclusions related to grade or subtype determination cannot yet be pronounced. Ultimately, if positive definitive data are available and validated, the position of the OCT in the practical diagnostic scenario of RM will be determined not only by accuracy parameters, but also by the technical expertise required—still considerable at the

moment—and its cost-effectiveness. Although out of the scope of the present analysis, a cost-effectiveness assessment is planned in our study.

Conclusions

Our interim analysis shows that OCT holds a higher diagnostic yield than conventional RMBs. OCT differentiates between benign and malignant RMs and between RCC and oncocytoma with similar sensitivity and PPV than RMB, although specificity and NPV of OCT are lower than that of RMB. These interim results support the continuation of our prospective study until final inclusion and the potential advantage of OCT in reducing ND results in a selected RM population. For the time being, efforts should focus on optimising OCT analysis to increase specificity and NPV.

References

1. Siegel RL, Miller KD, Jemal A. Cancer statistics 2016. *CA Cancer J Clin* 2016;66:7–30.
2. Nepple KG, Yang L, Grubb RL, Strobe SA. Population based analysis of the increasing incidence of kidney cancer in the United States: evaluation of age specific trends from 1975 to 2006. *J Urol* 2012; 187:32–8.
3. Ljungberg B, Bensalah K, Canfield S, et al. EAU guidelines on renal cell carcinoma: 2014 update. *Eur Urol* 2015;67:913–24.
4. Ljungberg B, Bensalah K, Bex A, et al. EAU guidelines on renal cell carcinoma. <http://uroweb.org/guideline/renal-cell-carcinoma/>.
5. Finelli A, Ismaila N, Bro B, et al. Management of small renal masses: american society of clinical oncology clinical practice guideline. *J Clin Oncol* 2017;35:668–80.
6. Johnson DC, Vukina J, Smith AB, et al. Preoperatively misclassified, surgically removed benign renal masses: a systematic review of surgical series and United States population level burden estimate. *J Urol* 2015;193:30–5.
7. Patel HD, Johnson MH, Pierorazio PM, et al. Diagnostic accuracy and risks of biopsy in the diagnosis of a renal mass suspicious for localised renal cell carcinoma: systematic review of the literature. *J Urol* 2016;195:1–8.
8. Blumenfeld AJ, Guru K, Fuchs GJ, Kim HL. Percutaneous biopsy of renal cell carcinoma underestimates nuclear grade. *Urology* 2010;76:610–3.
9. Divgi CR, Uzzo RG, Gatsonis C, et al. Positron emission tomography/ computed tomography identification of clear cell renal cell carcinoma: results from the REDECT trial. *J Clin Oncol* 2013;31:187–94.
10. Wagstaff PG, Ingels A, De Bruin DM, et al. Percutaneous needle based optical coherence tomography for the differentiation of renal masses: a pilot cohort percutaneous needle based optical coherence tomography for the differentiation of renal masses: a pilot cohort. *J Urol* 2015;195:1–8.
11. Su LM, Kuo J, Allan RW, et al. Fiber-optic confocal laser endomicroscopy of small renal masses: toward real-time optical diagnostic biopsy. *J Urol* 2016;195:486–92.
12. Optical biopsy to improve the diagnosis of kidney cancer. <https://clinicaltrials.gov/ct2/show/NCT02073110>.
13. Bossuyt PM, Reitsma JB, Bruns DE, et al. STARD 2015: an updated list of essential items for reporting diagnostic accuracy studies. *BMJ* 2015;351, h5527.
14. Muller BG, De Bruin DM, van den Bos W, et al. Prostate cancer diagnosis: the feasibility of needle-based optical coherence tomography. *J Med Imaging (Bellingham)* 2015;2, 37501.
15. Muller BG, de Bruin DM, Brandt MJ, et al. Prostate cancer diagnosis by optical coherence tomography: first results from a needle based optical platform for tissue sampling. *J Biophotonics* 2016;9: 490–8.
16. Muller BG, Swaan A, de Bruin DM, van den Bos W. Customized tool for validation of optical coherence tomography in differentiation of prostate cancer. *Technol Cancer Res Treat* 2017;16:57–65.
17. Barwari K, De Bruin DM, Faber DJ, Van Leeuwen TG, De Rosette JJ, Laguna MP. Differentiation between normal renal tissue and renal tumours using functional optical coherence tomography: a phase I in vivo human study. *BJU Int* 2012;110:415–20.
18. Wu J, Zhu Q, Zhu W, Chen W, Wang S. Comparative study of CT appearances in renal oncocytoma and chromophobe renal cell carcinoma. *Acta Radiol* 2015;57:500–6.
19. Marconi L, Dabestani S, Lam TB, et al. Systematic review and meta-analysis of diagnostic accuracy of percutaneous renal tumour biopsy. *Eur Urol* 2015;69:660–73.
20. Leveridge MJ, Finelli A, Kachura JR, et al. Outcomes of small renal mass needle core biopsy, non-diagnostic percutaneous biopsy, and the role of repeat biopsy. *Eur Urol* 2011;60:578–84.
21. Tsivian M, Rampersaud EN, Del Pilar Laguna Pes M, et al. Small renal mass biopsy – how, what and when: report from an international consensus panel. *BJU Int* 2014;113:854–63.
22. Park SY, Park BK, Kin CK, Kwon GY. Ultrasound-guided core biopsy of small renal masses: diagnostic rate and limitations. *J Vasc Interv Radiol* 2013;24(1):90–6.
23. Dave CN, Seifman B, Chennamsetty A, et al. Office-based Ultrasound-guided renal core biopsy is safe and efficacious in the management of Small Renal Masses. *Urology* 2017;102:26–30.

CHAPTER 3

3

Available ablation energies to treat cT1 renal cell cancer: Emerging technologies

PJ Zondervan, **M Buijs**, DM De Bruin, OM van Delden, KP Van Lienden

Abstract

Purpose An increasing interest in percutaneous ablation of renal tumours has been caused by the increasing incidence of SRMs, the trend toward minimally invasive nephron-sparing treatments, and the rapid development of local ablative technologies. In the era of shared decision making, patient preference for non-invasive treatments also leads to an increasing demand for image-guided ablation. Although some guidelines still reserve ablation for poor surgical candidates, indications may soon expand as evidence for the use of the two most validated local ablative techniques, cryoablation (CA) and radiofrequency ablation (RFA), is accumulating.

Methods A literature search was conducted to identify original research articles investigating the clinical outcomes of new emerging technologies, percutaneous MWA, percutaneous IRE, and SABR, in patients with primary cT1 localised renal cell cancer.

Results Due to the collaboration between experts in the field of biomedical engineering, urologists, interventional radiologists, and radiation oncologists, the improvements in ablation technologies have been evolving rapidly in the last decades. New emerging technologies such as microwave ablation (MWA), irreversible electroporation (IRE), and stereotactic ablative radiotherapy (SABR) seem to be getting ready for prime time.

Conclusion This topical paper describes the new emerging technologies for cT1 localised renal cell cancer and investigates how they compare to CA and RFA.

Introduction

With the increasing use of cross-sectional imaging, the subsequent rise in the incidence of SRMs, the evolution of new ablative technologies, and the aging population, percutaneous ablation of localised RCC in both fit and unfit patients is gaining more interest. The different guidelines advise to offer focal therapy only for the elderly or unfit patient, and until today the EAU guideline still does. The AUA guideline on the contrary is more progressive: They advise considering thermal ablation as an alternate approach for the management of cT1a renal masses < 3 cm in size [1, 2].

Focal therapy can be very attractive for patients for several reasons. Image-guided ablation is minimally invasive, allows for quick patient recovery, short hospital stay, fewer complications, and a smaller reduction in renal function as compared to surgery [3]. Cryoablation (CA) and radiofrequency ablation (RFA) are the most studied techniques to date with the longest outcomes reported and both are therefore advised as the designated modalities for SRMs in the various guidelines [1–4]. Yet, CA and RFA have their drawbacks and limitations. New competing emerging technologies such as microwave ablation (MWA), irreversible electroporation (IRE), and stereotactic ablative radiotherapy (SABR) are increasingly used, or under clinical investigation and appear promising.

The scope of this topical paper is to describe these emerging technologies and assess their potential roles as compared to the current standard techniques CA and RFA. A literature search was conducted to identify original research articles investigating the clinical outcomes of percutaneous MWA, percutaneous IRE, and SABR in patients with primary cT1 localised renal cell cancer.

Microwave ablation (MWA)

MWA is a thermal ablation technique, which uses electromagnetic waves through one or multiple antennas. The electromagnetic microwaves agitate water molecules in the surrounding tissue, producing friction and heat, causing cell death by coagulative necrosis [5].

One randomized controlled trial was published in 2012 comparing open partial nephrectomy (OPN), laparoscopic partial nephrectomy (LPN), open MWA, and laparoscopic MWA. Besides the fact that there was less blood loss, fewer complications, and less decline in postoperative renal function in favor of MWA, no difference was found in local recurrence-free survival with a median follow-up of 32 months. The major limitation of this study was the small number of inclusions: 48 underwent microwave ablation [6]. Regarding studies on percutaneous MWA, only case series have been published so far. Although concerns were raised initially about higher local recurrence and

complication rates for MWA in comparison to RFA and cryoablation, more recent data have shown that outcomes are comparable.

We selected original research studies with > 50 cases of percutaneous MWA in patients with cT1 localised RCC, and the results of seven studies are listed in Table 1 [7-13]. All of the studies were level of evidence 3, mainly retrospective observational studies.

MWA was performed with either ultrasound- or CT-guidance. The duration of ablation across the studies was mainly short (5–22.5 min), while the total procedure times took longer (22.5–45 min). The number of probes used ranged from 1 to 2, with one antenna used when tumour size < 2 cm, two antennas used when tumour size \geq 2 cm, and three antennas were used when tumour size was > 3 cm. With mean tumour sizes ranging from 2.3 cm to 3.2 cm, a low percentage of complications was reported (3.2–24.8%). Complications reported mainly consisted of hematuria, perirenal hematomas, or urinoma. The functional results after MWA showed only a decrease in renal function ranging from 1.1 to 8.4% across the studies.

Concerning oncological outcomes, the residual disease was reported ranging from 0 to 18.3%, and local recurrences ranged from 0 to 15.7%. With median follow-up periods ranging from 8 to 26 months, a low percentage of metastases was reported (0–2.9%). Overall survival ranged from 80.6% to 97%. DFS ranged from 87.9 to 97%, and CSS ranged from 97 to 100%. The major drawback is that any residual or recurrence during follow-up was mostly not proven with pathology but only on imaging. Another limitation of these studies is their retrospective nature, the relatively short follow-up, and the small tumour sizes. Although data on MWA seems promising, they have currently not reached the long-term outcomes of the thoroughly studied modalities using RFA and CA [1-3].

Potential advantages of MWA are shorter ablation and procedure times as compared with RFA and CA [15], less influence by the heat-sink effect of the blood circulation as compared to RFA [5,16] and the potential of MWA to achieve larger ablation zones than RFA (Table 4). In the future, MWA can potentially compete with CA for larger (cT1b) lesions. A potential disadvantage of MWA is the unpredictability of the ablation zone as compared to CA, but this may be resolved as technology improves.

Table 1: Summary of studies assessing percutaneous **Microwave Ablation** in localised cT1 Primary Renal Cell Carcinoma with > 50 cases.

| Study | Design | Level of evidence* | Technique | Number of Cases | Charlson Comorbidity Index | Tumour size Mean (cm) | Complications | Follow-Up (months) Median | Renal Function Decrease (%) | Residual Disease (%) | Local Recurrence (%) | Metastasis (%) | DFS (%) | OS (%) | CSS (%) |
|-------------------------------|---------------|--------------------|--------------------------------------|-----------------|----------------------------|-----------------------|-------------------------|--------------------------------|-----------------------------|---------------------------------------|--------------------------------------|----------------|-----------------|-----------------|-----------------|
| Li 2013 ⁷ | Prospective | 3 | US-guided, general anesthesia | 83 | NR | 3.2(+/- 1.6) | No severe complications | 26(3-74) CEUS and CT/MRI | NR | 18.3% CEUS, CT/MRI & Pathology proven | 8.4% CT/MRI, CEUS & Pathology proven | NR | NR | 96.4% | NR |
| Moreland 2014 ⁸ | Retrospective | 3 | US and CT-guided, general anesthesia | 53 | 3 (median) | 2.6(0.8-4.0) | 11.3% | 8(6-9) CT/MRI | 1.1% | No residual CT/MRI | No local recurrence CT/MRI | No metastasis | NR | NR | NR |
| Yu 2015 ⁹ | Retrospective | 3 | US-guided, Moderate sedation | 105 | 32% CCI>2 | 2.7(0.6-4.0) | 3.2% | 25.8(3.7-75.2) CEUS/CT/MRI | 3.2% | 13.3% CEUS/CT/MRI CT | 0.95% CT | 2.9% | 97% (5 years) | 82.6% (5 years) | 97% (5 years) |
| Dong 2016 ¹⁰ | Retrospective | 3 | US-guided, General anesthesia | 105 | NR | 2.9(0.6-6) | 24.8% | 25(1.13-93.23) CEUS and CT/MRI | 8.4% | NR | NR | NR | NR | NR | NR |
| Ierardi 2017 ¹¹ | Retrospective | 3 | CEUS, CT-guided or US-guided | 58 | NR | 2.36+/- 0.93 | 8.6% | 25.7 (3-72) CT | NR | 7% CT | 15.7% | NR | 87.9% (5 years) | 80.6% (5 years) | 96.5% (5 years) |
| Chan 2017 ¹² | Retrospective | 3 | CT-guided General anesthesia | 84 | NR | 2.5 | 4.8% | 24 CT | 7% | 8% CT | 3.8% | 2.4% | 95% (2 years) | 97% (2 years) | NR |
| Klapperich 2017 ¹³ | Retrospective | 3 | CT-guided General anesthesia | 96 | 3.6 +/- 1.5 (mean) | 2.6(1.2-4) | 11% | 15 (6-20) CT/MRI | 3.3% | No residual CT/MRI | 1% Pathology proven | No metastasis | NR (3 years) | 91% (3 years) | 100% (3 years) |

Residual tumour is defined as unablated residual tumour at initial follow-up imaging. Recurrence is defined as the appearance of tumour at the edge or in the ablation zone. DFS: Disease Free Survival, OS: Overall Survival, CSS: Cancer Specific Survival, NR: Not Reported. CCI: Charlson Comorbidity Index. *Level of evidence Oxford 2011 [14]

Irreversible electroporation (IRE)

IRE is a novel focal ablation technique based on the principle of electroporation of the cell membrane. By using ultrashort high-voltage electrical pulses, it causes nanopores in the cell membrane and consequently an increased cellular permeability causing cell death by apoptosis [17]. Although IRE is supposed to be a non-thermal ablation modality, a secondary rise in temperature has been shown [18]. Whether thermal damage accompanying the non-thermal damage is of any clinical relevance is still a matter of debate. A characteristic feature of IRE is that the lesions show a sharp demarcation zone between ablated and non-ablated tissue, making IRE particularly useful for planning more precise tumour ablation while preserving surrounding tissue. This can be an advantage in tumours in difficult, central locations or with a complex shape. Experience with IRE for renal tumours is limited. We selected original research studies for the safety and feasibility of IRE in primary RCC; the results of seven studies are listed in Table 2 [19-26].

All of the studies selected were level of evidence three or four (Table 2). Pech et al. demonstrated the feasibility and safety of IRE in 'an ablate and resect' clinical Phase 1 study in six patients [19], while Thompson performed IRE in ten patients [20]. Two retrospective studies performed by Trimmer [21] and Diehl [22] investigated the feasibility and short-term functional and oncologic outcomes after percutaneous IRE of 20 and 7 renal tumours, respectively. Wendler et al. have done extensive work on IRE in the IRENE study, in which patients underwent percutaneous CT-guided IRE and 4 weeks later radical or partial nephrectomy [23-25]. Canvasser et al. published about 42 renal tumours for which CT-guided IRE was performed [26]. Buijs et al. submitted a paper presenting the preliminary results of ten cases who underwent percutaneous IRE [27]. Percutaneous IRE was mainly performed CT-guided.

The numbers of needles used across all studies ranged from 3 to 4. If reported, procedure times ranged from 53 to 203 min, dependent on the tumour size and complexity of needle positioning and the shape needed to get the correct ablation zone. Mean tumour sizes ranged from 2.0 to 2.7 cm.

Mainly minor complications were reported and consisted of perinephric hematomas, post-procedural pain, and urinary retention. The major complications reported in two studies were transient gross hematuria in a hilar tumour and stage 1 acute kidney failure [22,27]. Renal function decline was minimal but was not always reported. Wendler et al. showed preservation of the urine collecting system: the urothelium showed signs of regeneration after 28 days, while the tumour and parenchyma showed clear necrosis and permanent cell destruction [25].

Follow-up was available in five of seven studies: the mean follow-up ranged from 6 to 25 months. A high but variable percentage of residual disease was reported (range 7–37.5%). Some of the authors suggested that residual tumour was most likely the result of probe malpositioning [21, 26, 27]. Wendler et al. have done extensive work on IRE in the IRENE study in which patients underwent percutaneous CT-guided IRE and 4 weeks later radical or partial nephrectomy. They demonstrated microscopic residual tumour cells in three out of eight biopsy-proven RCC cases. Although they questioned the clinical relevance of the microscopic tumour residues remaining in the non-viable ablation region, this still offers a possibility of repeat ablation in their opinion [23,24]. In their study, one patient showed local recurrence after 1 year. The studies that reported recurrences showed percentages ranging from 0 to 12.5% (Table 2).

Little is published concerning post-procedural imaging in these studies. Some showed a slightly larger hypodense area of the ablation zone, compared to the original tumour, and surrounding areas of enhancement in the perinephric fat [21]. Diehl et al. showed a progressive, significant decrease in treated tumour signal intensity on follow-up imaging, suggesting a treatment response rate of 100% at a mean follow-up of 6.4 months [22]. The limitation of some of the studies was the low number of biopsy-proven tumours treated [21,22,26].

A major drawback of IRE is the need for deep muscle relaxation and ECG synchronized pulsing during general anesthesia. The pulsatile application of electricity with a high current of around 20–50 A and a Voltage of 500–3000 V is a challenge for the anesthesiologist. It can give possible triggering of cardiac arrhythmias and severe muscle contractions or epileptic seizures when not synchronized with ECG or in the absence of neuromuscular blocking agents [28].

Although IRE seems feasible and safe, these results are preliminary and need technical improvement to ensure oncological results. Furthermore, the remaining questions are how do we know at what time the effect of IRE is successful, and how to interpret the imaging during follow-up, and what is the best imaging modality to use? All these questions are remaining and creating a need for further investigation. IRE is promising in selected cases (tumours near vital structures). The main disadvantages are the need for general anesthesia with deep muscle relaxation and long procedure times caused by the complex positioning of needles.

Table 2: Summary of studies assessing **Irreversible Electroporation (IRE)** in localised cT1 Primary Renal Cell Carcinoma.

| Study | Design | Level of evidence* | Technique | Number of Cases | Charlson Comorbidity Index | Tumour Size Mean | Complications | Follow-Up (months) | Renal Function Decrease | Residual Disease (%) | Local Recurrence (%) | Metastasis (%) | DFS (%) | OS (%) | CSS (%) |
|----------------------|-----------------------|--------------------|--|------------------|----------------------------|---------------------|---|--------------------------------|--------------------------------------|----------------------------------|--------------------------------|----------------|---------|--------|---------|
| Pech 2011 [19] | Phase I prospective | 3 | Open IRE, General ANS | 6 | NR | 2.7(range 2.0-3.9) | No complications | NR | NR | NR | NR | NR | NR | NR | NR |
| Thompson 2011 [20] | Prospective cohort | 3 | Percutaneous IRE US-, or CT-guided, General ANS | 10 (7 patients) | NR | 2.2 (range 1.6-3.1) | Cardiac arrhythmias, Partial ureteric obstruction | NR | NR | 2/7 residual at 3 months CT | NR | NR | NR | NR | NR |
| Trimmer 2015 [21] | Retrospective | 4 | Percutaneous CT-guided IRE, General ANS | 20 | NR | 2.2+/- 0.7 | Minor: Perinephric hematomas, pain, urinary retention | 1 year in 30% available CT/MRI | Creatinine -0.04 mg/dL after 6 weeks | 2/20 residual at 6 months CT/MRI | 1/20 recurrence at 1 yr CT/MRI | NR | NR | NR | NR |
| Diehl 2016 [22] | Retrospective | 4 | Percutaneous CT-guided IRE, General ANS | 7 (5 patients) | NR | 2.44 (1.5-3.8) | 2 minor complications: Hematuria, AKI | Mean 6.4 (3-11) | Creatinine -2.75 mL/min in 3 months | No residual MRI | NR | NR | NR | NR | NR |
| Wendler 2017 [23-25] | Phase 2a prospective, | 3 | Percutaneous CT-guided IRE, followed by resection, General ANS | 8 (7 patients) | Ranging 0-2 | Mean 2.2(1.5-3.9) | Hematuria 7/7, perirenal hematoma 2/7, pain 7/7 | Mean 25(15-36) | NR | 3/8 residual Pathology proven. | 1/8 recurrence | NR | NR | NR | NR |
| Canvasser 2017 [26] | Retrospective | 3 | Percutaneous CT-guided IRE, General ANS | 42 (41 patients) | NR | Mean 2.0(1.0-3.6) | 22% clavian grade I; perinephric hematoma, urinary retention, | Mean 22 (SD 12.4) | eGFR -6 mL/min | 3 failures/42 CT | 2/42 recurrence CT | NR | NR | NR | NR |

| Study | Design | Level of evidence* | Technique | Number of Cases | Charlson Comorbidity Index | Tumour Size Mean | Complications | Follow-Up (months) | Renal Function Decrease | Residual Disease (%) | Local Recurrence (%) | Metastasis (%) | DFS (%) | OS (%) | CSS (%) |
|-------------------------------------|---------------------|--------------------|---|-----------------|-------------------------------|------------------|--|--------------------|-----------------------------|----------------------|----------------------|----------------|---------|--------|---------|
| Buijs 2017 & 2018 [27 & submitted] | Prospective phase 2 | 3 | Percutaneous CT-guided IRE, General ANS | 10 | Mean CCI corrected for age: 7 | 2.2 (1.1-3.9) | 1x Grade 3: Obstruction ureter due to blood clot 1, 1x Grade 2: pyelonephritis 3x Grade 1: 1 perinefric hematoma, 1 painful miction, 1 hematuria | Mean 6 (3-12) | 2,6 % decrease after 1 year | 1/10 residual CT | No recurrences | NR | NR | NR | NR |

Residual is defined as enhancement reported at the first imaging after IRE in the ablation zone.

Recurrence is defined as new enhancement after a period of non-enhancement in or at the edge of the ablation zone.

AKI: Acute Kidney Insufficiency, US: Ultrasound, CT: Computed-Tomography, ANS: Anesthesia, DFS: Disease Free Survival, OS: Overall Survival, CSS: Cancer Specific Survival, NR: Not Reported. CCI: Charlson Comorbidity Index

*Level of evidence Oxford 2011 [14]

Stereotactic ablative radiotherapy (SABR)

Radiotherapy has been settled as a palliative treatment option in the armamentarium of the urologist in the metastasized setting for renal cell cancer. In the past, conventional radiotherapy had a limited role in the treatment of primary RCC largely due to the supposed radioresistance of RCC. In retrospect, this is mainly caused by the fact that too low doses were given. Due to the availability of new technologies that deliver high-dose stereotactic ablative radiotherapy, there has been a shift toward possible treatment options for primary RCC with curative intent. To date, SABR is mainly chosen as a treatment option for patients who are at high risk for anesthesia. Also, high-dose radiation seems to have an immunogenic effect in patients with RCC. The intense localised radiation provided by SABR would drive the release of antigens by tumours, inducing a tumour-specific T cell response [29].

We selected original research studies for primary RCC who underwent SABR with > 20 cases; besides a systematic review, only two studies were selected (Table 3). Siva et al. performed a systematic review on SABR for RCC with no tumour size restrictions in 2012. In total, ten publications describing 126 patients reported treatment with one to six fractions of SABR [30]. Recently the same group published a prospective study in which 37 patients with inoperable primary RCC underwent SABR. Tumours of < 5 cm received one single SABR of 26 Gy delivered, while in tumours \geq 5 cm 42 Gy was delivered in three fractions [31]. Furthermore, safety, efficacy, and survival were assessed in a multi-institutional setting in 223 patients from nine institutions. Both single-fraction SABR and multi-fraction SABR were given [32].

Tumour sizes ranged from 2.1 to 7.5 cm in the studies, representing not only cT1 but also cT2a tumours [31, 32]. Treatment-related toxicities were defined using Common Terminology Criteria of Adverse Events: severe toxicity ranging from 1.3 to 3.8% grade 3–4. Grade 1 toxicity ranged from 21.4 to 78%. Mainly fatigue, nausea, radiation dermatitis, and enteritis were reported. There was a relatively minor decrease in eGFR after SABR (5.5–11 mL/min) even when considering that tumour size was larger than that in the studies performing IRE of MWA. With a median follow-up ranging from median 9–57 months across the studies, the local control was excellent for patients with comorbid conditions, especially because the reported Charlson Comorbidity Index (CCI) was > 6 in 76% of the patients [31].

Single-fraction SABR was associated with better progression-free survival and cancer-specific survival. An interesting observation in the multi-institutional study was that patients receiving single-fraction SABR appear to be less likely to progress distantly or to die of cancer, something that authors did not fully understand [32]. A potential explanation

could be the enhanced abscopal effect of distant tumour cell eradication because of single-fraction irradiation. An alternative hypothesis is that during fractionated radiotherapy, circulating tumour cells are released in the circulation, which may still be viable after smaller doses of fractionated radiotherapy [32]. Concluding from these series, cT1 primary tumours, and even cT2 tumours, can be ablated in the unfit patient who is unable to undergo anesthesia with promising results.

Table3 Summary of studies assessing **Stereotactic Ablative Radiotherapy (SABR)** in localised Primary Renal Cell Carcinoma.

| Study | Design | Level of evidence* | Technique | Number of cases | Charlson Comorbidity Index | Tumour Size (cm) | Complications | Follow-Up (months) | Renal Function Decrease (%) | Residual Disease (%) | Local Recurrence (%) | Metastasis (%) | DFS (%) | OS (%) | CSS (%) |
|----------------|-------------------------------------|--------------------|--|-----------------|--------------------------------|------------------------------|---|--------------------------------|---|----------------------|--|----------------|--|---------------------------------|---------------------------------|
| Siva 2012 [30] | Systematic review | 2 | SABR 3, 4, and 5 fraction approaches used. Mostly used: 40Gy over 5 fractions. | 126 | NR | NR, but no size restrictions | Weighted rate of severe toxicity 3.8% Weighted rate of minor toxicity 21.4% Reported fatigue, nausea, radiation dermatitis and enteritis. | Median/mean ranged from 9-57.7 | NR | NR | Weighted local control 93.9% (range 84-100%) CT/MRI | NR | NR | NR | NR |
| Siva 2017 [31] | Prospective | 3 | Single 26Gy (for tumour size ≤5 cm) versus 3 fractions of 14Gy (for tumour size >5cm) SABR | 37 | 76% of the patients had CCI ≥6 | Median 4.8 (2.1-7.5) | 78% Grade 1-2 toxicity 3% Grade 3 toxicity Reported: Fatigue Chestwall pain Nausea | Median 24 | 11mL/min eGFR in 1 year | NR | 2 years Freedom for local progression 100% CT/MRI | NR | 2 years freedom from distant progression n 89% (CI 78-100) | 92% (2 years) | NR |
| Siva 2017 [32] | Multi-institutional pooled analysis | 3 | Both single-, and multifraction SABR included. Mean Gy 25 (14-70) | 223 | NR | Mean 4.36 (+/- 2.77) | 35.6% Grade 1-2 toxicity 1.3% Grade 3-4 toxicity Reported: Nausea Bowel toxicity | Median 30 | Mean decrease in eGFR 5.5 +/- 13.3 mL/min | NR | 1.4% Local control: 97.8% at 2 year and 4 year CT/MRI | 7.2% | PFS 77.4% (2 years) 65.4% (4 years) | 82.1% (2 years) 70.7% (4 years) | 95.7% (2 years) 91.9% (4 years) |

Local recurrence was defined using Response Evaluation Criteria in Solid Tumours, version 1.0.
Residual was not defined and not reported across all studies.

ANS: Anesthesia, DFS: Disease Free Survival, OS: Overall Survival, CSS: Cancer Specific Survival

NR: Not Reported. CCI: Charlson Comorbidity Index

*Level of evidence Oxford 2011 [14]

Table 4: Practical Pro & Cons of different types of percutaneous Ablation in cT1 RCC

| | Pro | Con |
|--------------|--|---|
| RFA | Single needle possible Coagulative properties Can be done under deep sedation, general anesthesia not mandatory Quicker than CA Good evidence available | Heat-sink effect No real-time monitoring of ablation zone Limited size of ablation zone Risk for urothelial damage |
| Cryoablation | Real-time monitoring of ablation zone possible Large ablation size possible Can be done under deep sedation, general anesthesia not mandatory Good evidence available | Heat-sink effect Multiple needles often required Risk for bleeding More time-consuming than RFA and MWA |
| MWA | Quicker than RFA and CA Higher temperatures than RFA Coagulative properties Can be done under deep sedation, general anesthesia not mandatory | No real-time monitoring of ablation zone Risk for urothelial damage Limited evidence available |
| IRE | Direct post-procedural monitoring possible No injury to surrounding structures Well suited for centrally located tumours | General anesthesia with muscle relaxation and EKG-triggering required Multiple parallel placed needles required More time-consuming than CA, RFA and MWA No sound evidence available |
| SABR | Truly non-invasive No anesthesia required No size limit | Renal function impairment No sound evidence available |

Considerations

In daily practice, it is challenging to decide which treatment modality is best for cT1 localised RCC. Due to the increasing incidence of SRMs and the aging population not fit for surgery, increased demand for ablations may be expected. In addition to this, we are confronted with the fit patient requesting for ablation, while for these patients partial nephrectomy is still advised. Following the paradigm of shared-decision making, it could be that even fitter patients will choose for focal therapy in the future. The AUA guideline advises considering thermal ablation as an alternate approach for the management of cT1a renal masses < 3 cm in sizes [2], while the EAU still advises offering CA or RFA only to elderly and/or comorbid patients with SRMs [1]. Both CA and RFA are the designated types of ablation advised by the different guidelines [2,3]. Whichever ablative technique is chosen, counseling should always include information regarding the likelihood of tumour persistence or local recurrence. Furthermore, a percutaneous approach is preferred over a surgical approach whenever feasible to minimize morbidity [2]. Recent studies on the

use of ablation in SRMs confirmed a decrease in the use of laparoscopic ablations [33]. Comparing RFA and CA, conflicting data regarding efficacy and oncological outcomes have been described [34-36]. In practice, RFA seems to be faster and cheaper, while CA takes more time, is more expensive, but can potentially be more precise in monitoring the ‘ice-ball’ during the procedure. Furthermore, CA seems to be more effective in cT1b tumours [37]. The majority of complications associated with ablation are minor. While CA has a higher chance for bleeding (up to 8%), RFA has fewer bleeding complications as a result of its coagulative effect (up to 4%) [38]. For RFA, the major complication is urothelial damage leading to urinary leak or possible stricture (up to 4.8%) [39]. On the contrary, CA produced less harm to the collecting system or ureter (1–2%) [40,41].

The advantage of CA is creating a large ‘ice-ball’, with multiple cryo-needles, in different sizes, which can be visualized during the procedure. This means real-time monitoring of the ablation is possible. RFA uses one or more probes, but the presumed ‘fire-ball’ cannot be visualized on CT during the procedure.

With the evolution of new technologies, MWA, IRE, and SABR have made their entrance. While the body of evidence for MWA in renal masses is still limited, it could have some potential advantages in ablating larger lesions possibly even in a shorter time compared to RFA or CA [15]. As oncological data will mature in the coming years for MWA, they probably will become comparable to RFA and CA. While MWA is routinely used for SRM to date, IRE is still under investigation. IRE has proven to be feasible and safe in small series but is by far not settled, and further research has to be done in the field. Even when IRE is to be introduced in clinical practice, it will solely be in selected cases: in centrally located tumours or when vital structures are very close. Patients are required to undergo general anesthesia with muscle relaxation.

SABR is safe with low toxicity, has no definite size limitation, is not limited by tumour location, and is thought to promote anti-tumour immunity. Even though the optimal dose and fractionation regimens are not yet definite, it could be the sole solution in some selected cases [31, 32]. The immunogenic effect seen in SABR is also suggested in other ablation types and the combination with immunotherapy such as immune checkpoint inhibition could be promising in the future.⁴² Further research in dose fractionation and oncological long-term follow-up in SABR has to settle the treatment type for SRMs.

The dilemma concerning which type of ablation should be used in selected cases is still unresolved. The type of ablation chosen for a cT1 renal cell cancer mostly depends on the experience and expertise of the urologist and interventional radiologist, and the available resources. The individual characteristics of each kidney tumour are different and make it necessary to adapt the type of ablation to this particular tumour. Proper case selection is very important when considering the use of ablative therapies. Furthermore, the condition

of the patient is vital in deciding the possibilities for the type of ablation. The percutaneous approach is preferred over the laparoscopic because of fewer complications and its minimal invasiveness [44]. The different types of ablation available offer a solution to give direction to this decision-making process when considering their pros and cons when evidence is more sound (Table 4, Fig. 1).

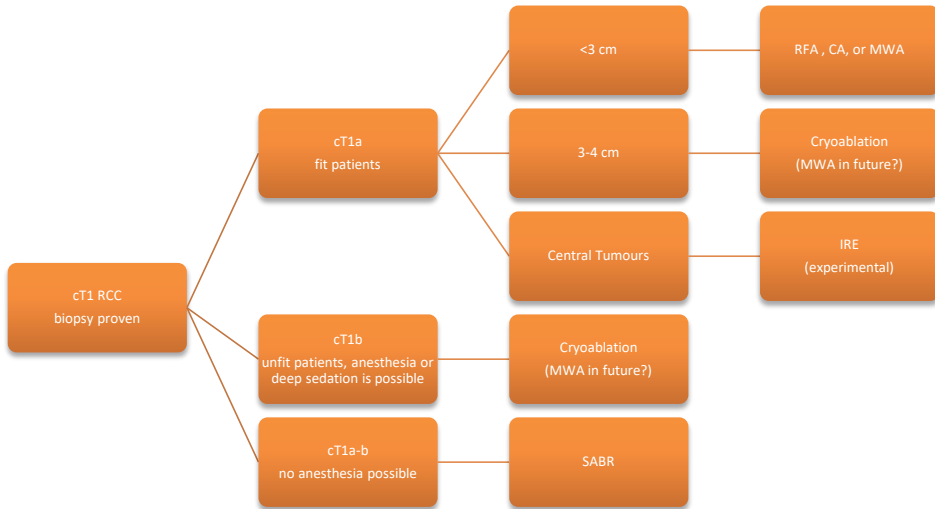


Fig. 1 Flowchart for guiding decision making for type of ablation in cT1 localised RCC. For SRMs in fit patient, different types of ablation are possible (CA, RFA, MWA, IRE in selected cases), while for cT1a- b tumours in unfit patients CA or SABR is advised. SRMs < 3 cm are expected to be in the favorable prognostic group [43], for this reason a cut-off value of tumour size 3 can be used, as bigger lesions and cT1b lesions are best treated with CA.³⁷

Conclusion

Image-guided percutaneous ablation for cT1 localised renal cell cancer has become a readily available and competing alternative for partial nephrectomy. Due to an expected increase in SRMs, an aging population, awareness of shared- decision making, patient preference, and rapid technical improvements, ablative therapy will become much more relevant in the near future. Image-guided ablative therapy is a good alternative for SRMs in fit patients but seems also a good solution in cT1b tumours in the unfit patient. As new emerging technologies are rising to compete with their historical counter partners, we will need to carefully evaluate them. As MWA, IRE, and SABR is introduced, the near future will learn if these new emerging technologies are ready for prime time and how they will eventually settle in the palette of image-guided ablation for cT1 localised renal cell carcinoma.

References

1. Ljungberg B, Bensalah K, Canfield S, Dabestani S, Hofmann F, Hora M, Kuczyk MA, Lam T, Marconi L, Merseburger A, Mulders P, Powles T, Staehler M, Volp A, Bex A (2015) EAU guidelines on renal cell carcinoma: 2014 update. *Eur Urol* 67:913–924
2. Campbell S, Uzzo RG, Allaf ME, Bass EB, Cadeddu JA, Chang A, Clark PE, Davis BJ, Derweesh IH, Giambarrresi L, Gervai DA, Hu SL, Lane BR, Leibovich BC, Pierorazio PM (2017) Renal mass and localised renal cancer: AUA guideline. *J Urol* 198:520–529.
3. Rivero JR, De la Cerda J, Wang H, Liss MA, Farrell AM, Rodriquez R, Suri R, Kaushik D (2018) Partial nephrectomy versus thermal ablation for clinical stage T1 Renal masses: systematic review and meta-analysis of more than 3900 patients. *J Vasc Interv Radiol* Jan 29(1):18–29
4. NCCN clinical practical guidelines in oncology, kidney cancer. Version 4.2018. https://www.nccn.org/professionals/physician_gls/pdf/kidney_blocks.pdf
5. Simon CJ, Dupuy DE, Mayo-Smith WW (2005) Microwave ablation: principles and applications. *Radiographics* 25(suppl 1):S69–S83
6. Guan W, Bai J, Liu J, Wang S, Zhuang Q, Ye Z, Hu Z (2012) Microwave ablation versus partial nephrectomy for small renal tumours: intermediate-term results. *J of Surg Oncol* 106:316–321
7. Li X, Liang P, Yu J et al (2013) Role of contrast-enhanced ultrasound in evaluating the efficiency of ultrasound guided percutaneous guided microwave ablation in patients with renal cell carcinoma. *Radiol Oncol* 47(4):398–404
8. Moreland AJ, Ziemlewicz TJ, Best S et al (2014) High-powered microwave ablation of T1a renal cell carcinoma: safety and initial clinical evaluation. *J Endourol* 28(9):1046–1052
9. Yu J, Zhang P, Liang G et al (2015) Midterm Results of percutaneous microwave ablation under ultrasound guidance versus retroperineal laparoscopic radical nephrectomy for small renal cell carcinoma. *Abdom Imaging* 40:3248–3256
10. Dong X, Li X, Yu J et al (2016) Complications of ultrasound-guided percutaneous microwave ablation of renal cell carcinoma. *OncoTargets Ther* 9:5903–5909
11. Ierardi AM, Puliti A, Angileri SA et al (2017) Microwave ablation of malignant renal tumours: intermediate-term results and usefulness of RENAL and mRENAL scores for predicting outcomes and complications. *Med Oncol* 34(97):1–9
12. Chan P, Velasco S, Vesselle G et al (2017) Percutaneous microwave ablation of renal cancers under CT guidance: safety and efficacy with a 2-year follow-up. *Clin Radiol* 72(9):786–792
13. Klapperich ME, Abel EJ, Ziemlewicz TJ et al (2017) Effect of tumour complexity and technique on efficacy and complications after percutaneous microwave ablation of stage 1a renal cell carcinoma: a single-center. Retrospective Study. *Radiol* 284(1):272–280
14. OCEBM Levels of Evidence Working Group, “The Oxford 2011 Levels of Evidence”. Oxford Centre for Evidence-Based Medicine. <https://www.cebm.net/2016/05/ocebml-levels-of-evidence/>
15. Zhou W, Arellano RS (2018) Thermal ablation of cT1 Renal cell carcinoma: a comparative assessment of technical performance, procedural outcome, and safety of microwave ablation, radiofrequency, and cryoablation. *J Vasc Interv Radiol* 29(7):943–951
16. Brace CL (2010) Microwave tissue ablation: biophysics, technology and applications. *Crit Rev Biomed Eng* 38(1):65–78
17. Davalos RV, Mir LM, Rubinsky B (2005) Tissue ablation with irreversible electroporation. *Ann Biomed Eng* 33(2):223–231
18. Wagstaff PGK, de Bruin DM, van den Bos et al (2014) Irreversible electroporation of the porcine kidney: temperature development and distribution. *Urol Oncol* 33:168.e1–168.e7
19. Pech M, Janitzky A, Wendler JJ, Strang C, Blaschke S, Dudeck O, Ricke J, Liehr UB (2011) Irreversible electroporation of renal cell carcinoma: a first-in-man phase I clinical study. *Cardiovasc Intervent Radiol* 34:132–138
20. Thompson KR, Cheung W, Ellis SJ, Federman D, Kavoudias H, Loarder-Oliver D, Roberts S, Evans P, Ball C, Haydon A (2011) Investigation of the safety of irreversible electroporation in humans. *J Vasc Interv Radiol* 22:611–621
21. Trimmer CK, Koshla A, Morgan M, Stephenson SL, Ozayar A, Cadeddu J (2015) Minimally invasive percutaneous treatment of small renal tumours with irreversible electroporation: a single center experience. *J Vasc Interv Radiol* 26(10):1465–1471

22. Diehl SJ, Rathmann N, Kostrzewa M, Manuel Ritter, Smakic A, Schoenberg SO, Kriegmair MC (2016) Irreversible electroporation for surgical renal masses in solitary kidneys: short-term interventional and functional outcome. *J Vasc Radiol* 27:1407–1413
23. Wendler JJ, Porsch M, Nitschke S, Köllermann J, Siedentopf S, Pech M, Fischback F, Ricke J, Schostak M, Liehr UB (2015) A prospective phase 2a pilot investigating focal percutaneous irreversible electroporation (IRE) ablation by nanoknife in patients with localised renal cell carcinoma (RCC) with delayed interval tumour resection (IRENE trial). *Contemp Clin Trials* 43:10–19
24. Wendler JJ, Pech M, Fischenback F, Jürgens B, Friebe B, Baumunk D, Porsch M, Blaschke S, Schindele D, Siedentopf S, Ricke J, Schostak M, Köllermann J, Liehr UB (2018) Initial assessment of the efficacy of irreversible electroporation (IRE) in the focal treatment of localised renal cell carcinoma (RCC) with delayed- interval kidney tumour resection (IRENE trial—an ablate-and- resect pilot study). *Urology* 114:224–232
25. Wendler JJ, Pech M, Köllermann J, Friebe B, Siedentopf S, Blaschke S, Schindele D, Porsch M, Baumunk D, Jürgens J, Fischback F, Ricke J, Schostak M, Böhm M, Liehr UB (2017) Upper-urinary-tract effects after irreversible electroporation (IRE) of human localised renal-cell carcinoma (RCC) in the IRENE pilot phase 2a ablate-and-resect Study. *Cardiovas Intervent radiol* accepted september 2017
26. Canvasser NE, Sorokin I, Lay AH, Morgan MSC, Ozayar A, Trimmer C, Cadeddu JA (2017) Irreversible electroporation of small renal masses: suboptimal oncologic efficacy in an early series. *World J Urol* 35:1549–1555
27. Buijs M, Van Lienden KP, Wagstaff PGK (2017) Irreversible electroporation for the ablation of renal cell carcinoma: a prospective, human, in vivo study protocol (IDEAL phase 2b). *JMIR Res Protoc* 6(2):e21
28. Nielsen K, Scheffer HJ, Vieveen JM, van Tilborg AJM, Meijer S, van Kuijk C, van der Tol MP, Meijerink MR, Bouwman RA (2014) Anaesthetic management during open and percutaneous irreversible electroporation. *Br J Anaesth* 113(6):985–992
29. Siva S, Kothari G, Muacevic A et al (2017) Radiotherapy for renal cell carcinoma: renaissance of an overlooked approach. *Nat Rev* 14(9):549–563
30. Siva S, Pham D, Gill S et al (2012) A systematic review of stereotactic radiotherapy ablation for primary renal cell carcinoma. *BJUI* 110:E737–E743
31. Siva S, Pham D, Kron T, Bressel M, Lam J, Tan TH, Chesson B, Shaw M, Chander S, Gill S, Brook NR, Lawrentschuk N, Murphy DG, Foroudi F (2017) Stereotactic ablative body radiotherapy for inoperable primary kidney cancer: a prospective clinical trial. *BJUI* 120:623–630
32. Siva S, Louie AV, Warner A, Muacevic A, Gandhidasan S, Ponsky L, Ellis R, Kaplan I, Mahadevan A, Chu W, Swaminath A, Onishi H, Teh B, Correa RJ, Lo SS, Staehler M (2018) Pooled analysis of stereotactic ablative radiotherapy for primary renal cell carcinoma: a report from the international radiosurgery oncology consortium for kidney (IROCK). *Cancer* 124(5):934–942
33. Mohapatra A, Potretzke AM, Weaver J et al (2017) Trends in managements of small renal masses: a survey of members of the endourological society. *J Kidney Cancer and VHL* 4(3):10–19
34. Kavoussi N, Canvasser N, Cadeddu J et al (2016) Ablative therapies for the treatment of small renal masses: a review of different modalities and outcomes. *Curr Urol Rep* 17(8):59
35. Atwell TD et al (2013) Percutaneous ablation of renal masses measuring 3.0 cm and smaller: comparative local control and complications after radiofrequency ablation and cryoablation. *AJR Am J Roengenol* 200:461–466
36. Samarasekera D et al (2013) Percutaneous radiofrequency ablation versus percutaneous cryoablation: long-term outcomes following ablation for renal cell carcinoma. *J Urol* 189:e737
37. Houston Thompson R, Atwell T, Schmit G et al (2015) Comparison of partial nephrectomy and percutaneous ablation for cT1 renal masses. *Eur Urol* 67:252–259
38. Atwell TD, Carter RE, Schmit GD et al (2012) Complications following 573 percutaneous renal radiofrequency and cryoablation procedures. *J Vasc Interv Radiol* 23(1):48–54
39. Balageas P, Cornelis F, Le Bras Y et al (2013) Ten year experience of percutaneous image guided radiofrequency ablation of malignant renal tumours in high-risk patients. *Eur Radiol* 23(7):1925–1932
40. Zargar H, Atwell TD, Cadeddu J et al (2016) Cryoablation for small renal masses: selection criteria, complications, and functional and oncological results. *Eur Urol* 69(1):116–128
41. Breen DJ, Bryant TJ, Abbas A et al (2013) Percutaneous cryoablation of renal tumours: outcomes from 171 tumours in 147 patients. *BJU Int* 112(6):758–765

42. Hickey RM, Kulik LM, Nimeiri H et al (2017) Immuno-oncology and its opportunities for interventional radiologists: immune checkpoint inhibition and potential synergies with interventional oncology procedures. *J Vasc Interv Radiol* 28:1487–1494
43. Bhindi B, Lose LM, Mason RJ et al (2017) Are we using the best tumour size cut-points for renal cell carcinoma staging? *Urology* 109:121–126
44. Aboumarkzouk OM, Ismail M, Breen DJ et al (2018) Laparoscopic vs percutaneous cryotherapy for renal tumours: a systematic review and meta-analysis. *J Endourol* 32(3):177–183

CHAPTER 4



Irreversible electroporation: State of the art

PGK Wagstaff, **M Buijs**, W van den Bos, DM de Bruin, PJ Zondervan, JJMCH de la Rosette, MP Laguna Pes

Abstract:

The field of focal ablative therapy for the treatment of cancer is characterised by an abundance of thermal ablative techniques that provide a minimally invasive treatment option in selected tumours. However, the unselective destruction inflicted by thermal ablation modalities can result in damage to vital structures in the vicinity of the tumour. Furthermore, the efficacy of thermal ablation intensity can be impaired due to thermal sink caused by large blood vessels in the proximity of the tumour. Irreversible electroporation (IRE) is a novel ablation modality based on the principle of electroporation or electropermeabilization, in which electric pulses are used to create nanoscale defects in the cell membrane. In theory, IRE has the potential of overcoming the aforementioned limitations of thermal ablation techniques. This review provides a description of the principle of IRE, combined with an overview of in vivo research performed to date in the liver, pancreas, kidney, and prostate.

Introduction

The past decades have yielded significant developments in the field of focal ablative therapy for the treatment of primary tumours or organ-confined distant metastases. Among the practiced techniques are cryoablation, radiofrequency ablation (RFA), microwave ablation, and high-intensity focused ultrasonography. These thermal ablative techniques provide a minimally invasive treatment option in selected tumours in multiple organs such as the liver, lung, pancreas, kidney, and prostate [1–6].

Focal tumour ablation requires precisely dosed and accurate targeting of the tissue to be ablated while preserving surrounding healthy tissues and vital structures such as blood vessels, nerves, and neighboring organs [7,8]. The unselective destruction inflicted by thermal ablation modalities can result in damage to vital structures in the vicinity of the tumour. Furthermore, the efficacy of thermal ablation intensity can be impaired due to “thermal sink”. The proximity of large vessels, bile ducts, or the renal collecting system can cause thermal fluctuations, leading to inconsistent ablation results [4,8].

Irreversible electroporation (IRE) is a novel ablation modality with the potential of overcoming the aforesaid limitations of thermal ablation techniques. This review describes the principle of IRE, combined with an overview of in vivo research performed to date in tumours of the liver, pancreas, kidney, and prostate (Table 1). It has to be noted that the development of IRE is simultaneous to that of related techniques based on the same principle, such as electrochemotherapy (ECT), which combines electroporation with chemotherapy [9,10]. This review is confined to IRE as an ablation technique and does not go into detail on ECT.

Evidence acquisition

For this nonsystematic review, we performed a literature search of PubMed for original and review articles written in English using the search terms “Irreversible Electroporation”, combined with “liver”, “pancreas”, “kidney”, and “prostate”. This search resulted in 203 hits, from which we selected 20 articles based on relevant contributions to clinical evaluation of IRE (Table 1). Case reports were excluded. The selected articles had been published from 2011 to 2015, and 40% of the papers were published in 2015. Levels of evidence were assigned to the selected articles according to the Oxford Centre for Evidence-based Medicine’s “Levels of Evidence” [11]. The reference lists of the selected papers were scrutinized for additional relevant articles (yielding 41 articles).

Table 1 Overview of clinical trials focusing on IRE in liver, pancreatic, kidney, and prostate tumours

| Author, year | Organ | Number of IRE ablations | FU method | FU term | Findings | Type of study | Level of evidence |
|---------------------------|--------|-------------------------|----------------------------|-------------------------|---|----------------------|-------------------|
| Thomson et al, 2011 [36] | Liver | 63 | CT | Directly, 1 mo and 3 mo | in humans, IRE of liver and kidney tumours is safe if pulses are synchronized with ECG | Prospective cohort | 4 |
| Kingham et al, 2012 [38] | Kidney | 10 | | | | | |
| | Liver | 65 | CT/MRI | Directly, 1/3/6 mo | IRE is safe for the treatment of liver tumours; one persistence and one recurrence observed | Retrospective cohort | 4 |
| Cannon et al, 2013 [40] | Liver | 48 | CT/MRI/PET, tumour markers | Directly, 3-monthly | initial ablation success in 100% of cases, local recurrence-free survival 60% at 1 year; nine low-grade AEs, all resolved | Prospective cohort | 4 |
| Silk et al 2014 [61] | Liver | 15 | CT | Directly, 1–2 mo | Local tumour recurrence in six of eleven patients (55%); one biliary stent placed, possibly due to contact of IRE electrode with bile duct | Retrospective cohort | 4 |
| Cheung et al, 2013 [41] | Liver | 18 | CT | 1 mo, 3-monthly | Complete ablation in 13 (72%) lesions; no recurrences at mean FU of 18 mo; no serious complications | Prospective cohort | 4 |
| Scheffer et al, 2014 [62] | Liver | 10 | Resection | Ablation– resection | Macroscopic vitality staining, nonviable IRE lesion covering complete tumour in eight of ten patients; microscopically, irreversible cell damage in the tumour-free margin of all specimens | Prospective cohort | 4 |

| Author, year | Organ | Number of IRE ablations | FU method | FU term | Findings | Type of study | Level of evidence |
|----------------------------|----------|-------------------------|---------------|--|--|----------------------|-------------------|
| Cheng et al, 2015 [42] | Liver | 6 | CT, resection | 1 mo, 3-monthly until liver transplant | imaging: complete response in all cases; pathology: five lesions with complete necrosis, one lesion with viable tumour cells <5% | Retrospective cohort | 4 |
| Niessen et al, 2015 [39] | Liver | 79 | CT/MRI | Directly, 1.5/3/6 mo | incomplete ablation in two cases; FU of 6 mo in 48 patients, 14 (29%) of whom showed local recurrence; risk factors for local recurrence: tumour volume and tumour type | Prospective cohort | 4 |
| Sugimoto et al, 2015 [37] | Liver | 6 | CEUS/CT/MRI | Directly, 1 wk, 1 mo, 3-monthly | Complete IRE ablation in five (83%) tumours; residual tumour in one case at 1 week; no serious complications | Prospective cohort | 4 |
| Narayanan et al, 2012 [45] | Pancreas | 15 | CT | Directly, 1 day, monthly | CT directly and 24 hours post-IRE showed patent vasculature in all cases; no severe complications or mortality occurred; grade 2 pancreatitis in one case, resolving spontaneously | Retrospective cohort | 4 |
| Paiella et al, 2015 [46] | Pancreas | 10 | CT | Directly, 1/2/3 mo | All cases treated successfully; overall survival: 7.5 mo; complications: pancreatic abscess (n=1) and pancreaticoduodenal fistula (n=1) | Prospective cohort | 4 |
| Martin et al, 2012 [47] | Pancreas | 27 | CT/MRI /PET | Discharge, 3-monthly | At 90 days, no signs of local recurrence in all patients; 17 possible IRE-related complications; grade 4/5 complications: bile leak (n=2) and portal vein thrombosis (n=2); one mortality at 70 days | Prospective cohort | 4 |

| Author, year | Organ | Number of IRE ablations | FU method | FU term | Findings | Type of study | Level of evidence |
|------------------------------|----------|-------------------------|------------|----------------------|---|----------------------|-------------------|
| Martin et al, 2013 [48] | Pancreas | 54 | CT/MRI/PET | Discharge, 3-monthly | improvement IRE vs standard therapy: local PFS 14 vs 6 mo, distant PFS 15 vs 9 mo; and overall survival of 20 vs 13 mo; a total of 57 AEs: bile leakage (n=2) and duodenal leakage (n=2); one mortality occurred | Prospective cohort | 4 |
| Martin et al, 2015 [49] | Pancreas | 200 | CT/MRI/PET | Discharge, 3-monthly | Median overall survival 24.9 mo (range: 4.9–85 mo); complication rate of 37% (median: grade 2, range: grades 1–5); local recurrence in six (3%) patients | Prospective cohort | 4 |
| Pech et al, 2011[18] | Kidney | 6 | Resection | Ablation– resection | No changes in laboratory blood results or cardiac function; pathology (H&E), swelling of the ablated cells but no actual dead cells; no viability staining performed | Prospective cohort | 4 |
| Trimmer et al, 2015 [52] | Kidney | 20 | CT/MRI | 6 wk, 6 mo, 10 mo | Residual tumour at 6 wk in two of 20 cases; 6 mo FU available in 15 cases, no signs of recurrence; 1 y FU available in six cases, recurrence in one case; no major complications observed | Retrospective cohort | 4 |
| wendler et al, 2015 [53] | Kidney | 3 | Resection | 4 wk | IRE lesions covering all tumours completely, no residual tumour in margins; very small tumour residues of unclear malignancy observed within the ablation zone, requiring additional investigation using viability staining | Prospective cohort | 4 |
| Onik and Rubinsky, 2010 [58] | Prostate | 16 | Biopsy | 3 wk | All patients remained continent and potent patients remained so after IRE; no evidence of cancer in ablated area in 15 cases; one patient refused biopsies | Prospective cohort | 4 |

| Author, year | Organ | Number of IRE ablations | FU method | FU term | Findings | Type of study | Level of evidence |
|------------------------------|----------|-------------------------|-----------|---------------|--|----------------------|-------------------|
| valerio et al, 2014 [59] | Prostate | 34 | MRI | 1 wk and 6 mo | Suspicion of residual disease in six patients, confirmed with biopsies in one case; complications: urinary retention (n=2), debris/ hematuria (n=6), dysuria (n=5),urinary tract infection (n=5) | Retrospective cohort | 4 |
| van den Bos et al, 2015 [29] | Prostate | 16 | Resection | 4 wk | Complete ablation of tissue within the IRE electrode configuration, no skip lesions; IRE ablation zone 2.5–2.9 times larger than IRE needle configuration | Prospective cohort | 4 |

Notes: Levels of evidence assigned according to *Oxford Centre for Evidence-based Medicine* – Levels of evidence (March 2009); Howick et al (<http://www.cebm.net/?o=1025>).³¹

Abbreviations: Ae, adverse event; CT, computed tomography; ECG, electrocardiogram; FU, follow-up; H&E, hematoxylin and eosin; IRE, irreversible electroporation; MRI, magnetic resonance imaging; mo, months; PET, positron emission tomography; PFS, progression-free survival; wk, weeks; y, years; CEUS, contrast-enhanced ultrasound.

IRE principle

IRE is based on the principle of electroporation or electropermeabilization, in which electric pulses are used to create nanoscale defects in the cell membrane. These defects, termed “nanopores” or “conductive pores”, permeate the cell membrane, permitting molecules to pass into the targeted cells [8,12,13]. Nanopore formation can be temporary (reversible electroporation), as used in the fields of gene transfection or ECT [9,14,15]. Above a certain electrical threshold, the “nanopores” become permanent, causing cell death due to the inability to maintain homeostasis (IRE), as used in the food industry for sterilization and, more recently, in medicine for tumour ablation [16–18]. The occurrence of IRE was initially considered an unwanted treatment side effect during reversible electroporation procedures. In the past decade, however, the focus has turned to IRE as an ablation modality, resulting in the development of a commercially available IRE console designed specifically for tissue ablation [8,19].

The presence of nanopores following the delivery of electrical pulses has been visualized using electron microscopy, showing temporary and permanent nanopores [12,13]. The pulse-induced disturbances of the cells as a whole were studied using fluorescence microscopy [20,21]. Because direct visualization of cell poration is difficult to follow over time, researchers have used indirect measures to quantify the effect of electroporation, such as changes in electrical conductivity or the uptake of dye following the admission of electrical pulses [22,23]. However, visualization of membrane pores following the application of pulses does not definitively prove them to be the cause of IRE-induced cell death. Furthermore, *ex vivo* and animal research results have shown that IRE using the current clinically practiced treatment settings causes a substantial increase in temperature in the targeted tissue [24–26]. This secondary temperature development raises the question regarding the extent of the IRE effect that is caused by the temperature change versus that due to cell membrane poration. Therefore, as the field of tumour ablation using IRE progresses at a rapid pace, its underlying mechanism remains a subject of debate [16,24,27].

If we assume instead of temperature development, the theory of cell membrane poration, IRE is not dependent on thermal energy and is therefore not influenced by “thermal sink”, promising consistent results in the vicinity of large vessels or the renal collecting system. Furthermore, IRE should be defined so as to limit damage to the cell membrane, spare tissue architecture, and minimize damage to blood vessels, nerves, and the renal collecting system [28]. IRE lesions show a sharp demarcation between ablated and nonablated tissues, whereas thermal ablation techniques show a transitional zone of partially damaged tissue wherein insufficient temperatures were reached for definitive ablation [29]. This indicates that IRE ablation boundaries can potentially be planned more precisely compared to conventional techniques.

IRE device and procedure

The first, and at the time of writing only, commercially available IRE console for clinical use in tissue ablation is the NanoKnife™, also registered as the HVP-01 Electroporation System (Angiodynamics Inc, Queensbury, NY, USA). The system carries a CE mark and has US Food and Drug Administration approval for soft tissue ablation. The NanoKnife™ platform consists of a low-energy direct current generator interfaced with a computer system equipped with user-friendly treatment planning software (Fig. 1A and B). The system has the capability of connecting up to six monopolar needle electrodes, 16 G in diameter, and covered in a retractable insulation sheath, allowing for the adjustment of the active tip length (Fig. 1C). Bipolar IRE electrodes are available; however, these are not commonly used after early animal research showed bipolar IRE to result in lower ablation volumes, combined with a higher risk of collateral damage [30].

Further parameters to be adjusted in IRE ablation are Voltage, pulse number, pulse length, electrode number, and electrode spacing. The parameters can be entered into the IRE console, which subsequently generates a two-dimensional (2D) representation of the ablation shape, perpendicular to the direction of the inserted needle electrodes (Fig. 1B). Knowledge on how to tailor IRE settings to specific tissue/tumour types remains limited. Research into the simulation of the IRE ablation zone, in order to aid IRE ablation planning, is underway but has not yet yielded accurate results [31]. Except for slight variations, IRE settings are similar for most research into tumour ablation. Currently practiced IRE settings for tumour ablation are Voltage 1,500 V/cm, 70–90 pulses of 70–90 μ s, electrode spacing 1.5–2 cm, and active electrode tip length 1–2.5 cm.

To prevent complications as a result of the administration of high-intensity electrical pulses, two main precautions are generally taken during IRE procedures. First, to prevent severe muscle contractions, IRE procedures take place under general anesthesia with additional muscle relaxation [32]. Second, the administered IRE pulses could potentially cause cardiac arrhythmia, depending on the distance of the ablation spot to the heart [36]. Therefore, synchronization of the IRE pulses with the cardiac rhythm is advised. A synchronization device can be interfaced to the IRE console to ensure accurate pulse timing (Fig. 1D). The IRE electrodes are positioned under computed tomography (CT) and/or ultrasound guidance in a similar manner to RFA or cryoablation probes. To guarantee an equal distribution of the electrical field, the electrodes need to be placed exactly parallel. External spacers are available to interlock the electrodes (Fig. 1C). In prostate ablations, a brachytherapy grid can be used for needle targeting and fixation [29].

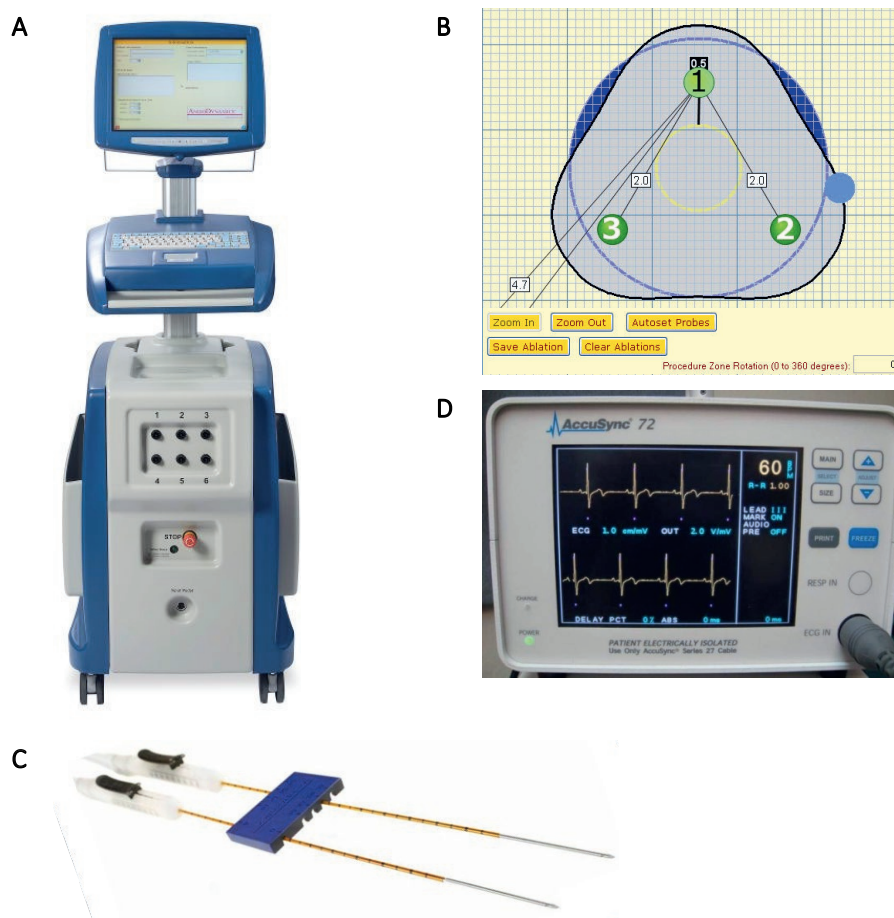


Fig. 1 IRE equipment. **Notes:** (A) The NanoKnife™ IRE console. (B) User-friendly treatment planning software generates a 2D representation of the ablation zone, perpendicular to the direction of the inserted needle electrodes. (C) Monopolar needle electrodes (16 G), covered in a retractable insulation sheath, allowing for adjustment of the active tip length. The blue spacer allows for parallel external fixation of the IRE needles. (D) AccuSync ECG synchronizer, allowing for synchronization of the iRe pulses with the cardiac rhythm. **Abbreviations:** ECG, electrocardiogram; IRE, irreversible electroporation; 2D, two-dimensional.

In vivo IRE results

Liver

Conventional thermal ablation techniques, specifically RFA, have been proven effective in the treatment of hepatic tumours in selected patients [33,34]. Thermal ablation in the liver is limited by the risk of thermal damage to large vessels, bile ducts, gall bladder, hepatic capsule, and extrahepatic organs [35]. Furthermore, the presence of large vessels may lead to a heat sink, impairing ablation results.

IRE of tumours of the liver is the most extensively investigated, with nine trials reporting on its efficacy and safety (Table 1). In terms of safety, all nine studies concluded that IRE was well tolerated by patients, and that IRE is safe for treating liver tumours under the condition that the procedure is electrocardiographically synchronized to the cardiac rhythm [36,37]. IRE was especially feasible in tumours close to major vital structures, for instance, bile ducts, portal veins, and arteries [38,39].

The tumour response rate varied from 50% to 98.1% [36–38,40–42]. Highest response rates were described in patients with a median tumour size of 1 cm in high-risk locations, such as perivascular regions and positions close to major biliary structures, investigated by Kingham et al [38]. Lowest response rates were demonstrated in patients with liver metastasis from numerous different primary tumours, fluctuating from 1.7 to 6.3 cm in size [36]. The overall local recurrences at a 6-month follow-up varied from 0% to 55% [38–41]. The aforementioned response rates and recurrences vary widely across studies, which is probably due to the heterogeneity of patient populations, ablation protocols, and tumour characteristics.

In conclusion, the success of IRE in the liver mainly depends on lesion size. Thomson et al reported that liver metastases >5 cm did not show any response concerning tumour control [36]. When four or more unipolar electrodes are required to ablate one lesion, the overall response rate decreases drastically. This is imaginable because it is technically challenging to place a multiple-needle array. Additionally, the field of electrical impulses is wider and therefore less controllable. A further risk factor associated with local recurrence after IRE is tumour type, with hepatocellular carcinoma (HCC) being less associated with recurrence than metastatic disease ($P=0.023$ for HCC, cholangiocellular carcinoma, or metastatic disease) [39].

Early results of IRE appear to be promising for small liver lesions close to vital structures, as no complications that were directly related to the IRE ablation were described. Nonetheless, comparative studies with conventional thermal ablative therapies need to be carried out to prove its oncological efficacy.

Pancreas

Pancreatic tumours are aggressive in nature. Furthermore, they are generally complicated to treat due to the proximity to vital structures, such as the portal vein, the celiac trunk, and the superior mesenteric vein [43]. In patients with unresectable locally advanced pancreatic cancer (LAPC), RFA has been shown to improve survival. However, RFA treatment is characterised by a high rate of complications [44].

Narayanan et al evaluated the safety of percutaneous pancreatic IRE in 15 ablations in 14 patients. No severe complications or mortality occurred [45]. One patient developed a

grade 2 pancreatitis, which resolved spontaneously. Similarly, Paiella et al reported on the safety and feasibility of pancreatic IRE in ten patients diagnosed with unresectable LAPC [46]. Two complications were observed, namely, a pancreatic abscess and a pancreaticoduodenal fistula, both in the same patient.

A considerable amount of experience in pancreatic IRE has been obtained by the research of Martin et al [47–49]. Starting with a pilot study in 27 patients, aimed at studying the safety and feasibility of pancreatic IRE, 17 possible IRE-related complications were reported in four patients, ranging from grades 1 to 5 [47]. Grade 4 and grade 5 complications consisted of bile leak (n=2) and portal vein thrombosis (n=2). One mortality occurred at 70 days post-IRE. This was due to portal vein thrombosis, which was presumably induced or worsened by the IRE treatment. At a 90-day follow-up, none of the patients showed signs of local recurrence [47]. In a subsequent study, Martin et al reported on pancreatic IRE in a group of 54 unresectable LAPCs [48]. When comparing IRE patients to those on standard therapy, an improvement in local progression-free survival was observed (14 vs 6 months; $P=0.01$), distant progression-free survival (15 vs 9 months; $P=0.02$), and overall survival (20 vs 13 months; $P=0.03$). A total of 67 adverse events were reported in 32 patients of the IRE group, including two cases of bile leakage and two cases of duodenal leakage. One mortality occurred post-pancreatic IRE [48]. A recent analysis of 200 LAPC stage III patients treated with IRE in addition to conventional chemotherapy and radiation therapy showed equally promising results [49]. Median overall survival in these patients was 24.9 months (range: 4.9–85 months), at a complication rate of 37% (median: grade 2, range: grades 1–5). In six (3%) patients, a local recurrence was observed [49].

According to these studies, IRE has proven to be an effective treatment in pancreatic carcinomas, with an improvement in progression-free survival and overall survival when compared to chemotherapy or chemoradiation therapy. However, a few limitations deserve consideration. Sample sizes are small and therefore confine the clinical evidence. We recommend that trials should be repeated with larger populations. Additionally, complication rates are high and severe in nature. A major part of the aforementioned studies included unresectable pancreatic carcinomas, a population that is known for its high morbidity and mortality. Due to high complication rates and the aggressive nature of these tumours, it might be difficult to determine the overall effect of IRE in pancreatic carcinomas. However, the first results indicate that IRE is a suitable option and should be considered in patients diagnosed with unresectable pancreatic carcinoma.

Kidney

The alternative for nephron-sparing surgery is the use of RFA or cryoablation in selected patients presenting with a small renal mass (≤ 4 cm). Oncologic outcomes of ablative therapies are slightly lower compared to the results from conventional surgery. This is,

however, balanced by a lower complication rate and preservation of renal function [50,51]. Thermal ablative treatments are contraindicated for tumours near the renal collecting system, the large blood vessels, or the abdominal organs. IRE could potentially extend the application of focal therapy in kidney cancer if proven safe and reliable in these high-risk locations.

The first-in-human study into the feasibility and safety of IRE ablation of renal cell carcinoma was performed by Pech et al [18]. This “ablate-and-resect” pilot study included six patients with a renal mass requiring radical nephrectomy. IRE was performed under anesthesia immediately before resection of the kidney. In one patient, a single intraoperative supraventricular extrasystole was encountered, without any further electrocardiographic abnormalities during follow-up. Histopathological examination, using hematoxylin and eosin staining, of the resected tumours showed swelling of the ablated cells, but no actual dead cells were observed [18]. No additional viability staining was performed.

Thomson et al investigated the safety of IRE in renal masses in their multiple organ (liver, lung, and kidney) IRE study. IRE of the kidney was performed in ten tumours of seven patients [36]. One patient developed an obstruction of the ureter, which previously had been obstructed as a result of RFA ablation treatment. None of the remaining patients showed signs of stricture while the ureter or collecting system was within the ablation zone. Two patients suffered transient hematuria, both of whom had received IRE treatment extending into the central portion of the kidney. Two patients required a second IRE treatment after 3 months of follow-up [36].

Trimmer et al reported on 20 cases of IRE in small renal masses, with 1 year of imaging follow-up [52]. Two out of the 20 cases presented with residual tumour at 6-week follow-up imaging and were treated with salvage RFA. Six-month follow-up was available in 15 cases showing no signs of recurrence. One-year follow-up was available in six cases, showing recurrence in one case, which was treated by partial nephrectomy. No major complications were observed [52].

The most recent report on renal mass IRE is from Wendler et al, providing preliminary results of a trial in which the IRE lesions are resected 4 weeks post-ablation [53]. This interim report describes the results in the first three patients and gives a detailed report on the histopathology of an IRE ablation zone. The IRE lesions cover all three tumours completely, with no residual tumour in the margins. Very small tumour residues of unclear malignancy have been observed within the ablation zone. The viability, and with that the oncological consequence, of these small residues is unclear. The authors aim to perform additional viability staining in more patients to further investigate this issue [53].

It is concluded that IRE is safe and feasible in the treatment of kidney tumours. No major complications occurred in any of the studies. Nonetheless, the golden standard, a laparoscopic partial nephrectomy, is a highly effective minimally invasive treatment, which is accompanied by very low complication rates and side effects. Therefore, we consider that IRE should be considered in patients diagnosed with renal tumours close to vital structures as only a second-line treatment.

Prostate

Prostate cancer is the most prevalent form of cancer in men, with an increase in the detection of localised disease in the Western world due to the use of prostate-specific antigen testing and improved imaging techniques [29,54]. Conventional therapies in prostate cancer (prostatectomy and radiotherapy) are associated with high incidence of treatment side effects. Common side effects resulting from the destructive nature of conventional treatment include urinary incontinence (0%–20%), bowel problems (22%–36%), and erectile dysfunction (19%–74%) [55–57]. Focal therapies, including IRE, have the potential to reduce these burdens by sparing vital structures such as the urethra and the neurovascular bundles.

The first to report on the use of IRE in prostate cancer were Onik and Rubinsky, 58 treating 16 patients with localised cancer for whom preservation of potency and continence was a major concern. All patients were continent immediately upon removal of the catheter 0–3 days posttreatment. Patients who were potent before remained so after IRE treatment. However, two patients who received bilateral IRE treatment required 6 months for full return of potency. Treatment success was determined after 3 weeks by transperineal biopsies. Fifteen patients showed no evidence of cancer in the targeted area, with one patient refusing follow-up. In one patient, a microfocus Gleason 6 cancer was found outside the targeted area [58].

Valerio et al performed IRE of prostate cancer in 34 patients, assessing safety and feasibility [59]. A total of 12 grade 1 complications and ten grade 2 complications occurred. Follow-up consisted of multiparametric magnetic resonance imaging (MRI) at 1 week and 6 months post-IRE. Complications included urinary retention (n=2; 6%), debris/hematuria (n=6; 18%), dysuria (n=5; 15%), and urinary tract infection (n=5; 15%). Six patients (18%) showed suspicion of residual disease, four of whom underwent a secondary treatment. Only one patient had histological confirmation of treatment failure, through transperineal biopsies, and decided to undergo a radical prostatectomy [59].

Recently, Van den Bos et al performed an ablate-and- resect study, performing IRE in 16 prostate cancer patients 4 weeks prior to radical prostatectomy [29]. Their study focused on safety and feasibility, not specifically targeting the prostate cancer, and therefore did not

present results on cancer-free rates. However, pathology results showed complete ablation of tissue (necrosis and fibrosis) within the IRE electrode configuration. Furthermore, the IRE ablation zones were found to extend beyond the IRE needles, with three needle ablations being 2.9 times larger than the needle configuration and four needle ablations being 2.5 times larger. Importantly, no skip lesions were observed within the needle configuration [29].

In theory, focal treatment in prostate cancer is a promising approach as current conventional therapies have a lot of limitations. Radical prostatectomy and radiotherapy both have poor functional outcomes, with high rates of urinary incontinence and erectile dysfunction. It is believed that IRE has the potential to overcome these side effects. However, to date, there is little evidence on the oncological outcome and no long-term results of IRE in prostate cancer are available. To our knowledge, there is sufficient evidence to say that IRE is a safe and effective focal treatment modality in prostate cancer, but a large trial is needed to warrant its oncological efficacy.

Considerations and future perspectives

The introduction of new treatment techniques should adhere to a standardized methodology, such as the IDEAL recommendations [60]. Following such guidelines will result in a stepwise, safe, and scientifically valid evaluation of the new technique at hand. Research into in vivo IRE is focusing on several different organs simultaneously, with progress being at a different stage for each field. Although IRE research in liver and pancreas is leading the way, it is important to not take these results as evidence for the safety and efficacy of IRE in other organs, that is, skipping ahead in the organ-specific evaluation of IRE.

Several trials are expected to provide additional evidence on in vivo IRE in the near future. The COLDFIRE-II trial (NCT02082782) is aimed at including 29 patients with colorectal liver metastasis for treatment with percutaneous CT-guided IRE, with follow-up by positron emission tomography (PET)-CT and PET-MRI. The same research group is finalizing the results of the PANFIRE trial (NCT01939665), having included 15 patients with locally advanced pancreatic adenocarcinoma, treated with percutaneous IRE and subsequently followed by cross-sectional imaging (CT/MRI) and blood tumour markers. Two further trials focusing on IRE in pancreatic cancer are the IMPALA trial (NL44713.018.13) and the pancreatic IRE trial (NL45048.058.13) at the Leiden University (the Netherlands).

Although the evidence on IRE in different organs is rapidly expanding, most results remain in the form of low-quality cohort studies, to be graded as level 4 of evidence [11]. Different groups are collaborating by pooling IRE data in registries. Uniform and central collection of data will result in larger data sets, allowing for more substantial evaluation of IRE safety and

efficacy. Examples of such registries are the Soft Tissue Ablation Registry (STAR) and the prostate IRE registry (NCT02255890) of the Clinical Research Office of the Endourological Society (CROES). A considerable improvement on the available evidence will come from the CROES coordinated multicenter randomized controlled trial (RCT) (level 2b) into IRE in prostate cancer (NCT01835977). This recently started RCT will compare the IRE safety and efficacy between a focal IRE ablation and extended IRE ablation of the prostate.

For IRE to evolve into an accepted segment of standard therapy more research is needed, directed at tissue-specific device settings and ablation protocols, further evaluation of early ablation results, and follow-up methods, completed by studies focused on long-term oncological outcomes. At this phase of development, it is essential to perform IRE as much as possible in the setting of a clinical trial. As it involves the use of a medical device instead of a pharmacological product, the optimal way to proceed is following the recommendations of the IDEAL collaboration [60]. This evaluation equals surgical innovation to the different phases of pharmacological research. IRE has been described for the IDEAL stage 2a (development phase). To develop IRE into a minimally invasive treatment device, results should be compared with a standard test at use in Phase IIb and Phase III RCT trials. The best trial for the clinical evaluation of a new technique is an RCT. These trials are, however, seldom undertaken because they are time-consuming and expensive. The common trial design, a prospective cohort, should consist of a strict treatment protocol in combination with a clearly defined population. If inclusion in a trial is not possible, patient data should at least be pooled uniformly in a centrally coordinated registry.

Conclusion

IRE is showing promising results in early clinical research. The prospect of treating tumours in the vicinity of vital structures gives IRE a potential edge over conventional ablation techniques, which are mainly thermal in nature. However, for IRE to evolve into a clinically accepted ablation technique, further development is needed on multiple fronts, namely, tissue-specific device settings/protocols, ablation monitoring, and follow-up imaging, as well as long-term oncological outcomes. At this stage of development, it is essential to perform IRE in the setting of well-designed clinical trials and, if trial participation is not possible, at least to pool patients in a registry. Furthermore, as electrical properties vary among different tissue types, it is important not to interchange outcomes between organs, undermining the organ-specific evaluation of IRE.

References

1. Lencioni R, Cioni D, Della Pina C, Crocetti L. Hepatocellular carcinoma: new options for image-guided ablation. *J Hepatobiliary Pancreat Sci.* 2010; 17:399–403.
2. Sharma A, Abtin F, Shepard JA. Image-guided ablative therapies for lung cancer. *Radiol Clin North Am.* 2012;50:975–999.
3. Volpe A, Cadeddu JA, Cestari A, et al. Contemporary management of small renal masses. *Eur Urol.* 2011;60:501–515.
4. Olweny EO, Cadeddu JA. Novel methods for renal tissue ablation. *Curr Opin Urol.* 2012;22:379–384.
5. Valerio M, Ahmed HU, Emberton M, et al. The role of focal therapy in the management of localised prostate cancer: a systematic review. *Eur Urol.* 2014;66:732–751.
6. van den Bos W, Muller BG, Ehdaie B, Scardino P, de la Rosette JJ. What is still needed to make focal therapy an accepted segment of standard therapy? *Curr Opin Urol.* 2014;24:247–255.
7. Rubinsky B, Onik G, Mikus P. Irreversible electroporation: a new ablation modality – clinical implications. *Technol Cancer Res Treat.* 2007; 6:37–48.
8. Wagstaff PG, de Bruin DM, Zondervan PJ, et al. The efficacy and safety of irreversible electroporation for the ablation of renal masses: a prospective, human, in-vivo study protocol. *BMC Cancer.* 2015;15:165.
9. Miklavcic D, Mali B, Kos B, Heller R, Sersa G. Electrochemotherapy: from the drawing board into medical practice. *Biomed Eng Online.* 2014;13:29.
10. Yarmush ML, Golberg A, Sersa G, Kotnik T, Miklavcic D. Electroporation-based technologies for medicine: principles, applications, and challenges. *Annu Rev Biomed Eng.* 2014;16:295–320.
11. Oxford Centre for Evidence-based Medicine – Levels of Evidence. Howick J, Phillips B, Ball C, et al, Centre for Evidence-Based Medicine, University of Oxford; 2009. Available from: <http://www.cebm.net/oxford-centre-evidence-based-medicine-levels-evidence-march-2009/>. Accessed October 1, 2015.
12. Lee EW, Wong D, Prikhodko SV, et al. Electron microscopic demonstration and evaluation of irreversible electroporation-induced nanopores on hepatocyte membranes. *J Vasc Interv Radiol.* 2012;23:107–113.
13. Chang DC, Reese TS. Changes in membrane-structure induced by electroporation as revealed by rapid-freezing electron-microscopy. *Biophys J.* 1990;58:1–12.
14. Neumann E, Schaeferfritter M, Wang Y, Hofschneider PH. Gene-transfer into mouse lymphoma cells by electroporation in high electric fields. *EMBO J.* 1982;1:841–845.
15. Mir LM, Orlowski S, Belehradec J, Paoletti C. Electrochemotherapy potentiation of antitumour effect of bleomycin by local electric pulses. *Eur J Cancer.* 1991;27:68–72.
16. Al-Sakere B, Andre F, Bernat C, et al. Tumour ablation with irreversible electroporation. *PLoS One.* 2007;2:e1135.
17. Olweny EO, Kapur P, Tan YK, Park SK, Adibi M, Cadeddu JA. Irreversible electroporation: evaluation of nonthermal and thermal ablative capabilities in the porcine kidney. *Urology.* 2013;81:679–684.
18. Pech M, Janitzky A, Wendler JJ, et al. Irreversible electroporation of renal cell carcinoma: a first-in-man phase I clinical study. *Cardiovasc Intervent Radiol.* 2011;34:132–138.
19. Bertacchini C, Margotti PM, Bergamini E, Lodi A, Ronchetti M, Cadossi R. Design of an irreversible electroporation system for clinical use. *Technol Cancer Res Treat.* 2007;6:313–320.
20. Kinoshita K, Ashikawa I, Saita N, et al. Electroporation of cell-membrane visualized under a pulsed-laser fluorescence microscope. *Biophys J.* 1988; 53:1015–1019.
21. Hibino M, Shigemori M, Itoh H, Nagayama K, Kinoshita K. Membrane conductance of an electroporated cell analysed by submicrosecond imaging of transmembrane potential. *Biophys J.* 1991;59:209–220.
22. Jiang CL, Davalos RV, Bischof JC. A Review of basic to clinical studies of irreversible electroporation therapy. *IEEE Trans Biomed Eng.* 2015;62:4–20.
23. Granot Y, Ivorra A, Maor E, Rubinsky B. In vivo imaging of irreversible electroporation by means of electrical impedance tomography. *Phys Med Biol.* 2009;54:4927–4943.
24. van Gemert MJ, Wagstaff PG, de Bruin DM, et al. Irreversible electroporation: just another form of thermal therapy? *Prostate.* 2015;75(3): 332–335.
25. Wagstaff PG, de Bruin DM, van den Bos W, et al. Irreversible electroporation of the porcine kidney: temperature development and distribution. *Urol Oncol.* 2015;33(4):168.e1–168.e7.

26. van den Bos W, Scheffer HJ, Vogel JA, et al. Thermal energy during irreversible electroporation and the influence of different ablation parameters. *J Vasc Interv Radiol*. Epub 2015 Dec 17.
27. Davalos RV, Bhonsle S, Neal RE. Implications and considerations of thermal effects when applying irreversible electroporation tissue ablation therapy. *Prostate*. 2015;75:1114–1118.
28. Golberg A, Yarmush ML. Nonthermal irreversible electroporation: fundamentals, applications, and challenges. *IEEE Trans Biomed Eng*. 2013;60:707–714.
29. van den Bos W, de Bruin DM, Jurhil RR, et al. The correlation between the electrode configuration and histopathology of Irreversible Electroporation ablations in prostate cancer patients. *World J Urol*. Epub 2015 Aug 22.
30. Tracy CR, Kabbani W, Caddeu JA. Irreversible electroporation (IRE): a novel method for renal tissue ablation. *BJU Int*. 2011;107: 1982–1987.
31. Wimmer T, Srimathveeravalli G, Gutta N, et al. Planning irreversible electroporation in the porcine kidney: are numerical simulations reliable for predicting empiric ablation outcomes? *Cardiovasc Intervent Radiol*. 2015;38:182–190.
32. Nielsen K, Scheffer HJ, Vieveen JM, et al. Anaesthetic management during open and percutaneous irreversible electroporation. *Br J Anaesth*. 2014;113:985–992.
33. Bruix J, Sherman M. Management of hepatocellular carcinoma: an update. *Hepatology*. 2011;53:1020–1022.
34. Cho YK, Kim JK, Kim MY, Rhim H, Han JK. Systematic review of randomized trials for hepatocellular carcinoma treated with percutaneous ablation therapies. *Hepatology*. 2009;49:453–459.
35. Teratani T, Yoshida H, Shiina S, et al. Radiofrequency ablation for hepatocellular carcinoma in so-called high-risk locations. *Hepatology*. 2006;43:1101–1108.
36. Thomson KR, Cheung W, Ellis SJ, et al. Investigation of the safety of irreversible electroporation in humans. *J Vasc Interv Radiol*. 2011;22: 611–621.
37. Sugimoto K, Moriyasu F, Kobayashi Y, et al. Irreversible electroporation for nonthermal tumour ablation in patients with hepatocellular carcinoma: initial clinical experience in Japan. *Jpn J Radiol*. 2015;33:424–432.
38. Kingham TP, Karkar AM, D'Angelica MI, et al. Ablation of perivascular hepatic malignant tumours with irreversible electroporation. *J Am Coll Surg*. 2012;215:379–387.
39. Niessen C, Igl J, Pregler B, et al. Factors associated with short-term local recurrence of liver cancer after percutaneous ablation using irreversible electroporation: a prospective single-center study. *J Vasc Interv Radiol*. 2015;26:694–702.
40. Cannon R, Ellis S, Hayes D, Narayanan G, Martin RC. Safety and early efficacy of irreversible electroporation for hepatic tumours in proximity to vital structures. *J Surg Oncol*. 2013;107:544–549.
41. Cheung W, Kavounoudias H, Roberts S, Szkandera B, Kemp W, Thomson KR. Irreversible electroporation for unresectable hepatocellular carcinoma: initial experience and review of safety and outcomes. *Technol Cancer Res Treat*. 2013;12:233–241.
42. Cheng RG, Bhattacharya R, Yeh MM, Padia SA. Irreversible electroporation can effectively ablate hepatocellular carcinoma to complete pathologic necrosis. *J Vasc Interv Radiol*. 2015;26:1184–1188.
43. Yeo CJ. Pancreatic cancer – in brief. *Curr Probl Cancer*. 2002;26:170.
44. Pandya GJ, Shelat VG. Radiofrequency ablation of pancreatic ductal adenocarcinoma: the past, the present and the future. *World J Gastro- intest Oncol*. 2015;7:6–11.
45. Narayanan G, Hosein PJ, Arora G, et al. Percutaneous irreversible electroporation for downstaging and control of unresectable pancreatic adenocarcinoma. *J Vasc Interv Radiol*. 2012;23:1613–1621.
46. Paiella S, Butturini G, Frigerio I, et al. Safety and feasibility of Irreversible Electroporation (IRE) in patients with locally advanced pancreatic cancer: results of a prospective study. *Dig Surg*. 2015;32:90–97.
47. Martin RC, McFarland K, Ellis S, Velanovich V. Irreversible electroporation therapy in the management of locally advanced pancreatic adenocarcinoma. *J Am Coll Surg*. 2012;215:361–369.
48. Martin RC, McFarland K, Ellis S, Velanovich V. Irreversible electroporation in locally advanced pancreatic cancer: potential improved overall survival. *Ann Surg Oncol*. 2013;20(suppl 3):S443–S449.
49. Martin RC, Kwon D, Chalikonda S, et al. Treatment of 200 locally advanced (Stage III) pancreatic adenocarcinoma patients with irreversible electroporation: safety and efficacy. *Ann Surg*. 2015;262: 486–494.
50. Katsanos K, Mailli L, Krokidis M, McGrath A, Sabharwal T, Adam A. Systematic review and meta-analysis of thermal ablation versus surgical nephrectomy for small renal tumours. *Cardiovasc Intervent Radiol*. 2014;37:427–437.
51. Wagstaff P, Ingels A, Zondervan P, de la Rosette JJ, Laguna MP. Thermal ablation in renal cell carcinoma management: a comprehensive review. *Curr Opin Urol*. 2014;24:474–482.

52. Trimmer CK, Khosla A, Morgan M, Stephenson SL, Ozayar A, Cadeddu JA. Minimally invasive percutaneous treatment of small renal tumours with irreversible electroporation: a single-center experience. *J Vasc Interv Radiol*. 2015;26(10):1465–1471.
53. Wendler JJ, Ricke J, Pech M, et al. First delayed resection findings after irreversible electroporation (IRE) of human localised renal cell carcinoma (RCC) in the IRENE pilot Phase 2a trial. *Cardiovasc Intervent Radiol*. 2015;39(2):239–250.
54. Jemal A, Siegel R, Xu J, Ward E. Cancer statistics, 2010. *CA Cancer J Clin*. 2010;60:277–300.
55. Resnick MJ, Koyama T, Fan KH, et al. Long-term functional outcomes after treatment for localised prostate cancer. *N Engl J Med*. 2013;368:436–445.
56. Ficarra V, Novara G, Ahlering TE, et al. Systematic review and meta-analysis of studies reporting potency rates after robot-assisted radical prostatectomy. *Eur Urol*. 2012;62:418–430.
57. Ficarra V, Novara G, Rosen RC, et al. Systematic review and meta-analysis of studies reporting urinary continence recovery after robot-assisted radical prostatectomy. *Eur Urol*. 2012;62:405–417.
58. Onik G, Rubinsky B. Irreversible electroporation: first patient experience focal therapy of prostate cancer. In: Rubinsky B, editor. *Irreversible Electroporation*. Berlin Heidelberg: Springer-Verlag; 2010:235–247.
59. Valerio M, Stricker PD, Ahmed HU, et al. Initial assessment of safety and clinical feasibility of irreversible electroporation in the focal treatment of prostate cancer. *Prostate Cancer Prostatic Dis*. 2014; 17:343–347.
60. McCulloch P, Altman DG, Campbell WB, et al. No surgical innovation without evaluation: the IDEAL recommendations. *Lancet*. 2009; 374:1105–1112.
61. Silk MT, Wimmer T, Lee KS, et al. Percutaneous ablation of peribiliary tumours with irreversible electroporation. *J Vasc Interv Radiol*. 2014;25:112–118.
62. Scheffer HJ, Nielsen K, van Tilborg AA, et al. Ablation of colorectal liver metastases by irreversible electroporation: results of the COLD- FIRE-I ablate-and-resect study. *Eur Radiol*. 2014;24:2467–2475.

CHAPTER 5

5

Irreversible electroporation for the ablation of renal cell carcinoma: A prospective, human, in-vivo trial

M Buijs, KP van Lienden, PGK Wagstaff, MJV Scheltema, DM de Bruin, PJ Zondervan, OM van Delden, TG van Leeuwen, JJMCH de la Rosette, MP Laguna Pes

Abstract

Background: Irreversible electroporation (IRE) is an emerging technique delivering electrical pulses to ablate tissue, with the theoretical advantage to overcome the main shortcomings of conventional thermal ablation. Recent short-term research showed that IRE for the ablation of renal masses is a safe and feasible treatment option. In an ablate and resect design, histopathological analysis 4 weeks after IRE demonstrated that the renal tumours were completely covered by ablation zone. In order to develop a validated long-term IRE follow-up study, it is essential to obtain clinical confirmation of the feasibility, safety and efficacy of this novel technology. Additionally, follow-up after IRE ablation obliges verification of a suitable imaging modality.

Objective: The objectives of this study are feasibility, safety and clinical efficacy of IRE ablation for renal masses and to evaluate the use of cross-sectional imaging modalities in the follow-up after IRE in renal tumours. This study conforms to the recommendations of the IDEAL Collaboration and can be categorized as a phase II trial.

Methods: In this prospective clinical trial, IRE will be performed in 20 patients aged 18 years and older presenting with a solid enhancing small renal mass (SRM) (≤ 4 cm) who are candidates for ablation. Magnetic resonance imaging (MRI) and contrast-enhanced ultrasound (CEUS) will be performed at 1-day pre-IRE and 1-week post-IRE. Computed tomography (CT), CEUS, and MRI will be performed at 3 months, 6 months, and 12 months post-IRE.

Results: Presently, the recruitment of patients has started and the first inclusions are completed. Preliminary results and outcomes are expected in 2018.

Conclusions: To establish the position of IRE ablation for treating renal tumours, a structured stepwise assessment in clinical practice is required. This study will offer fundamental knowledge on the feasibility, safety and clinical efficacy of IRE ablation for SRMs, potentially positioning IRE as an ablative modality for renal tumours and accrediting future research with long-term follow-up.

Introduction

Ablative Therapy in Renal Cell Carcinoma

Due to the widespread detection of small renal masses (SRMs), a gradual but sustained rise in the incidence of renal tumours 4 cm or less (cT1a, according to the TNM [tumour/node/metastasis] staging system) has been observed [1-4]. At present, the reference standard therapy in the management of SRMs is nephron-sparing surgery like partial nephrectomy [5]. However, a significant interest is sparked in minimally invasive therapies, including cryoablation and radiofrequency ablation (RFA). Literature shows that thermal ablation compared to partial nephrectomy is characterised by a slightly higher recurrence rate but also accompanied by a lower complication rate [6,7]. Nevertheless, a growing body of research advocates that in selected patients similar oncological results can be obtained compared to those accomplished in surgical resection [8]. Current guidelines recommend primary ablative therapy in patients who are (1) not suitable for surgery, (2) have a genetic predisposition for developing multiple tumours, and (3) are diagnosed with bilateral tumours or have a solitary kidney and are at risk of complete loss of renal function after surgery [9-11].

Ablation of undesirable tissue depends on accurate dosing and adequate targeting of tumour destruction while sparing vital structures such as adjacent organs, collecting system, or major vessels [12,13]. Due to temperature fluctuations that are accompanied by the thermal character of cryoablation and RFA, it is thought that the destruction process of the tumour is unselective [14,15]. Ablation effects and tissue heating may be less effective in proximity to blood vessels as a result of thermal drainage by regional vascular flow impairing the extent of coagulation, in the literature termed as a “heat sink” effect [9,16]. Additionally, collateral damage to underlying vital structures can occur, as the natures of these structures are susceptible to extreme temperatures. Therefore according to guidelines, renal tumours located near the hilum or the proximal ureter are not suitable for thermal ablation, forming a niche in the ablative treatment of renal tumours [10].

Irreversible Electroporation in Renal Cell Carcinoma

An emerging technique among the assortment of ablative modalities is called irreversible electroporation (IRE). It is based on high-voltage electrical pulses transferred between 2 or more needle electrodes. Charging the cell membrane causes holes in the membrane called nanopores, resulting in increased permeability of the cell and subsequent cell death [13,17-20].

Theoretically, the mechanism of action of IRE does not rely on temperature changes. Therefore it has been postulated that it has the potential to overcome the current limitations of thermal ablative modalities like cryoablation and RFA [12]. However, using

the current clinical device settings, a temperature rise is to be expected as shown by Wagstaff et al in an animal model [21].

Concerning IRE ablation in renal tumours, 4 studies have been performed in humans [20,22-24]. All studies concluded that the safety of IRE in humans is warranted as long as electrocardiogram (ECG) synchronization is used.

Trimmer et al made a start in safety and clinical efficacy, describing post-ablation features on cross-sectional imaging. Although these initial results seem promising and appear similar to conventional ablative techniques, a few limitations deserve consideration. The study design is retrospective, and the follow-up was limited. Imaging was available in 15 out of 20 patients (75%) at 6-month follow-up and only in 6 out of 20 patients (30%) at 1-year follow-up [23].

Thomson et al performed IRE in various organs, including 10 renal tumours in 7 patients. One patient (14%) developed a ureteral stricture after IRE ablation in an area of the ureter that previously had been obstructed by RFA. Other centrally located tumours did not show any major complications. A total of 2 patients (29%) experienced minor complications consisting of transient hematuria [24]. Wendler et al were the first to provide histopathological data of IRE in renal tumours of 3 patients, showing complete coverage of the tumour within the ablation zone with preservation of the renal parenchyma [25]. Very small tumour residues of unclear malignant potential were found within the ablation zone. Unfortunately, the clinical significance of these residues remained unclear and impossible to follow-up since the tumours had been resected.

Rationale

The first human studies have proven the safety of IRE for the ablation of SRMs. Initial results on the clinical efficacy of IRE are promising and imply that effective oncological management is achievable. Clinical outcomes should be investigated in a small prospective patient population to provide essential data before embarking on a randomized trial. We, therefore, plan to perform a study aiming at the feasibility, safety and clinical efficacy of IRE in SRMs, with a specific focus on post-ablation follow-up with cross-sectional imaging. Research on IRE in liver tumours has demonstrated that the ablation success of IRE decreases with tumour size above 4 cm [24]. According to current guidelines, ablative treatment is only offered to patients with SRMs (≤ 4 cm) [10]. Therefore, we aim to investigate IRE ablation in renal masses up to 4 cm. This prospective, human, in vivo trial is an essential step to safely progress to larger randomized trials on IRE of SRMs. This study conforms to the recommendations of the IDEAL (idea, development, exploration, assessment, long-term study) Collaboration and can be categorized as a phase II [26].

Methods

Study Objectives

- To determine the safety and feasibility of IRE ablation of SRMs (≤ 4 cm) by evaluating device and procedural adverse events using Common Terminology Criteria for Adverse Events (CTCAE) version 4.0
- To determine the clinical efficacy of IRE ablation for SRMs (≤ 4 cm) assessed by the recurrence and residual disease rate at follow-up using cross-sectional imaging
- To evaluate the use of computed tomography (CT), magnetic resonance imaging (MRI), and contrast-enhanced ultrasound (CEUS) in the visualization of (non)complete ablation to assess the radiological extent of the ablation zone at 1 week, 3 months, 6 months, 9 months and 1 year after IRE
- To evaluate perioperative outcomes after IRE ablation of SRMs (≤ 4 cm) such as (1) renal function, measured by creatinine levels and estimated glomerular filtration rate (eGFR), (2) average length of hospital stay, (3) quality of life, and (4) postoperative pain score after IRE, measured by a visual analog scale (VAS) and analgesics use

Population

A total of 20 patients with solid enhancing SRMs on cross-sectional imaging qualifying for ablative therapy will be enrolled in this study. Eligible patients are 18 years of age and older and will receive a biopsy of the SRM before the procedure. All inclusions are reviewed for safety and eligibility by a nephrologist participating in the research project. The inclusion and exclusion criteria for this study are listed in Table 1.

Table 1. Selection criteria. Severe cardiovascular disease is defined as the diagnosis of myocardial infarction, uncontrolled angina, significant ventricular arrhythmias, stroke, or severe cardiac failure (New York Heart Association class III and IV) within 6 months prior to inclusion.

| |
|--|
| Inclusion criteria: |
| <ul style="list-style-type: none">• Age 18 years and older• Solid enhancing SRM on cross-sectional imaging suspect for RCC• Candidate for ablation• Signed informed consent |
| Exclusion criteria: |
| <ul style="list-style-type: none">• Irreversible bleeding disorders• Inability to stop anticoagulation therapy• Implantable cardioverter-defibrillator or pacemaker |

Study Design

This is a prospective, human, in vivo study among 20 patients presenting with solid enhancing SRM on cross-sectional imaging suspect for RCC. Preoperatively, imaging is required through CT, MRI, and CEUS. Furthermore, serum creatinine levels and VAS scores are obtained. A biopsy of the SRM will be performed prior to the ablation. IRE ablation will be performed using CT guidance, and ablation success will be measured directly after the ablation through contrast-enhanced CT. Device-related adverse events will be registered using the CTCAE version 4.0 guideline. At 1 week post-ablation, only CEUS and MRI will be performed to limit exposure to ionizing radiation. At 3 months, 6 months, and 12 months post-ablation, CEUS, MRI, and CT will be performed. Additionally, at these time points, serum creatinine levels and VAS scores will be obtained, and quality of life will be assessed through Short Form 36 (SF-36) questionnaires. The residual and recurrent disease will be assessed through tissue enhancement on cross-sectional imaging. When imaging appears suspicious for recurrence or residual disease, a percutaneous renal core biopsy will be performed. A study flowchart demonstrating the investigations is outlined in Fig. 1.

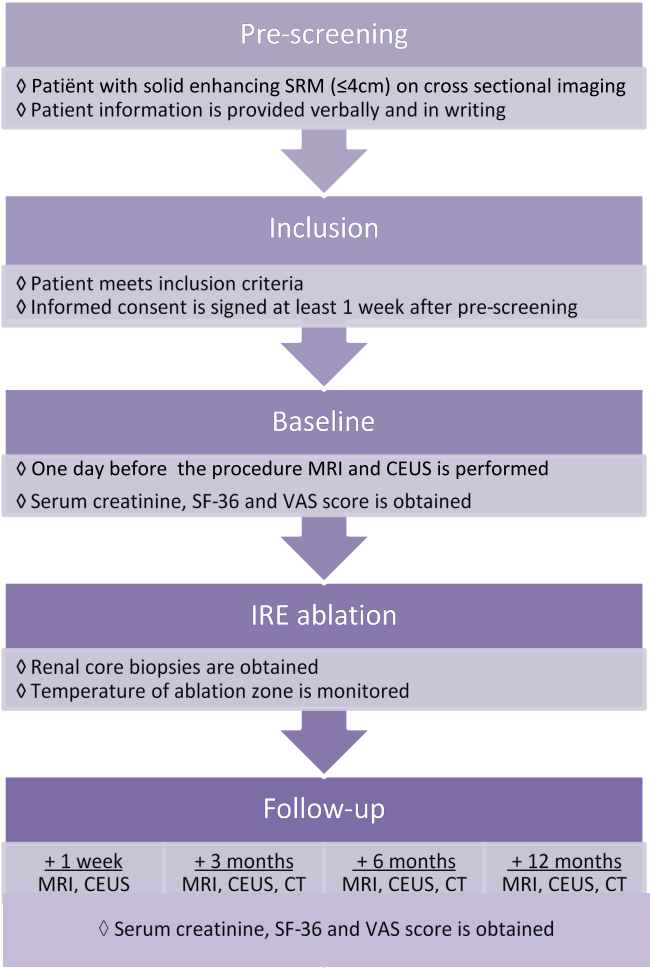


Fig. 1. Study design flowchart.
Study Procedures

Renal Core Biopsy (Standard)

According to the ablation protocol of the Academic Medical Center University Hospital, percutaneous renal core biopsies will be obtained prior to the IRE procedure. At least 2 core biopsies will be acquired for pathological examination.

Irreversible Electroporation Ablation (Study Intervention)

In this study, IRE ablation is performed using the NanoKnife IRE device (AngioDynamics Inc) (Fig. 2, A), also registered as the HVP-01 electroporation system. The IRE system contains a low energy direct current generator, a footswitch, and 19G monopolar needle electrodes (15 or 25 cm length). Regulatory authorities have approved both the device and the electrodes through a Conformité Européenne certificate for the use of cell membrane electroporation. Additionally, the US Food and Drug Administration has granted 510(k) clearance with premarket notifications (K060054, K080202, K080376, K080287). Granted 510(k) components are all approved for surgical ablation of soft tissue.

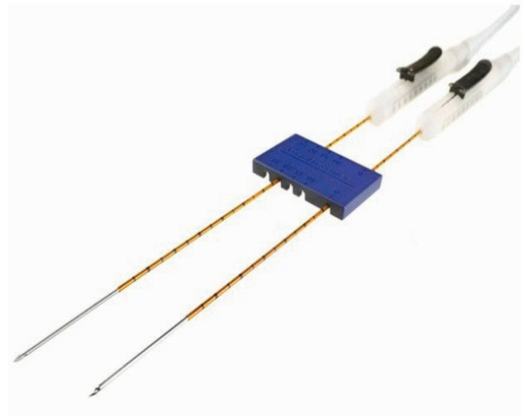
The IRE procedure will be performed at the radiology department CT room with the patient under general anesthesia including deep muscle relaxation to prevent severe muscle contraction [27]. CT imaging will be performed with the patient in the prone or lateral position, dependent on tumour location and position of adjacent organs such as intestines. An interventional radiologist cooperating with a urological surgeon and a resident urology, all experts on percutaneous ablative procedures, will perform the IRE procedure. IRE pulses will be synchronized with ECG under the supervision of an anesthesiologist. Prior to ablation, a (second) set of biopsies will be obtained to confirm histopathology. Guided by CT and accompanied by an external spacer for fixation, needle electrodes will be placed (Fig. 2B). The number of probes and probe placement will be attuned for specific tumour size and location, granting 15 mm between the electrodes with an active tip length of 15-25 mm. IRE pulses with pulse intensity of 1500 V/cm will be delivered in 90 consecutive pulses of 90 μ s. Settings are used to disrupt the cell membrane potential in order to achieve irreversible permeability of the cell and subsequent apoptosis. Van den Bos et al demonstrated that with current settings the ablation zone is completely ablated without leaving any skip lesions within the electrode configuration [28].

The primary cycle of IRE is estimated to be 5 to 10 minutes, with a total operating time of approximately 90 minutes. Immediately after IRE has been performed, a contrast-enhanced CT will be made to assess immediate technical success and to detect acute complications. It is expected that patients will be discharged 24 to 36 hours after the IRE procedure. Before the patient's discharge, quality of life and postprocedural pain will be assessed through SF-36 questionnaire and VAS score respectively. At 1 week after the

procedure, VAS score and SF-36 questionnaire will be obtained and cross-sectional imaging by CEUS and MRI will be performed.



A



B

Fig. 2. A. The NanoKnife IRE console. B. The console operates with 19G monopolar needle electrodes, which are bundled together using the external spacers.

Computed Tomography Imaging (Standard)

As provided per ablation protocol, CT imaging will take place during the diagnostic phase and during the procedure. According to our ablation surveillance protocol, follow-up CT imaging will be performed at 3 months, 6 months, 1 year, 1.5 years, 2 years, 2.5 years, and 3 years after IRE ablation. After this, patients will be followed up yearly for up to 10 years. This is the standardized follow-up after ablative therapy at our institution (see Fig. 1). Patients with an eGFR below 60 mL/min/1.73 m² will undergo pre- and post hydration in order to prevent contrast-induced nephropathy according to our hospital protocol. Patients with an eGFR below 30 mL/min/1.73 m² are excluded from CT imaging.

CT imaging will be performed in a supine position in a dual-source CT system, SOMATOM Force (Siemens Medical Solutions), or in a Sensation 64-slice CT scanner (Siemens Medical Solutions). First, a survey scan from the upper border of the diaphragm to the ischium bone will be made. Next, noncontrast series in the same section will be performed.

Subsequently, 100 mL of Ultravist-300 diluted with NaCl 0.9% will be administered intravenously with a speed of 4 mL/s to achieve enhancement. Following contrast injection, arterial and corticomedullary phase series will be obtained after 45 seconds and 90 seconds, respectively. Source images will be reconstructed in coronal and sagittal planes using multiplanar reconstruction in the venous and delayed series.

Contrast-Enhanced Ultrasound and Magnetic Resonance Imaging (Study Intervention)

Baseline CEUS will be obtained from 1 day to 3 months before IRE, and 1 week, 3 months, 6 months, and 12 months after IRE. Baseline MRI will be obtained from 1 day to 3 months before IRE, and 1 week, 3 months, 6 months, and 12 months after IRE (see Fig. 1). This frequency was established in order to assess lesion size and characteristics.

CEUS imaging encompasses microbubbles of 3 to 5 μm as a contrast agent to visualize blood flow. The phospholipid-coated microbubbles demonstrate regional tissue vascularization, including the tissue-specific microvasculature. This study uses a Philips iU22 (Phillips Healthcare) device united with a third-generation intravenous ultrasound contrast agent (SonoVue) for optimal imaging. Sonovue contrast agent is characterised by a distribution half-life of 1 minute and an elimination half-life of 6 minutes when intravenously administered [29].

MRI will be performed with the patient in the supine position using a 1.5 Tesla AVANTO MRI scanner (Siemens Healthcare) with a 16-channel body matrix array coil. According to our kidney tumour protocol, a minimum of 9 sequences will be performed: T2-trufi with fat suppression, T1-fl2d contrast-enhanced in and out of phase, T2-haste, T1-vibe unenhanced, and dynamic series at 0, 30, 60, and 90 seconds post arrival of contrast in the thoracic aorta. Intravenous contrast agent Gadovist (Bayer Pharma) of 0.1 mmol per kg of body weight will be administered at a rate of 2 mL/sec for enhancement.

Sample Size

Our sample size was deliberated based on previous similar study designs that used comparable sample sizes of 6 to 20 patients [20,23-25]. In this phase of research (phase II IDEAL Collaboration), a small cohort of N=20 was chosen to acquire the first results to progress to a large trial. A sample size of 20 patients does not permit reliable comparative statistical analysis. In this study, IRE is intended as a curative therapy. Consequently, there will be no exploration of the number of probes and configuration settings.

Potential Benefits and Risks

Conventional focal ablative therapies, RFA, and cryoablation are indicated in patients presenting with an SRM who are poor surgical candidates or who are (genetically) predisposed to develop multiple tumours and are at risk of significant loss of renal function after surgery. For this study, IRE ablation will be offered to this group of patients in our institution. Early research into renal IRE has proven that procedural safety and the periprocedural burden are comparable to conventional ablative therapies. The lack of long-term oncological follow-up poses a potential risk as patients cannot be counseled on the risk of residual or recurrent tumour. Post-IRE follow-up will be equal to post cryoablation and post-RFA follow-up and therefore does not carry an additional burden concerning ionizing radiation. When renal function appears to decrease to eGFR below 30 mL/min/1.73 m², only MRI and CEUS will be performed to prevent contrast-induced nephropathy. Furthermore, potential risks associated with IRE ablation for renal tumours using the NanoKnife system are listed in Table 2.

Table 2: Potential risks associated with IRE of renal tumours.

| Potential Hazards of renal IRE ablation | Potential Effects |
|--|---|
| Excessive energy delivery | Muscle contraction, burn, damage to critical anatomical structure, unintended tissue ablated, bradycardia/hypotension, vagal stimulation/asystole, electrical shock, myocardial infarction, stroke, death |
| Insufficient/ no energy delivery | Ineffective ablation, no ablation |
| Unintended mains or patient circuit Voltage exposure to patient or user | Electrical shock |
| Incorrect timing of pulse delivery | Transient arrhythmia, prolonged arrhythmia, stroke, death |
| Unintended interference with implanted devices containing electronics or metal parts | Myocardial infarction, stroke, death |
| Unexpected movement of the device and displacement of the electrodes | Hypotension, damage to critical anatomical structure, pneumothorax, mechanical perforation, haemorrhage, unintended tissue ablated, electrical shock, death |
| Sterile barrier breach | Infection, sepsis |

Data Safety Monitoring Board

The study will be monitored by a data safety monitoring board (DSMB) consisting of an independent urologist and a clinical epidemiologist. This team will monitor patient safety and treatment efficacy data during the study. Monitoring procedures are predetermined and described in the DSMB charter, approved by the institutional review board (IRB) of the Academic Medical Center University Hospital in Amsterdam. Additional DSMB meetings can be called at any time if deemed necessary by the DSMB or the principal investigator.

Analysis

The NanoKnife console produces 2-dimensional images including a prediction of the ablation zone, which is perpendicular to the needle. The AMIRA (FEI) software package system will bundle the 2-dimensional ablation zone cross-sections around the length of the exposed tip. This will estimate the following:

- Ablation zone volume (cm³)
- 3-Dimensional reconstruction
- Ablation zone shape/symmetry

An experienced urologist will evaluate CT and MRI images for the following characteristics :

- The volume of ablation zone (cm³)
- Shape of ablation zone
- Residual tumour on ablation zone border
- Skip lesions or signs of recurrence within ablation zone
- Transition zone between ablated and normal renal tissue
- Damage to adjacent vital structures

For MRI and CT, whole-mount ablation zone will be calculated. The AMIRA software system will be used to obtain a 3-dimensional kidney and ablation zone. CEUS will be performed by an interventional radiologist and will be used for 2-dimensional imaging only.

Ethical Consideration

The IRB of the Academic Medical Center, Amsterdam, approved this study protocol (2016_055). The protocol has been registered with the Dutch Central Committee on Research Involving Human Subjects (NL56935.018.16) and is entered in the ClinicalTrials.gov database (NCT02828709). The study is conducted following the ethical principles and standards of Good Clinical Practice which have their origin in the Declaration

of Helsinki (Fortaleza, Brazil, October 2013). Potential candidates will receive the study information both verbally and in writing. They will be granted at least 1 week to decide on participation. Written informed consent will be acquired from all participants. If deemed necessary, supplementary information will be provided verbally or in writing.

Availability of Data and Materials

The study initiator, international coordinating researcher, and biostatistician have access to all data. All data is available for audit, and all data will be published in an international peer-reviewed medical journal. The datasets created in the current study are not publicly available due to protecting the privacy of participants but are available from the corresponding author on reasonable request.

Results

At the time of writing the trial is recruiting patients, with 2 inclusions completed. The expected inclusion rate is 1 patient every 6 weeks, resulting in an estimated inclusion period of 2 years. Hence we calculate that we will recruit the full sample size within 2 years. Additionally, early results on the outcome of residual tumour disease, quality of life, and safety and feasibility will be acquired within 2 years (see Fig. 3). The imaging follow-up in this study is 1 year for each patient (see Fig. 1); therefore, we expect to complete the study in 2019.

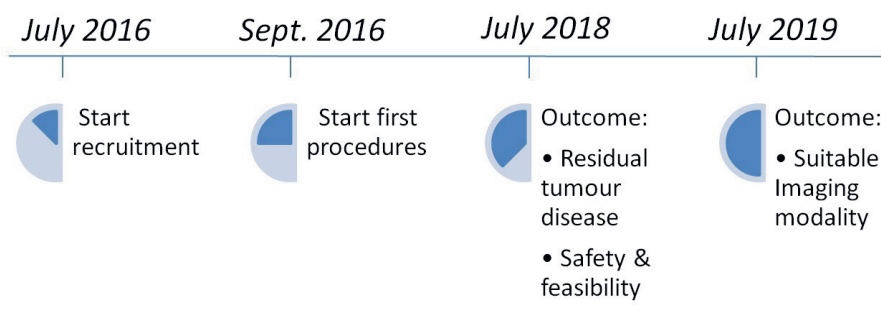


Fig. 3. Planned timeline of recruitment, enrollment, and outcome.

Discussion

Principal Findings

IDEAL phase I research into IRE in renal tumours has shown encouraging short-term outcomes, paving the way for small-scale follow-up studies. In our opinion, it is crucial to prospectively investigate the feasibility, safety and clinical efficacy of IRE in renal tumours to serve as a solid base for a large randomized trial. We aim to determine the clinical effect of IRE by assessing the presence of enhancement on cross-sectional imaging during follow-up as it is advised in thermal ablation [30]. Whereas IRE is a novel ablation technology, posttreatment radiological features in CT scan or MRI are still ill-defined. However, retrospective preliminary research suggests the radiological pattern is similar to the one described after thermal ablation [23].

Limitations

A limitation within our study is the absence of histopathological confirmation post-IRE. In literature, 2 *in vivo* studies have revealed the IRE ablation effects in a histopathologic analysis. The first study resected the renal tumour immediately after ablation, demonstrating preliminary IRE ablation effect on a cellular level. In this study no definite cell death was observed, implying that IRE effects are not directly established. Wendler et al resected the ablated tumours 4 weeks after the IRE procedure, showing that the ablation zone covered the renal tumours completely. Nonetheless, within the ablation zone very small residues of tumour have been found of uncertain malignancy [22] in 3 cases described. Studies in animal models have demonstrated that the effect of IRE is partially achieved after 3 to 4 weeks [31-33]. Yet resecting ablated RCCs in humans after longer than 4 weeks is not acceptable when ablation is used in a curative setting. Hence, the only way to provide insight into the clinical value of these minimal tumour residues is to thoroughly follow patients with intensive imaging studies after IRE ablation. Even though renal mass biopsy during the follow-up targeting the ablation zone may contribute to histopathological confirmation, it would have brought additional burden in a fragile population and would not have been an irrefutable proof of complete ablation. Therefore, as provided by the consensus that ablation success in kidney tumours is assessed by radiological characteristics [30], success in our study will be assessed exclusively based on radiological features.

Conclusions

In our study, IRE parameters (1500 V/cm, active tip length 15-25 mm, inter-electrode spacing 1 to 2 cm, 90 treatment pulses after 10 sufficient test pulses) were chosen because several clinical studies confirmed that on a histopathological level the ablation zone is completely ablated within the electrode configuration without leaving skip lesions [25,28]. Due to the small sample size and the design of the study, we do not intend to explore different IRE configurations and probe settings.

IRE promises consistent ablation results due to its 'nonthermal' character and is therefore theoretically suitable for centrally located tumours. However, recent literature has investigated the temperature rise of IRE ablation in porcine kidneys and livers, demonstrating a significant temperature rise when repetitive high-intensity pulses are applied [21,34]. Al-Sakere et al showed that when a high amount of energy is applied in a small number of pulses, a significant temperature rise occurs (a phenomenon called Joule heating). In current literature, a solution has been suggested in which the same amount of energy is applied in more pulses, which could result in a mild temperature increase [18,35]. Other factors that can influence the temperature in IRE ablation are varying Voltage, pulse length, the distance between electrodes, active tip length, and electrode configuration [35]. Furthermore, early clinical practice of IRE in renal tumours close to vital structures demonstrated that no major complications occurred, suggesting that thermal damage of IRE is not clinically significant, and centrally located tumours are suitable for IRE [24].

For the follow-up of renal masses, the most frequently used imaging modality is contrast-enhanced CT. Multiple studies have demonstrated that MRI and CEUS are adequate imaging techniques for follow-up after IRE [36-40]. However, the use of contrast-enhanced CT scans in the follow-up after kidney ablation might be precluded because of potential nephrotoxicity or ionizing radiation exposure in young patients. In the population of patients that receive ablation for their renal mass comorbidity, older age and decrease in renal function are common since their presence entails a clear indication for ablative therapy. Furthermore, MRI, applicable to a broader range of the ablated population, may not be easily available and may increase costs. Hence, in this population, it is vital to investigate whether other imaging modalities will detect recurrences and residual disease in renal masses with the same accuracy as CT and MRI.

Nononcological outcomes of IRE have been minimally investigated in renal tumours. A total of 2 small studies described serum creatinine levels and demonstrated no significant changes in renal function or transient increase of creatinine which resolved after 1 month [23,24]. Postprocedural pain and length of stay are described by Thomson et al in the liver, kidney,

and lung (N=36, kidney tumours n=4). While 4 patients were admitted longer than 24 hours, none of these patients had kidney tumours.

Postprocedural pain was registered through analgesics use, demonstrating 2 patients who required intravenous or intramuscular analgesics. No patient required prolonged analgesic use after discharge. Quality of life has not been reported in current IRE literature. Insight in non-oncological outcomes, including quality of life, is urgently required since treatment decision making is often influenced by this. Particularly in the ablation population, meaning elderly patients with multiple comorbidities, quality of life after an intervention is of great importance.

Categorized as a level 2 study according to the IDEAL classification, this study will provide prospective information on kidney IRE ablation with an extensive description of the radiological evolution of the ablated lesion along time as well as mid-term oncological outcomes. Lastly, we will provide prospective data on quality of life, kidney function, pain level, and duration of admittance after IRE.

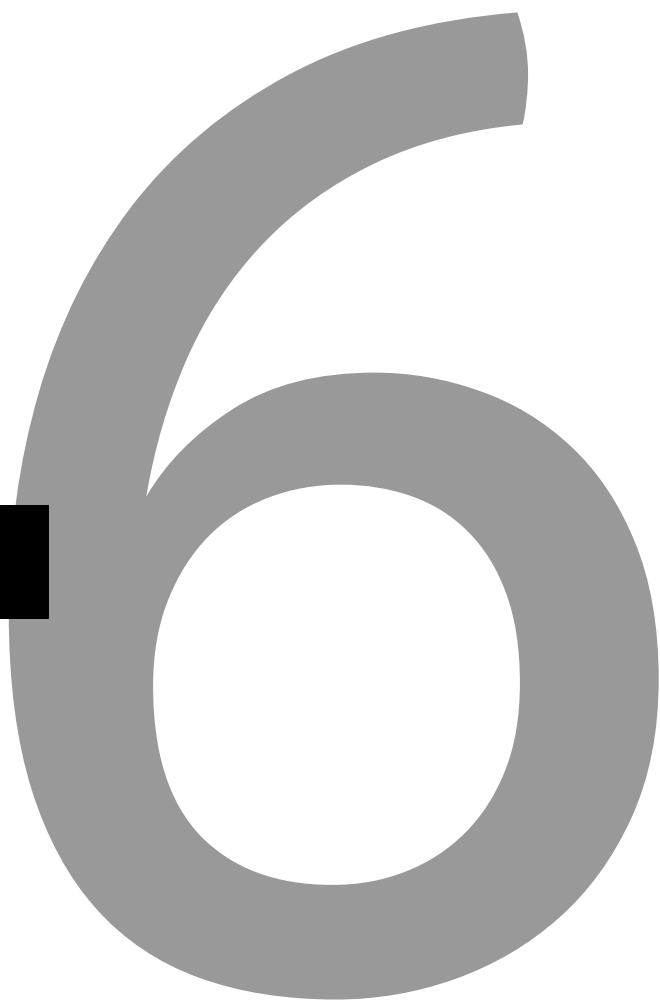
References

1. Chow WH, Devesa SS, Warren JL, Fraumeni JF. Rising incidence of renal cell cancer in the United States. *JAMA* 1999 May 05;281(17):1628-1631. [Medline: 10235157]
2. Hollingsworth JM, Miller DC, Dignault S, Hollenbeck BK. Rising incidence of small renal masses: a need to reassess treatment effect. *J Natl Cancer Inst* 2006 Sep 20;98(18):1331-1334 [FREE Full text] [doi: 10.1093/jnci/djj362] [Medline: 16985252]
3. Jemal A, Siegel R, Xu J, Ward E. Cancer statistics, 2010. *CA Cancer J Clin* 2010;60(5):277-300 [FREE Full text] [doi: 10.3322/caac.20073] [Medline: 20610543]
4. Mathew A, Devesa SS, Fraumeni JF, Chow W. Global increases in kidney cancer incidence, 1973-1992. *Eur J Cancer Prev* 2002 Apr;11(2):171-178. [Medline: 11984136]
5. Volpe A, Cadeddu JA, Cestari A, Gill IS, Jewett MA, Joniau S, et al. Contemporary management of small renal masses. *Eur Urol* 2011 Sep;60(3):501-515. [doi: 10.1016/j.eururo.2011.05.044] [Medline: 21664040]
6. Wagstaff P, Ingels A, Zondervan P, de la Rosette JJM, Laguna M. Thermal ablation in renal cell carcinoma management: a comprehensive review. *Curr Opin Urol* 2014 Sep;24(5):474-482. [doi: 10.1097/MOU.000000000000084] [Medline: 25051022]
7. Katsanos K, Mailli L, Krokidis M, McGrath A, Sabharwal T, Adam A. Systematic review and meta-analysis of thermal ablation versus surgical nephrectomy for small renal tumours. *Cardiovasc Intervent Radiol* 2014 Apr;37(2):427-437. [doi: 10.1007/s00270-014-0846-9] [Medline: 24482030]
8. Hafron J, Kaouk JH. Ablative techniques for the management of kidney cancer. *Nat Clin Pract Urol* 2007 May;4(5):261-269. [doi: 10.1038/ncpuro0802] [Medline: 17483811]
9. Olweny EO, Cadeddu JA. Novel methods for renal tissue ablation. *Curr Opin Urol* 2012 Sep;22(5):379-384. [doi: 10.1097/MOU.0b013e328355ecf5] [Medline: 22706069]
10. Ljungberg B, Bensalah K, Canfield S, Dabestani S, Hofmann F, Hora M, et al. EAU guidelines on renal cell carcinoma: 2014 update. *Eur Urol* 2015 May;67(5):913-924. [doi: 10.1016/j.eururo.2015.01.005] [Medline: 25616710]
11. Van PH, Becker F, Cadeddu JA, Gill IS, Janetschek G, Jewett MA, et al. Treatment of localised renal cell carcinoma. *Eur Urol* 2011 Oct;60(4):662-672. [doi: 10.1016/j.eururo.2011.06.040] [Medline: 21726933]
12. Rubinsky B, Onik G, Mikus P. Irreversible electroporation: a new ablation modality—clinical implications. *Technol Cancer Res Treat* 2007 Feb;6(1):37-48 [FREE Full text] [Medline: 17241099]
13. Davalos RV, Mir IL, Rubinsky B. Tissue ablation with irreversible electroporation. *Ann Biomed Eng* 2005 Feb;33(2):223-231. [Medline: 15771276]
14. Lane BR, Moinedjeh A, Kaouk JH. Acute obstructive renal failure after laparoscopic cryoablation of multiple renal tumours in a solitary kidney. *Urology* 2005 Mar;65(3):593. [doi: 10.1016/j.urology.2004.09.044] [Medline: 15780398]
15. Johnson DB, Solomon SB, Su L, Matsumoto ED, Kavoussi LR, Nakada SY, et al. Defining the complications of cryoablation and radio frequency ablation of small renal tumours: a multi-institutional review. *J Urol* 2004 Sep;172(3):874-877. [doi: 10.1097/01.ju.0000135833.67906.ec] [Medline: 15310987]
16. Ogan K, Jacomides L, Dolmatch BL, Rivera FJ, Dellaria MF, Josephs SC, et al. Percutaneous radiofrequency ablation of renal tumours: technique, limitations, and morbidity. *Urology* 2002 Dec;60(6):954-958. [Medline: 12475648]
17. Deipolyi AR, Golberg A, Yarmush ML, Arellano RS, Oklu R. Irreversible electroporation: evolution of a laboratory technique in interventional oncology. *Diagn Interv Radiol* 2014;20(2):147-154 [FREE Full text] [doi: 10.5152/dir.2013.13304] [Medline: 24412820]
18. Al-Sakere B, André F, Bernat C, Connault E, Opolon P, Davalos RV, et al. Tumour ablation with irreversible electroporation. *PLoS One* 2007;2(11):e1135 [FREE Full text] [doi: 10.1371/journal.pone.0001135] [Medline: 17989772]
19. Olweny EO, Kapur P, Tan YK, Park SK, Adibi M, Cadeddu JA. Irreversible electroporation: evaluation of nonthermal and thermal ablative capabilities in the porcine kidney. *Urology* 2013 Mar;81(3):679-684. [doi: 10.1016/j.urology.2012.11.026] [Medline: 23290141]
20. Pech M, Janitzky A, Wendler JJ, Strang C, Blaschke S, Dudeck O, et al. Irreversible electroporation of renal cell carcinoma: a first-in-man phase I clinical study. *Cardiovasc Intervent Radiol* 2011 Feb;34(1):132-138. [doi: 10.1007/s00270-010-9964-1] [Medline: 20711837]

21. Wagstaff PGK, de Bruin DM, van den Bos W, Ingels A, van Gemert MJC, Zondervan PJ, et al. Irreversible electroporation of the porcine kidney: temperature development and distribution. *Urol Oncol* 2015 Apr;33(4):168.e1-168.e7. [doi: 10.1016/j.urolonc.2014.11.019] [Medline: 25557146]
22. Wendler JJ, Porsch M, Nitschke S, Köllermann J, Siedentopf S, Pech M, et al. A prospective Phase 2a pilot study investigating focal percutaneous irreversible electroporation (IRE) ablation by NanoKnife in patients with localised renal cell carcinoma (RCC) with delayed interval tumour resection (IRENE trial). *Contemp Clin Trials* 2015 Jul;43:10-19. [doi: 10.1016/j.cct.2015.05.002] [Medline: 25962890]
23. Trimmer CK, Khosla A, Morgan M, Stephenson SL, Ozayar A, Cadeddu JA. Minimally invasive percutaneous treatment of small renal tumours with irreversible electroporation: a single-center experience. *J Vasc Interv Radiol* 2015 Oct;26(10):1465-1471. [doi: 10.1016/j.jvir.2015.06.028] [Medline: 26250855]
24. Thomson KR, Cheung W, Ellis SJ, Federman D, Kavounoudias H, Loader-Oliver D, et al. Investigation of the safety of irreversible electroporation in humans. *J Vasc Interv Radiol* 2011 May;22(5):611-621. [doi: 10.1016/j.jvir.2010.12.014] [Medline: 21439847]
25. Wendler JJ, Ricke J, Pech M, Fischbach F, Jürgens J, Siedentopf S, et al. First delayed resection findings after irreversible electroporation (IRE) of human localised renal cell carcinoma (RCC) in the IRENE pilot phase 2a trial. *Cardiovasc Intervent Radiol* 2016 Feb;39(2):239-250. [doi: 10.1007/s00270-015-1200-6] [Medline: 26341653]
26. McCulloch P, Altman DG, Campbell WB, Flum DR, Glasziou P, Marshall JC, et al. No surgical innovation without evaluation: the IDEAL recommendations. *Lancet* 2009 Sep 26;374(9695):1105-1112. [doi: 10.1016/S0140-6736(09)61116-8] [Medline: 19782876]
27. Nielsen K, Scheffer HJ, Vieveen JM, van Tilborg AAJM, Meijer S, van KC, et al. Anaesthetic management during open and percutaneous irreversible electroporation. *Br J Anaesth* 2014 Dec;113(6):985-992 [FREE Full text] [doi: 10.1093/bja/aeu256] [Medline: 25173767]
28. van den Bos W, de Bruin DM, Jurhill RR, Savci-Heijink CD, Muller BG, Varkarakis IM, et al. The correlation between the electrode configuration and histopathology of irreversible electroporation ablations in prostate cancer patients. *World J Urol* 2016 May;34(5):657-664 [FREE Full text] [doi: 10.1007/s00345-015-1661-x] [Medline: 26296371]
29. Schneider M. Characteristics of SonoVue. *Echocardiography* 1999 Oct;16(7, Pt 2):743-746. [Medline: 11175217]
30. Zondervan PJ, Wagstaff PGK, Desai MM, de Bruin DM, Fraga AF, Hadaschik BA, et al. Follow-up after focal therapy in renal masses: an international multidisciplinary Delphi consensus project. *World J Urol* 2016 Dec;34(12):1657-1665 [FREE Full text] [doi: 10.1007/s00345-016-1828-0] [Medline: 27106492]
31. Deodhar A, Monette S, Single GW, Hamilton WC, Thornton R, Maybody M, et al. Renal tissue ablation with irreversible electroporation: preliminary results in a porcine model. *Urology* 2011 Mar;77(3):754-760. [doi: 10.1016/j.urology.2010.08.036] [Medline: 21111458]
32. Wendler JJ, Porsch M, Hühne S, Baumunk D, Buhtz P, Fischbach F, et al. Short- and mid-term effects of irreversible electroporation on normal renal tissue: an animal model. *Cardiovasc Intervent Radiol* 2013 Apr;36(2):512-520. [doi: 10.1007/s00270-012-0452-7] [Medline: 22893419]
33. Tracy CR, Kabbani W, Cadeddu JA. Irreversible electroporation (IRE): a novel method for renal tissue ablation. *BJU Int* 2011 Jun;107(12):1982-1987 [FREE Full text] [doi: 10.1111/j.1464-410X.2010.09797.x] [Medline: 21044244]
34. Faroja M, Ahmed M, Appelbaum L, Ben-David E, Moussa M, Sosna J, et al. Irreversible electroporation ablation: is all the damage nonthermal? *Radiology* 2013 Feb;266(2):462-470. [doi: 10.1148/radiol.12120609] [Medline: 23169795]
35. van den Bos W, Scheffer HJ, Vogel JA, Wagstaff PGK, de Bruin DM, de Jong MC, et al. Thermal energy during irreversible electroporation and the influence of different ablation parameters. *J Vasc Interv Radiol* 2016 Mar;27(3):433-443. [doi: 10.1016/j.jvir.2015.10.020] [Medline: 26703782]
36. Mahmood F, Hansen RH, Agerholm-Larsen B, Jensen KS, Iversen HK, Gehl J. Diffusion-weighted MRI for verification of electroporation-based treatments. *J Membr Biol* 2011 Apr;240(3):131-138 [FREE Full text] [doi: 10.1007/s00232-011-9351-0] [Medline: 21380763]
37. Padia SA, Johnson GE, Yeung RS, Park JO, Hippe DS, Kogut MJ. Irreversible electroporation in patients with hepatocellular carcinoma: immediate versus delayed findings at MR Imaging. *Radiology* 2016 Jan;278(1):285-294. [doi: 10.1148/radiol.2015150031] [Medline: 26523493]
38. van den Bos W, de Bruin DM, van Randen A, Engelbrecht MRW, Postema AW, Muller BG, et al. MRI and contrast-enhanced ultrasound imaging for evaluation of focal irreversible electroporation treatment: results from a phase

- I-II study in patients undergoing IRE followed by radical prostatectomy. *Eur Radiol* 2016 Jul;26(7):2252-2260 [FREE Full text] [doi: 10.1007/s00330-015-4042-3] [Medline: 26449559]
40. Wiggermann P, Zeman F, Niessen C, Agha A, Trabold B, Stroszczynski C, et al. Percutaneous irreversible electroporation (IRE) of hepatic malignant tumours: contrast-enhanced ultrasound (CEUS) findings. *Clin Hemorheol Microcirc* 2012;52(2-4):417-427. [doi: 10.3233/CH-2012-1615] [Medline: 22986756]
41. Niessen C, Jung EM, Beyer L, Pregler B, Dollinger M, Haimerl M, et al. Percutaneous irreversible electroporation (IRE) of prostate cancer: Contrast-enhanced ultrasound (CEUS) findings. *Clin Hemorheol Microcirc* 2015;61(2):135-141. [doi: 10.3233/CH-151985] [Medline: 26410867]

CHAPTER 6



Feasibility and safety of irreversible electroporation (IRE) in patients with small renal masses: Results of a prospective study

M Buijs, PJ Zondervan, DM de Bruin, KP van Lienden, A Bex, OM van Delden

Abstract

Background: Irreversible electroporation (IRE) has the potential to overcome limitations of thermal ablation, enabling small renal mass (SRM) ablation near vital structures.

Purpose: To assess feasibility and safety of percutaneous IRE for the treatment of SRMs.

Materials and methods: This prospective study is a phase 2 trial (NCT02828709) of IRE for patients with SRMs. Primary endpoints are feasibility and safety. Device- and procedural-adverse events were assessed by Clavien-Dindo and Common Terminology Criteria for Adverse Events version 4.0 grading systems. Technical feasibility was assessed by recording the technical success of the procedures. Technical success was evaluated by performing a CT immediately after ablation where complete tumour coverage and nonenhancement were evaluated. Tumour characteristics and patient characteristics, procedural- and anesthesia details, postprocedural events, and perioperative complications were recorded.

Results: Ten SRMs were included with a mean tumour size of 2.2 cm (range 1.1–3.9 cm) were treated with IRE. Renal mass biopsies revealed 7 clear cell and 1 papillary renal cell carcinoma. Two renal mass biopsies were non-diagnostic. The median follow-up was 6 months (range 3–12 months). Technical success was achieved in 9 out of 10 cases. One patient had a grade 3 Clavien-Dindo complication (1/10, 95% Confidence interval (CI) 0.0179–0.4041). Mean anesthesia time was 3.7 hours (range 3–5 hours), mean procedural time was 2.1 hours (range 1 hour 45 minutes–2 hours 30 minutes) and mean ablation time was 50 minutes (range 20 minutes–1 hour 45 minutes). The creatinine preoperative and postoperative (1 week, 3 months, 6 months, and 12 months) did not significantly differ. In total, 8 out of 10 cases did not experience postoperative pain.

Conclusion: IRE in SRMs is safe and feasible. Renal function is not affected by IRE and postoperative pain is rare. Anesthesia time and procedural time are a potential concern.

Introduction

Renal cell carcinoma (RCC) is one of the most lethal malignancies among urological cancers, and its incidence is increasing mainly due to the rise of the small renal masses (SRMs; <4cm) [1]. Thermal ablation is a nephron-sparing, minimal-invasive approach with the aim to obtain local tumour control while maintaining a low toxicity profile. Guidelines generally recommend thermal ablation in elderly, comorbid patients, or in patients with a high risk of complete loss of renal function following surgery [2,3]. Although results are good, thermal ablation still has its limitations including the so-called heat sink effect, in which perfused blood vessels nearby the tumour cause inconsistent ablation effect [4]. Additionally, centrally located tumours are unsuitable for thermal ablation due to damage to the collecting system and the increased risk of bleeding and strictures [5,6].

Irreversible electroporation (IRE) is an electricity-based ablation modality, creating small nanopores in the cell membrane of tumour tissue while sparing connective tissue of the collecting system and vital structures [7]. Few retrospective studies regarding IRE in SRMs in humans have been published on safety and feasibility [8–11]. Translating IRE into clinical practice requires a prospective assessment of its feasibility and safety following the idea, development, exploration, assessment, long-term study (IDEAL) criteria. Hence, phase 2 studies are needed before the implementation of a new technology. The primary objective of this report is to assess feasibility and safety of IRE for the treatment of SRMs in a prospective IDEAL phase 2 study. The secondary objective is to assess the functional outcome by measuring the renal function and postoperative pain.

Materials and methods

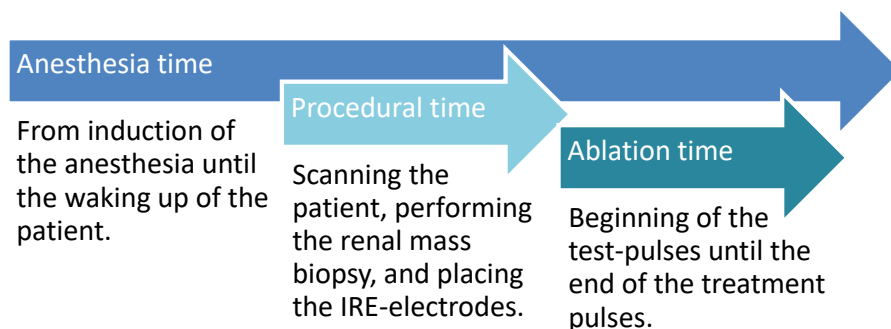
Study design and patients

This prospective, IDEAL phase 2, human, in vivo study on feasibility and safety of IRE in SRMs study was approved by the local Institutional Review Board (2016_55/NCT02828709). The study was implemented according to the study protocol as previously reported [12]. Trial registration has been completed at the Dutch Central Committee on Research Involving Human Subjects (NL56935.018.16, www.ccmo.nl) and in the clinicaltrials.gov database (NCT02828709). This study conforms to the recommendations of the IDEAL collaboration and can be categorized as a phase 2 trial [13]. Primary endpoints were feasibility and safety. All patients gave written informed consent. Inclusion criteria were age ≥ 18 years, a SRM with contrast enhancement on cross-sectional imaging suspect for RCC, signed informed consent, and candidate for ablative therapy. As a part of shared decision making, different treatment options for cT1a tumours were discussed with the patients including surgery, active surveillance, and ablation. The patient indications as well as the post-ablation scans were evaluated by a multidisciplinary kidney

tumour panel including medical oncologists, interventional radiologists, and urologists. Single kidneys were also included as this is an indication for ablative therapy. All patients were admitted the day before the procedure and discharged the day after the procedure. The total sample size was planned on 20 SRMs according to the study protocol.

IRE procedure

Ablation was performed using the IRE device (Nanoknife, AngioDynamics, Queensbury, NY, USA) under general anesthesia with deep muscle relaxation [14]. The console comprises a low energy direct current generator, a footswitch, and 19G monopolar needle electrodes (15 or 25 cm length). IRE electrodes were placed percutaneously under CT guidance by an interventional radiologist experienced in IRE in conjunction with a resident urology and/or urologist. A full neuromuscular blockade was achieved to prevent muscle contraction. Renal mass biopsy (RMB) was performed during the diagnostic workup or during the procedure prior to the ablation. The electrodes were placed to delineate the border between tumour tissue and normal renal parenchyma. Three to 6 electrodes with an active tip exposure of 15 mm to 25 mm, depending on the size of the tumour, were used to deliver pulses. The delivery of pulses was synchronized with the patients' ECG. First, 10 test pulses of 90 ms using $1,500 \text{ V/m}^3$ were administered, after which the Voltage was adjusted to achieve 20 to 40 Ampere. Second, when sufficient Ampere was reached, 90 pulses of 90 ms were administered. When the depth of the tumour exceeded 20-25 mm, a pullback (retraction of electrodes) was performed or the active tip length was adjusted in order to cover the entire tumour. Immediately after ablation, a contrast-enhanced CT was performed to assess the absence of ablation zone enhancement, coverage of the tumour, and to detect acute complications. Ablation time (beginning of the test pulses until the end of the 90 treatment pulses), procedural time (the time for scanning, performing RMB and placing electrodes), and anesthesia time (from induction of anesthesia until the anaesthesiologist transfers the care of the patient to the postanesthesia care unit) were recorded (supplementary Fig. 1). Additionally, perioperative complications and technical success were recorded.



Supplementary Fig. 1: Schematic view of the definitions of the procedural-, ablation- and anesthesia time.

Feasibility and safety

The safety of IRE was assessed by evaluating the device and procedural adverse events (AEs) using the Clavien-Dindo (CD) and Common Terminology Criteria for Adverse Events (CTCAE) version 4.0 grading systems postoperatively and during the follow-up [15–17]. Tumour characteristics were described using the Renal and Padua classification [18,19]. Patient comorbidities were described according to the age-adjusted Charlson comorbidity index (ACCI) [20]. The feasibility of IRE was assessed by recording the technical success of the ablation, determined by obtaining a contrast-enhanced CT immediately after IRE. As instructed by guidelines, technical success was established when ablation was able to treat the tumour according to the protocol, and when the ablation zone covered the whole tumour [21]. Serum creatinine was measured preoperative, and at 1 week, 3 months, 6 months, and 12 months post-IRE. The pain was measured preoperative, and at 1 day, 1 week, 3 months, and 12 months post-IRE.

Results

From September 2016 until January 2018, 10 SRMs were included and treated in 10 treatment sessions (9 patients, 6 male, 3 female; mean age 68 years old [range 60–77 years]). Patient and tumour characteristics are described in Table 1. The median follow-up was 6 months (range 3–12 months). Fig. 1 shows the MRI pre-IRE (tumour) and the post-IRE ablation zone. The renal mass biopsies demonstrated 7 clear cell RCCs, 2 non-diagnostic cases, and 1 papillary RCC. One patient was diagnosed with bilateral SRMs and underwent bilateral ablation on 2 separate treatment sessions (SRM 5 and 6). In total 9 out of 10 SRMs (8 out of 9 patients) were discharged the day after the IRE procedure.

IRE procedure

Ablation and operative data are displayed in Table 2. Mean anesthesia time was 3.7 hours (range 3–4 hours). The mean ablation time was 50 minutes (range 20 minutes–1 hour 45 minutes). The mean procedural time was 2.1 hours (range 1 hour 45 minutes–2 hours 30 minutes).

Safety

All AEs are depicted in Table 3. Five AEs occurred in 4 patients within the first month after ablation. The five AEs consisted of one CD grade 3b (95% CI 0.0179–0.4041), one CD grade 2 (95% CI 0.0179–0.4041), and three CD Grades 1 (95% CI 0.1078–0.6032).

CD grade 3b, CTCAE grade 3: Case 2 had a single kidney and developed an increase in creatinine 1 day after the IRE procedure due to a blood clot that partially obstructed the ureter. A double J ureteric stent was inserted under general anesthesia and admission was prolonged with 6 nights. Subsequently, the renal function returned back to the preoperative level 3 weeks after the procedure and the double J ureteric stent was removed. The patient did not require dialysis and did not have any lasting symptoms.

CD grade 2, CTCAE grade 3: Case 8 developed pyelonephritis 17 days after the IRE procedure, which required admission for 2 nights and IV antibiotics.

Grade 1 CD, Grade 1 CTCAE: Case 8 also developed a perinephric hematoma during the procedure, which was observed on the CT made immediately after ablation (Grade 1 CD, Grade 1 CTCAE). There were no signs of active bleeding. The hematoma was visible on imaging at 1 week post-IRE but was not visible anymore at 3 months post-IRE. Case 9 experienced painful micturition during 3 days after the procedure (Grade 1 CD, Grade 1 CTCAE), which resolved spontaneously within a week after the IRE. Case 7 had an episode of painless hematuria without passage of clots 5 days after ablation, which lasted for 2 days and resolved spontaneously (Grade 1 CD, Grade 1 CTCAE). All patients recovered without any permanent sequela.

In total, 9 out of 10 cases returned back to preoperative renal function 1 week after ablation. All the cases retained preoperative renal function within 3 weeks after ablation. There was no urinary leakage or retention. No patient required dialysis.

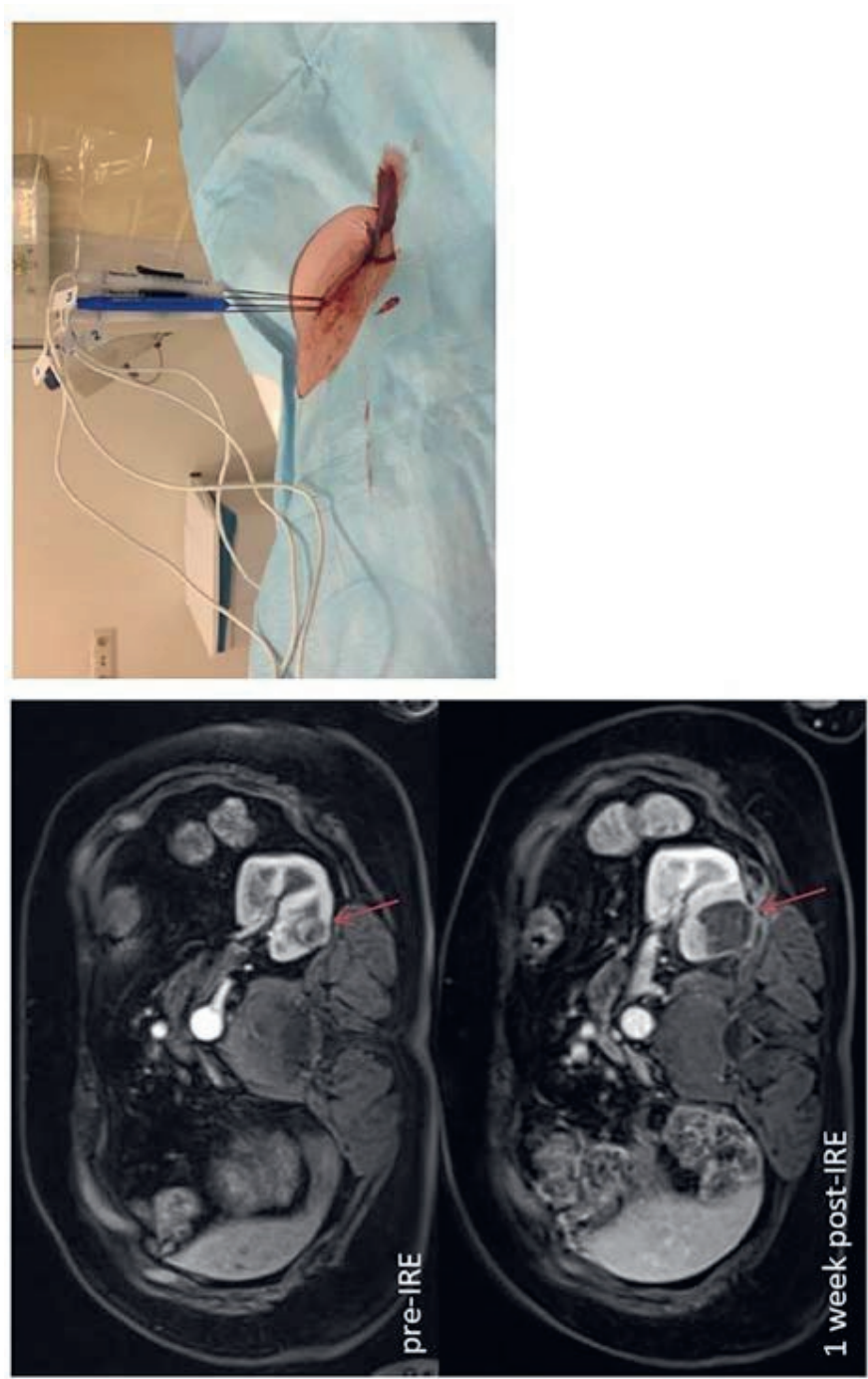


Fig. 1. Left: MRI of pre-IRE tumour (red arrow), MRI and post-IRE ablation zone (red arrow). Right: Picture of IRE electrodes (blue and white) during the procedure. Note the sharp demarcation of the ablation zone. The operator percutaneously applies high Voltage to the tumour. IRE = irreversible electroporation.

Table 1: Patient- and tumour characteristics, IRE data and technical feasibility. RMB: Renal Mass Biopsy; AZ: Ablation Zone; ccRCC: clear cell Renal Cell Carcinoma; pRCC: papillary Renal Cell Carcinoma. A: anterior; p: posterior, x: middle. x*: antioagulant medication stopped before ablation and restarted after ablation. TNM was uniformly used according to the seventh edition of the TNM 2009 classification system.

| | Case 1 | Case 2 | Case 3 | Case 4 | Case 5 | Case 6 | Case 7 | Case 8 | Case 9 | Case 10 |
|---------------------------|-------------------------|-------------|-------------|-------------|-------------|-------------|-------------------------|------------------------|------------|-------------|
| Patient data | | | | | | | | | | |
| Age | 72 | 60 | 68 | 66 | 60 | 60 | 77 | 77 | 70 | 73 |
| Male | x | x | | x | x | x | | | x | x |
| Anticoagulant med | x* | x* | | x | x* | x* | | | x | |
| ACCI | 6 | 7 | 10 | 12 | 5 | 5 | 5 | 10 | 7 | 5 |
| Solitary kidney | | x | x | x | | | | | | |
| Serum creatinine (μmol/L) | 88 | 194 | 85 | 144 | 77 | 82 | 70 | 82 | 122 | 112 |
| Tumour data | | | | | | | | | | |
| size lesion (cm) | 1.8 | 1.5 | 1.8 | 1.7 | 2.7 | 2.8 | 3.9 | 2.3 | 2 | 1.1 |
| dimensions lesion (cm) | 1.8x1.8x2.0 | 1.5x2.0x1.0 | 1.8x1.7x2.1 | 1.7x1.7x1.8 | 2.7x2.4x2.4 | 2.8x2.8x2.6 | 3.9x3.9x3.7 | 2.3x2.3x2.3 | 2x2.1x2.5 | 1.1x1.4x1.4 |
| Side; Location pole | L; middle | R; lower | L; upper | R; middle | R; upper | L; lower | L; central | R; upper | L; lower | L; upper |
| a/p/x | a | p | p | a | p | p | p | p | a | x |
| PADUA | 9 | 8 | 9 | 8 | 9 | 8 | 10 | 7 | 6 | 6 |
| RENAL | 7 | 6 | 6 | 5 | 8 | 6 | 8 | 5 | 5 | 4 |
| Biopsy | ccRCC F2 | ccRCC F2 | ccRCC F3 | ccRCC F2 | pRCC T1 F1 | ND | ND | ccRCC F2 | ccRCC F2 | ccRCC F1 |
| TNM | cT1aG2cN0c | cT1aG2cN0c | cT1aG3pN1p | cT1aG2cN0p | cT1aG1cN0c | cT1aGxcN0c | cT1aGxcN0c | cT1aG2cN0c | cT1aG2cN0c | cT1aG1cN0c |
| | M0 | M0 | M1 | M1 | M0 | M0 | M0 | M0 | M0 | M0 |
| In proximity to | 1mm calyx 12mm colon | 5mm calyx | na | na | na | 5mm calyx | 1mm spleen 1mm calyx | 2mm liver 2mm calyx | 5mm calyx | 5mm colon |

Technical feasibility

Technical success was achieved in 9 out of 10 cases. One patient (Case 7) had a growing and enhancing lesion 3 months after ablation on CT. Retrospective evaluation by the multidisciplinary kidney tumour panel of the procedural CT scan performed immediately after ablation and the CT scan performed 1 week after ablation revealed the residual tumour. This tumour was the largest of the cohort with a size of 3.9 x 3.9 x 3.7 cm.

One technical problem was encountered during the procedure of Case 1. Throughout the ablation, the IRE console measured a high current error between 1 electrode pair during the pullback. Hence, the device was shut down twice during the procedure. The Voltage was reduced to 600 v/ cm³ and the pulses were divided into 3 times 30 pulses instead of 1 time 90 pulses. After this, the procedure was completed without problems.

Table 2: IRE data and operative data. Intervention time: Time for scanning, performing the biopsy, and placing IRE needles. Ablation time: Time for test pulses and treatment pulses. Anaesthesia time: time that patient was under general anaesthesia. Technical success: Coverage of tumour by ablation zone and enhancement, assessed on CT performed immediately after ablation.

| | Case 1 | Case 2 | Case 3 | Case 4 | Case 5 | Case 6 | Case 7 | Case 8 | Case 9 | Case 10 |
|----------------------------------|-------------|-----------|---------------|---------------|-----------|--------------|---------------------------|-----------|-----------|---------------|
| IRE data | | | | | | | | | | |
| No. of electrodes; configuration | 4; square | 4; square | 3; triangular | 3; triangular | 4; square | 4; square | 6; pentagonal with centre | 4; square | 4; square | 3; triangular |
| Pullback | yes | no | no | no | yes | yes | yes | yes | yes | no |
| Tip exposure (cm) | 1.5 | 1.5 | 2.5 | 2.5 | 1.5 | 1.5 | 2.5 | 1.5 | 1.5 | 2.5 |
| Pulse length (µs) | 90 | 90 | 90 | 90 | 90 | 90 | 90 | 90 | 90 | 90 |
| Min Ampere | 19 | 22 | 31 | 21 | 22 | 25 | 22 | 25 | 21 | 28 |
| Max Ampere | 50 | 29 | 41 | 29 | 32 | 35 | 32 | 38 | 41 | 36 |
| Min Voltage | 600 | 1500 | 2250 | 1650 | 1980 | 2850 | 2080 | 1650 | 1620 | 2250 |
| Max Voltage | 2340 | 3000 | 2850 | 2400 | 3000 | 3000 | 2850 | 3000 | 2970 | 3000 |
| Anaesthesia time | 4 hrs | 4.5 hrs | 3 hrs | 3 hrs | 4 hrs | 3 hrs 45 min | 4 hrs | 3 hrs | 4 hrs | 3 hrs |
| Ablation time | 1 hr 45 min | 40 min | 45 min | 30 min | 1 hr | 30 min | 1 hour 20 min | 45 min | 1 hr | 20 min |
| Intervention time | 2 hrs | 3 hrs | 2 hrs | 2 hrs | 2 hrs | 2 hrs 30 min | 1 hour 45 min | 2 hrs | 2 hrs | 1 hr 45 min |
| ECG-abnormalities | no | no | no | no | no | no | no | no | no | no |
| Technical success | yes | yes | yes | yes | yes | yes | no | yes | yes | yes |
| Enhancement AZ | no | no | no | no | no | no | no | no | no | no |
| Coverage of tumour by AZ | yes | yes | yes | yes | yes | yes | no | yes | yes | yes |

Table 3 Adverse events post-IRE.

| Case | AE description | Treatment | Length stay | CD grade | CTCAE Grade |
|------|--|---|-------------|----------|-------------|
| 2 | Increase creatinine due to partially blocked ureter because of a blood clot. 1-day post-IRE until 7 days post-IRE. | JJ inserted under general anaesthesia and prolonged admission | 6 nights | 3b* | 3* |
| 7 | Episode of painless haematuria (light rosé colour). 5 days post-IRE until 7 days post-IRE. | No treatment | NA | 1 | 1 |
| 8 | Perinephric hematoma developed during the electrode placement, which was visible on imaging until 1 week after ablation. | No treatment | NA | 1 | 1 |
| 8 | Pyelonephritis with fever. 17 days post-IRE until 22 days post-IRE. | IV antibiotics and admission | 5 nights | 2* | 3* |
| 9 | Painful micturition. 3 days post-IRE until 5 days post-IRE. | Urine stick and sediment was negative, hence no treatment | NA | 1 | 1 |

NA = not applicable.

* Serious adverse event (SAE).

Functional results

The average creatinine serum was not significantly different pre-IRE vs. 1 week, 3 months, 6 months, and 12 months post-IRE (Fig. 2). In total, 2 out of 10 cases experienced mild to moderate pain at 1-day post-IRE (Case 2 and Case 8). Case 2 had an obstructed ureter by a blood clot (Grade 3 CD) and Case 8 had a perinephric hematoma (Grade 1 CD). In both cases, the pain was resolved 1-week post-IRE.

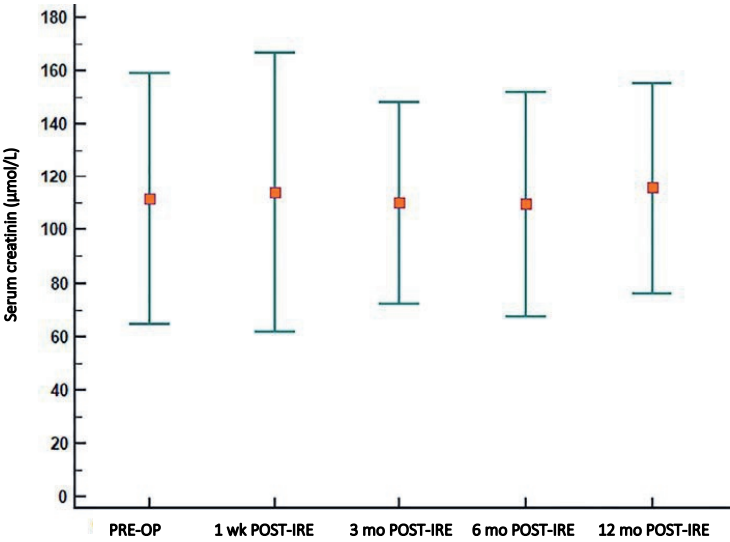


Fig. 2. The serum creatinine in $\mu\text{mol/L}$ (Y-axis) and the timeline (X-axis). Mean creatinine preoperative was $112 \mu\text{mol/L}$ (std dev 19.3 , CI $62.0\text{--}161.3$), mean creatinine 1 week post-IRE was $114.2 \mu\text{mol/L}$ (std dev 21.4 , CI $59.1\text{--}169.2$), mean creatinine 3 months post-IRE was $110.2 \mu\text{mol/L}$ (std dev 15.4 , CI $70.4\text{--}149.9$), mean creatinine 6 months post-IRE was $109.7 \mu\text{mol/L}$ (std dev 17.3 , CI $65.3\text{--}154.1$), and mean creatinine 12 months post-IRE was $115.7 \mu\text{mol/L}$ (std dev 16.2 , CI $74.1\text{--}157.2$). Preoperative vs. 1 week post-IRE, 3 months post-IRE, 6 months post-IRE, and 12 months post-IRE were not significantly different. std dev = standard deviation.

Discussion

IRE is characterised by high-Voltage delivery of electrical pulses, proposing a potentially safe treatment for centrally located tumours, and overcoming limitations of thermal ablation. We report the feasibility and safety of renal IRE in a prospective IDEAL phase 2 study. IRE was feasible for treating SRMs, with a high immediate technical success rate. IRE was well tolerated by patients, even in SRMs located near vital structures.

RCC patients become increasingly more comorbid and older. Shared decision making and patient preferences result in the increased use of ablation. A recent meta-analysis has demonstrated similar recurrence rates and distant metastasis rates for partial nephrectomy vs. thermal ablation. However, the study was limited by heterogeneity among studies and the lack of randomized trials [22]. IRE has been proposed to overcome

the heat sink limitation of thermal ablation. Additionally, centrally located SRMs that face a radical nephrectomy and consequently an impaired renal function can potentially be treated less invasively and in a nephron-sparing manner if IRE proves to be a safe and effective technique [23]. For these SRMs, IRE could potentially be a suitable treatment.

A limitation of our study is the small sample size. This pilot study was intended to precede a larger trial which will emphasize long-term endpoints. At the start of this project IRE for kidney cancer was still in the developmental stage, warranting us to start with a pilot study to prove feasibility and short-term safety before embarking on a larger study with more inclusions. Hence, adhering to IDEAL guidelines, it would not seem ethical to include a large number of patients at this stage. We initially planned to include 20 cases. This number did not contain a formal sample size calculation and was mainly based on previous renal IRE studies, which included 3 to 20 cases [10,11,25,26]. Considering the high immediate technical success rate in the first 10 cases, a larger sample size was not required to prove feasibility. Therefore, we will proceed to a large trial to determine long-term clinical efficacy and safety. An amendment including the reduced sample size and the reason for stopping at 10 patients has been reviewed and accepted by the Institutional Review Board.

To date, no recurrences have occurred in our study population. One patient, Case 7, had a residual tumour on cross-sectional imaging at 3 months post-IRE (1/10). The residual tumour was not biopsy-proven but was highly suspicious on imaging. The patient underwent additional cryoablation and 3 months afterward cross-sectional imaging showed no enhancement. The RMB that was obtained prior to the cryoablation demonstrated a high grade, clear cell RCC.

During the ablation of Case 1, a technical error occurred. Due to the input of high Voltage, the Ampere outcome exceeded the border of 60 Ampere, hence, the device shut down. Adjusting the Voltage input produced a reasonable Ampere (21 Amperes) and still within the borders for adequate tumour destruction (20-40 Ampere). The patient has remained recurrence-free to date.

To date, renal IRE has been prospectively investigated in only 3 studies [8, 10,24] of which 2 studies are an ablate & resect study. It is well known that retrospective safety analysis underreports AEs with high inter-rater variability, and is mainly outcome-driven. Wendler et al. demonstrated in a prospective, ablate & resect study in 7 patients, that IRE results in major damage to tumour tissue while sparing the urine collecting system or allowing for regeneration of the urothelium [7]. Thomson prospectively proved safety and efficacy in 7 patients with kidney tumours [10].

In our prospective study, we demonstrated IRE to be safe. One postoperative CD grade 3 AE occurred (an obstructed ureter by a blood clot) which, given the nature of the event,

seems to be related to the procedure of needle-based ablation, and not specifically to the electricity-based ablation effect. It is thought that the electrode punctured the collecting system, causing a small bleeding in the collecting system. The decrease in renal function was resolved within 3 weeks and the patient did not require dialysis.

Additionally, the pyelonephritis (CD grade 2) occurred 17 days after IRE ablation. Taking the long interval between the infection and the IRE ablation into account, it is uncertain if the infection was a direct result of the percutaneous ablation. Nevertheless, if so, it was a consequence of the ablation, this event seems to be procedure-related and not device-related. A total of 3 CD Grade 1 events occurred and were all transient and self-limiting. The demonstrated toxicity profile seems to be comparable to the renal IRE ablation in the literature [9,10,24,25].

Comorbidity and age generally increase the risk of complications and the ACCI in our population is high (mean ACCI 7 [range 5–12]), designating a high-risk population. Comparing complications with thermal ablation cohorts is therefore challenging, given the lower comorbidity rate and the large cohorts [27].

One case showed a residual tumour in retrospective. This technical failure was probably caused by an incorrect placed electrode, not entirely covering the tumour. This tumour was also the largest of the cohort measuring 3.9 x 3.9 x 3.7 cm and adjacent to the collecting system. The patient preferred additional ablation over surgery and underwent cryoablation of the residual tumour.

The long anesthesia time and procedural time is a potential concern as described earlier by Wendler et al., as increased anesthesia time increases the risk for complications [12]. On the contrary, the ablation time in our series is short with a mean of 50 minutes (range 20 minutes–1 hour 45 minutes). It appears that placing the needles is feasible, but time-consuming due to the need for precise- and multi-needle placement. For IRE specifically, the electrodes have to be placed in the borders of the tumour.

Conclusions

Renal IRE ablation in SRMs is safe and feasible. IRE offers a high immediate technical success rate in SRMs and is well tolerated with a low toxicity profile. Renal function is not affected by IRE. Pain postoperative was rare and only occurred in patients with complications. Long procedural time and anesthesia time is a disadvantage of the technique.

References

1. Siegel RL, Miller KD, Jemal A. Cancer statistics 2016. *CA Cancer J Clin* 2016;66:7–30.
2. Campbell SC, Novick AC, Belldgrun A, et al. Guideline for management of the clinical T1 renal mass. *J Urol* 2009;182:1271–9. <https://doi.org/10.1016/j.juro.2009.07.004>.
3. Ljungberg B, Bensalah K, Canfield S, et al. EAU guidelines on renal cell carcinoma: 2014 update. *Eur Urol* 2015;67:913–24.
4. Lay AH, Faddegon S, Olweny EO, et al. Oncologic efficacy of radio frequency ablation for small renal masses: clear cell vs papillary subtype. *J Urol* 2015;194:653–7. <https://doi.org/10.1016/j.juro.2015.03.115>.
5. Atwell TD, Carter RE, Schmit GD, et al. Complications following 573 percutaneous renal radiofrequency and cryoablation procedures. *J Vasc Interv Radiol* 2012;23:48–54. <https://doi.org/10.1016/j.jvir.2011.09.008>.
6. Littrup PJ, Ahmed A, Aoun HD, et al. CT-guided percutaneous cryotherapy of renal masses. *J Vasc Interv Radiol* 2007;18:383–92. <https://doi.org/10.1016/j.jvir.2006.12.007>.
7. Wendler JJ, et al. Upper-urinary-tract effects after irreversible electroporation (IRE) of human localised renal-cell carcinoma (RCC) in the IRENE pilot phase 2a ablate-and-resect study. *Cardiovasc Interv Radiol* 2017. <https://doi.org/10.1007/s00270-017-1795-x>.
8. Pech M, Janitzky A, Wendler JJ, et al. Irreversible electroporation of renal cell carcinoma: a first-in-man phase I clinical study. *Cardiovasc Interv Radiol* 2011;34:132–8. <https://doi.org/10.1007/s00270-010-9964-1>.
9. Diehl SJ, Rathmann N, Kostrzewa M, et al. Irreversible electroporation for surgical renal masses in solitary kidneys: short-term interventional and functional outcome. *J Vasc Interv Radiol* 2016;27:1407–13. <https://doi.org/10.1016/j.jvir.2016.03.044>.
10. Thomson KR, Cheung W, Ellis SJ, et al. Investigation of the safety of irreversible electroporation in humans. *J Vasc Interv Radiol* 2011;22:611–21. <https://doi.org/10.1016/j.jvir.2010.12.014>.
11. Trimmer CK, Khosla A, Morgan M, et al. Minimally invasive percutaneous treatment of small renal tumours with irreversible electroporation: a single-center experience. *J Vasc Interv Radiol* 2015;26:1465–71. <https://doi.org/10.1016/j.jvir.2015.06.028>.
12. Buijs M, van Lienden KP, Wagstaff PG, et al. Irreversible electroporation for the ablation of renal cell carcinoma: a prospective, human, in vivo study protocol (IDEAL phase 2b). *JMIR Res Protoc* 2017;6: e21. <https://doi.org/10.2196/resprot.6725>.
13. McCulloch P, Altman DG, Campbell WB, et al. No surgical innovation without evaluation: the IDEAL recommendations. *Lancet* 2009;374:1105–12. [https://doi.org/10.1016/S0140-6736\(09\)61116-8](https://doi.org/10.1016/S0140-6736(09)61116-8).
14. Nielsen K, Scheffer HJ, Vieveen JM, et al. Anaesthetic management during open and percutaneous irreversible electroporation. *Br J Anaesth* 2014;113:985–92. <https://doi.org/10.1093/bja/aeu256>.
15. Dindo D. The Clavien–Dindo classification of surgical complications. In: Cuesta MA, Bonjer HJ, eds. *Treatment of postoperative complications after digestive surgery*, London: Springer London; 2014:13–7.
16. National Institute of Cancer. Common terminology criteria for adverse events (CTCAE). NIH Publ 2010;2009:0–71. <https://doi.org/10.1080/00140139.2010.489653>.
17. Mitropoulos D, Artibani W, Graefen M, Remzi M. Guidelines on reporting and grading of complications after urologic surgical procedures. *Eur Urol* 2012;61(2):341–9. <https://doi.org/10.1016/j.eururo.2011.10.033>.
18. Kutikov A, Smaldone MC, Egleston BL, et al. Anatomic features of enhancing renal masses predict malignant and high-grade pathology: a preoperative nomogram using the RENAL nephrometry score. *Eur Urol* 2011;60:241–8. <https://doi.org/10.1016/j.eururo.2011.03.029>.
19. Hew MN, Baseskioglu B, Barwari K, et al. Critical appraisal of the Padua classification and assessment of the R.E.N.A.L. nephrometry score in patients undergoing partial nephrectomy. *J Urol* 2011;186:42–6. <https://doi.org/10.1016/j.juro.2011.03.020>.
20. Radovanovic D, Seifert B, Urban P, et al. Validity of Charlson comorbidity index in patients hospitalised with acute coronary syndrome. Insights from the nationwide AMIS plus registry 2002–2012. *Heart* 2014;100:288–94. <https://doi.org/10.1136/heartjnl-2013-304588>.
21. Ahmed M, Solbiati L, Brace CL, et al. Image-guided tumour ablation: standardization of terminology and reporting criteria—a 10-year update. *Radiology* 2014;273:241–60. <https://doi.org/10.1148/radiol.14132958>.

22. Rivero JR, De La Cerda J 3rd, Wang H, et al. Partial nephrectomy versus thermal ablation for clinical stage t1 renal masses: systematic review and meta-analysis of more than 3,900 patients. *J Vasc Interv Radiol*. 2017. <https://doi.org/10.1016/j.jvir.2017.08.013>.
23. Scosyrev E, Messing EM, Sylvester R, et al. Renal function after nephron-sparing surgery versus radical nephrectomy: results from EORTC randomized trial 30904. *Eur Urol* 2014;65:372–7 <https://doi.org/10.1016/j.eururo.2013.06.044>.
24. Wendler JJ, Ricke J, Pech M, et al. First delayed resection findings after irreversible electroporation (IRE) of human localised renal cell carcinoma (RCC) in the IRENE pilot phase 2a trial. *Cardiovasc Intervent Radiol*. 2015. <https://doi.org/10.1007/s00270-015-1200-6>.
25. Canvasser NE, Sorokin I, Lay AH, et al. Irreversible electroporation of small renal masses: suboptimal oncologic efficacy in an early series. *World J Urol* 2017: 1–7. <https://doi.org/10.1007/s00345-017-2025-5>.
26. Wendler JJ, Ricke J, Pech M, et al. Initial assessment of clinical feasibility, safety and efficacy of NanoKnife irreversible electroporation (IRE) in the focal treatment of localised renal cell carcinoma (RCC) with delayed interval tumour resection (IRENE trial). *Eur Urol Suppl* 2017;16:e102–3. [https://doi.org/10.1016/S1569-9056\(17\)30129-X](https://doi.org/10.1016/S1569-9056(17)30129-X).
27. Psutka SP, Feldman AS, McDougal WS, et al. Long-term oncologic outcomes after radiofrequency ablation for T1 renal cell carcinoma. *Eur Urol* 2013;63:486–92. <https://doi.org/10.1016/j.eururo.2012.08.062>.

7

CHAPTER 7

MRI and CT in the follow-up after irreversible electroporation (IRE) for the treatment of small renal masses

M Buijs, DM de Bruin, PGK Wagstaff, PJ Zondervan, MJV Scheltema, MW Engelbrecht, MP Laguna Pes, KP van Lienden

Abstract

Purpose: Ablation plays a growing role in the treatment of small renal masses (SRMs) due to its nephron-sparing properties and low invasiveness. Irreversible electroporation (IRE) has the potential, although still experimental, to overcome current limitations of thermal ablation. No prospective imaging studies exist of the ablation zone in the follow-up after renal IRE in humans. Objectives are to assess computed tomography (CT) and magnetic resonance imaging (MRI) on the ablation zone volume (AZV), enhancement and imaging characteristics after renal IRE.

Methods: Prospective phase 2 study of IRE in nine patients with ten SRMs. MRI imaging was performed pre-IRE, 1 week, 3 months, 6 months and 12 months after IRE. CT was performed pre-IRE, perioperatively (direct after ablation), 3 months, 6 months and 12 months after IRE. AZVs were assessed by two independent observers. Observer variation was analysed. Evolution of AZVs, and the relation between the needle configuration volume (NCV; planned AZV) and CT- and MRI volumes were evaluated.

Results: Eight SRMs were clear cell renal cell carcinomas, one SRM was a papillary renal cell carcinoma and one patient had a non-diagnostic biopsy. On CT, median AZV increased perioperatively until 3 months post-IRE (respectively, 16.8 cm³ and 6.2 cm³) compared to the NCV (4.8 cm³). On MRI, median AZV increased 1 week post-IRE until 3 months post-IRE (respectively, 14.5 cm³ and 4.6 cm³) compared to the NCV (4.8 cm³). At 6 months the AZV starts decreasing (CT 4.8 cm³; MRI 3.0 cm³), continuing at 12 months (CT 4.2 cm³, MRI 1.1 cm³). Strong correlation was demonstrated between the planning and the post-treatment volumes. Inter-observer agreement between observers was excellent (CT 95% CI 0.82-0.95, MRI 95% CI 0.86-0.96). All SRMs appeared non-enhanced immediately after ablation, except for one residual tumour. Subtraction images confirmed non-enhancement on MRI in unclear enhancement cases (3/9). Directly after IRE, gas bubbles, perinephric stranding and edema were observed in all cases.

Conclusion: The AZV increases immediately on CT until 3 months after IRE. On MRI, the AZV increases at 1 week until 3 months post-IRE. At 6 months the AZV starts decreasing until 12 months post-IRE on both CT and MRI. Enhancement was absent post-IRE, except for one residual tumour. Gas bubbles, perinephric stranding and edema are normal findings directly post-IRE.

Introduction

Given the ageing population and increased incidental detection of small renal masses (≤ 4 cm, SRMs), focal therapies such as cryoablation (CA) and radiofrequency ablation (RFA) gained interest due to their nephron-sparing properties and minimal invasiveness. A potential drawback of CA and RFA is a lower efficacy in the proximity of vessels or the renal collecting system (heat sink effect) [1,2]. This may lead to an inadequate ablation and consequently residual- or recurrent disease [3]. Additionally, vital structures (vessels, collecting system) can be damaged by the thermal process, causing necrosis and leading to perioperative or even long-term complications [4,5]. Irreversible electroporation (IRE), an electricity-based ablation modality, has the potential to circumvent these limitations as collagen structures, extracellular matrix and vital structures appears to be less affected to IRE compared to tumour tissue [6,7].

Multiple studies have shown that renal IRE is safe and feasible [8–12]. Except for one retrospective study with limited follow-up data [8], no previous study focused on the imaging characteristics and volume of the ablation zone (AZ) after renal IRE.

In pancreas, liver and prostate, volume and ablation zone characteristics are investigated and described to guide the follow-up [13–15]. Renal cell carcinoma (RCC) is very different from those tumours and comprises a wide variation of subtypes and inherently clinical behaviour. Real-time image assessment using contrast enhanced computed tomography (CT) is incorporated in renal ablation procedures to evaluate immediate technical success and to detect acute complications. In renal IRE it is yet unknown if the planned ablation size correlates with the definite ablation size, since IRE is an experimental ablation modality. Besides the two-dimensional, schematic needle-position that is created on the IRE generator at time of the ablation, no pre-treatment model exists that can predict the size and volume of the AZ. Currently, imaging in the follow-up is the only feedback on effectivity of the ablation. In order to detect residual disease, early recurrence, and for planning and predicting the AZ, detailed knowledge on the imaging characteristics of post-treatment AZ and their evolution over time is vital. Therefore the objective of this manuscript is to prospectively determine the IRE induced ablation zone volume (AZV) and its evolution over time using CT and magnetic resonance imaging (MRI). Second objective is to prospectively report on the imaging characteristics and enhancement of the AZ using CT and MRI.

Methods:

Study design

This prospective, human, in-vivo, IDEAL (Idea, development, exploration, assessment, long-term study) phase 2 study is approved by the local Institutional Review Board (IRB) (protocol decision number 2016_055). The study was executed according to the study protocol as previously reported [16]. All patients gave written informed consent. Trial registration has been completed at the National Central Committee on Research Involving Human Subjects and in the clinicaltrials.gov database (NCT02828709).

Patients

Patients were consecutively included in the study and treated with percutaneous IRE between September 2016 and January 2018. Recruitment found place at the urology outpatient clinic. Inclusion criteria consisted of age ≥ 18 years, a solid, enhancing SRM on cross-sectional imaging suspicious for RCC, signed informed consent, and candidate for ablative therapy [16]. Exclusion criteria were irreversible bleeding disorder, implantable cardioverter-defibrillator or pacemaker, severe cardiovascular disease, inability to stop anticoagulants (new oral anticoagulants or coumarin derivatives) and inability for deep muscle relaxation and general anaesthesia. The follow-up was 12 months. The indications for ablative therapy as well as the assessments on recurrence and residual diseases on post-IRE scans were evaluated in the multidisciplinary kidney board panel, consisting of interventional radiologists, urologists, nephrologists and oncologists.

IRE procedure

As described in the study protocol [16], IRE ablation was performed using the IRE generator and associated needles (Nanoknife[®], AngioDynamics, Queensbury, New York, United States of America (USA)) under general anesthesia with deep muscle relaxation [17]. The procedure was performed at the interventional radiology department. Prior to the ablation, a renal mass biopsy was performed according to guidelines [18]. IRE electrodes were placed percutaneously under CT guidance by an interventional radiologist experienced in IRE together with an urologist and a urology resident. The electrodes were positioned at the edge of the tumour. Maximum space between the needles was 2 – 2.4 cm. Three to six electrodes with an active tip exposure length of 15 mm to 25 mm, depending on the size of the tumour, were used to deliver the pulses. Immediately after the ablation a contrast-enhanced CT was performed to assess enhancement, volume and characteristics of the perioperative AZ.

Imaging follow-up schedule

Baseline CT- and MRI-imaging were obtained from 1 day to 3 months prior to the ablation. MRI was performed at 1 week, 3 months, 6 months and 12 months post-IRE. CT was performed according to our institutional protocol for follow-up of renal mass ablation at 3 months, 6 months and 12 months post-IRE. As renal ablation patients receive substantial doses of ionizing radiation it was deemed unethical to perform additional CT scan at 1 week post-IRE.

Magnetic Resonance Imaging

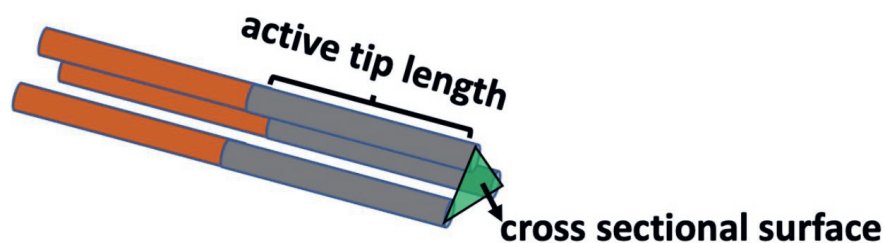
A 1.5 Tesla AVANTO MRI scanner (Siemens Healthcare, Erlangen, Germany) with a surface phased, 16-channel body array matrix coil was utilized. A coronal T2 weighted localizing sequence was performed using fast imaging with balanced steady-state free precession (bSSFP) to confirm kidney location. Transverse diffusion-weighted images (b0, b500 sec/mm²; matrix 134×134; field of view (FOV) 380 mm; slice thickness 6mm) were acquired. Breath-hold T2 weighted bSSFP transverse sequences with and without fat-suppression (matrix 384 x 230; FOV 350 mm; slice thickness 5mm) were acquired, followed by single shot breath hold half fourier acquisition (HASTE) in coronal and transverse planes (Matrix 320 x 256; FOV 400 mm; slice thickness 6mm). Finally, breath-hold transverse unenhanced and contrast-enhanced T1-weighted three-dimensional transverse fat-suppressed spoiled gradient-echo images (matrix 320×240; FOV 400 mm; slice thickness 3mm) were acquired before and at 0, 30, 60 and 90 sec post arrival of contrast in the thoracic aorta. A coronal post-contrast plane was acquired at 90 sec. For contrast enhancement, Gadopentetate dimeglumine 0.2 ml/kg (Gd-DTPA) (Gadovist 1.0, Bayer Pharma, Leverkusen, Germany; 0.1mmol/kg of body weight) was administered at a rate of 2 ml/sec using a power injector (Medrad, Warrendale, Pennsylvania, USA) followed by a 20 ml saline flush.

Computed Tomography

Scans were made on 384-slice CT scanner in supine position (SOMATOM Force, Siemens Healthcare, Erlangen, Germany). The renal tumour protocol consisted of a three phase contrast enhanced CT, with a slice thickness of 3 mm, after injection of 100 mL of contrast agent (Ultravist-300) with 4 mL/sec to achieve enhancement. First, a pre-contrast scan was obtained. The arterial phase and corticomedullary phase were acquired after 45 sec and 90 sec respectively. Patients with an eGFR of 30-60 ml/min/1.73 m² were prehydrated according to our institutional protocol at the time.

Tumour- and ablation zone volume

Volumes were measured using volume software (AGFA IMPAX Client 6.6.1.4024). The volumes were separately measured by two independent observers. The tumour volume (TV) and ablation zone volume (AZV) were measured by the observers, by manually delineating the lesion in every slice on both CT and MRI. Based on this, the volume was calculated using the volume software [19]. The TV and the AZV were measured using the corticomedullary phase and in the dynamic series of CT and MRI respectively. The needle configuration volume (NCV) was defined as the volume between the active needle ends prior to the ablation. The cross-sectional surface between the IRE electrodes given by the software on the IRE console was multiplied by the active tip length (Supplementary Fig. 1). The perioperative AZV was defined as the AZV on contrast-enhanced CT performed at the end of the IRE procedure. The post-IRE AZV was defined as the AZV on cross-sectional imaging performed at 1 week (MRI only), 3 months (MRI and CT), 6 months (MRI and CT) and 12 months (MRI and CT) after IRE.



Supplementary Fig. 1: The needle configuration volume is assessed prior to IRE ablation according to positioned needles. The cross-sectional surface between the IRE electrodes given by the software on the IRE console was multiplied by the active tip length to determine the volume (based on the calculation of the volume of a prism).

Imaging analysis

Characteristics were evaluated by an abdominal radiologist, an interventional radiologist and a resident urology in consensus. On CT, characteristics of the AZ were evaluated. CT enhancement was measured by delineating a region of interest (ROI) within the tumour/AZ. Density measurements were evaluated in hounsfield units (HU). Lesion enhancement was calculated as follows: Three equally spaced CT slices were selected. In each slice a circular region of interest (ROI) was delineated within the AZ, excluding necrotic or cystic areas. The average HU value of all pixels within the three ROIs was calculated and used for analysis. On MRI, signal intensity and diffusion restriction (DR) were evaluated in post-contrast dynamic images, diffusion weighted images (DWI), T2 weighted

imaging, and non-contrast-enhanced sequences. To confirm enhancement subtraction images were made.

Statistical methods

For both CT- and MRI volumes, inter-observer reliability was assessed using the intra-class coefficient (ICC). ICC estimates and their 95% confidence intervals (ICs) were calculated based on mean-rating (k=2), consistency, and two way random-effects model, according to McGraw and Wong [20]. The 95% confidence intervals (CIs) of the ICC estimate guided the interpretation [21]: Values below 0.5 are interpreted as poor reliability, between 0.5 and 0.75 as moderate reliability, between 0.75 and 0.9 as good reliability, and values greater than 0.90 indicated excellent reliability.

Both raters were blinded to each other results. The volume and enhancement measurements were expressed as medians and interquartile range (IQR) since the data were not normally distributed. Comparison of the volume on CT with the volume on MRI per time point was illustrated using Bland-Altman plots. Regression analysis was executed to analyse relation between the planned volumes (NCV), and the CT-AZVs and MRI-AZVs. Statistical analyses were performed using MedCalc Statistical Software for mac, version 15.8 (MedCalc Software, Ostend, Belgium).

Sample size

This imaging study is a part of a safety and feasibility pilot study [16]. For the aim of this study evaluation of ten IRE treated SRMs were required.

Results

Patients

Nine patients with ten SRMs with a median age of 68 years (IQR 60-77) were treated and included. Patient- and tumour characteristics are summarized in table 1 and table 2. Two patients had chronically impaired renal function preoperatively (stage 3B). Three patients had a solitary kidney. The follow-up was 12 months in all patients, except for one patient in whom residual tumour was diagnosed at 3 months. This patient (SRM 7) underwent salvage cryoablation and was therefore excluded from follow-up after 6 months. One patient had a non-diagnostic biopsy during ablation (SRM 6). The same patient was diagnosed with bilateral tumours and underwent bilateral IRE ablation in two separate sessions (SRM 5; right and SRM 6; left). One patient was unable to undergo MRI due to claustrophobia. One pre-IRE MRI was missing as the patient was referred from another hospital.

Table 1: Patient characteristics. *=Anticoagulant medication stopped before ablation and restarted after ablation; Y=yes; N=no; SRM=Small renal mass; ACCI = age-adjusted Charlson comorbidity index; SRM 5 and 6 are respectively the right and left kidney of the same patient

| | SRM 1 | SRM 2 | SRM 3 | SRM 4 | <u>SRM 5</u> | <u>SRM 6</u> | SRM 7 | SRM 8 | SRM 9 | SRM 10 |
|--------------------------------|-------|-------|-------|-------|--------------|--------------|-------|-------|-------|--------|
| <i>Patient characteristics</i> | | | | | | | | | | |
| Age | 72 | 60 | 68 | 66 | 60 | 60 | 77 | 77 | 70 | 73 |
| Male | Y | Y | N | Y | Y | Y | N | N | Y | Y |
| Solitary kidney | N | Y | Y | Y | N | N | N | N | N | N |
| Serum creatinine (µmol/L) | 88 | 194 | 85 | 144 | 77 | 82 | 70 | 82 | 122 | 112 |
| Anticoagulant meds | Y* | Y* | N | Y | Y* | Y* | N | N | Y | N |
| Age-adjusted CCI | 6 | 7 | 10 | 12 | 5 | 5 | 5 | 10 | 7 | 5 |

Table 2: Tumour characteristics. A = anterior; P=posterior; AZ = ablation zone; ccRCC = clear cell renal cell carcinoma; pRCC = papillary renal cell carcinoma; IRE = irreversible electroporation; RMB = renal mass biopsy; na: not applicable; SRM=Small renal mass; cm=centimeter; PADUA= Preoperative Aspects and Dimensions Used for an Anatomical; RENAL score = Radius (tumour size as maximal diameter), Exophytic/endophytic properties of the tumour, Nearness of tumour deepest portion to the collecting system or sinus, Anterior (a)/posterior (p) descriptor and the Location relative to the polar line. SRM 5 and 6 are respectively the right and left kidney of the same patient.

| | SRM 1 | SRM 2 | SRM 3 | SRM 4 | SRM 5 | SRM 6 | SRM 7 | SRM 8 | SRM 9 | SRM 10 |
|--|------------------|------------------|------------------|------------------|------------------|------------------|------------------|------------------|------------------|------------------|
| <i>SRM characteristics</i> | | | | | | | | | | |
| Diameter (cm) | 1.8 | 1.5 | 1.8 | 1.7 | 2.7 | 2.8 | 3.9 | 2.3 | 2 | 1.1 |
| Dimensions (cm) | 1.8x1.8x2.0 | 1.5x2.0x1.0 | 1.8x1.7x2.1 | 1.7x1.7x1.8 | 2.7x2.4x2.4 | 2.8x2.8x2.6 | 3.9x3.9x3.7 | 2.3x2.3x2.3 | 2x2.1x2.5 | 1.1x1.4x1.4 |
| Side; Location pole | L; interpolar | R; lower | L; upper | R; interpolar | R; upper | L; lower | L; central | R; upper | L; lower | L; upper |
| A/P/X | a | p | p | a | p | p | p | p | a | x |
| PADUA | 9 | 8 | 9 | 8 | 9 | 8 | 10 | 7 | 6 | 6 |
| RENAL | 7 | 6 | 6 | 5 | 8 | 6 | 8 | 5 | 5 | 4 |
| Biopsy | ccRCC F2 | ccRCC F2 | ccRCC F3 | ccRCC F2 | pRCC T1 F1 | ND | ccRCC F2 | ccRCC F2 | ccRCC F2 | ccRCC F1 |
| In proximity to vital structure | 1mm from calyx | 5mm from calyx | na | na | na | 5mm from calyx | 1mm from spleen | 2mm from liver | 5mm from calyx | 5mm from colon |
| | 12mm from colon | | | | | | 1mm from calyx | 2mm from calyx | | |
| TNM | cT1aG2cN0c M0 | cT1aG2cN0c M0 | cT1aG3pN1p M1 | cT1aG2cN0p M1 | cT1aG1cN0c M0 | cT1aGxcN0c M0 | cT1aGxcN0c M0 | cT1aG2cN0c M0 | cT1aG2cN0c M0 | cT1aG1cN0c M0 |

CT for the evaluation of IRE

Tumour and ablation zone volume

ICC was 0.91 (95% CI 0.82-0.95). The median tumour volume (TV) on CT is 9.5 cm³ (IQR 7.1-14.4 cm³). The median NCV is 4.8 cm³ (IQR 3.6-9.4 cm³). The median perioperative AZV (immediately after ablation) is 16.8 cm³ (IQR 14.3-19.6 cm³) and 3.5 times larger compared to the NCV. At 3 months post-IRE the median AZV is 6.2 cm³ (IQR 4.4-9.4 cm³). At 6 months and 12 months the median AZV was 4.8 cm³ (IQR 3.9-7.4 cm³), and 4.2 cm³ (IQR 2.5-5.5 cm³), respectively. Volume outcomes are described in Fig. 1 and table 3 respectively.

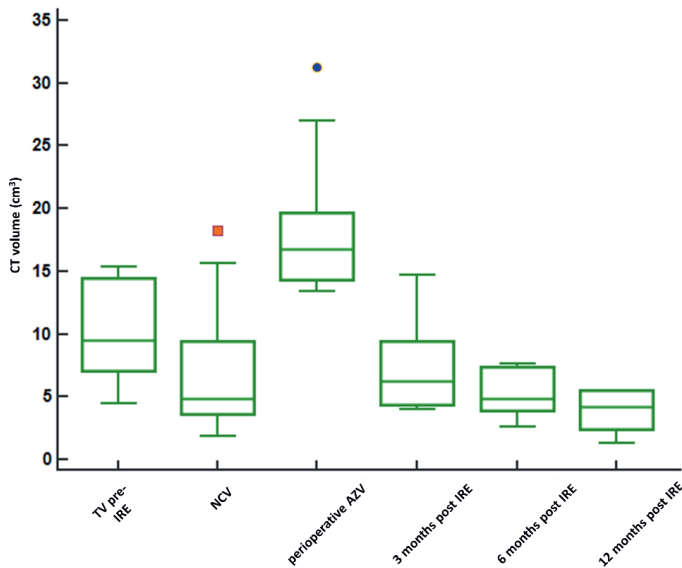


Fig. 1a: CT volumes in cm³ over time (median, 25th-75th percentile). On X-axis from left to right: Tumour volume (TV) pre-IRE 9.5 cm³ (IQR 7.1-14.4 cm³); Needle configuration volume (NCV) 4.8 cm³ (IQR 3.6-9.4 cm³); Perioperative ablation zone volume immediately after ablation (perioperative AZV) 16.8 cm³ (IQR 14.3-19.6 cm³); 3 months post-IRE AZV 6.2 cm³ (IQR 4.4-9.4 cm³); 6 months post-IRE AZV 4.8 cm³ (IQR 3.9-7.4 cm³); 12 months post-IRE AZV 4.2 cm³ (IQR 2.5-5.5 cm³). One outlier resembles SRM 7 with an initial tumour size of 3.9x3.9x3.7 cm.



Fig. 1b: Evolution through time of CT ablation zone. From left to right: Tumour pre-IRE (4.5 cm³); Perioperative ablation zone immediately after ablation (14.8 cm³); 3 months post-IRE ablation zone (4.4 cm³); 6 months post-IRE ablation zone (3.9 cm³); 12 months post-IRE ablation zone (2.5 cm³). Notice the proximity of the tumour pre-IRE (green arrow) and the ablation zone post-IRE (orange arrow) to the ureter (yellow arrow) and the renal vasculature in the hilum (blue arrow).

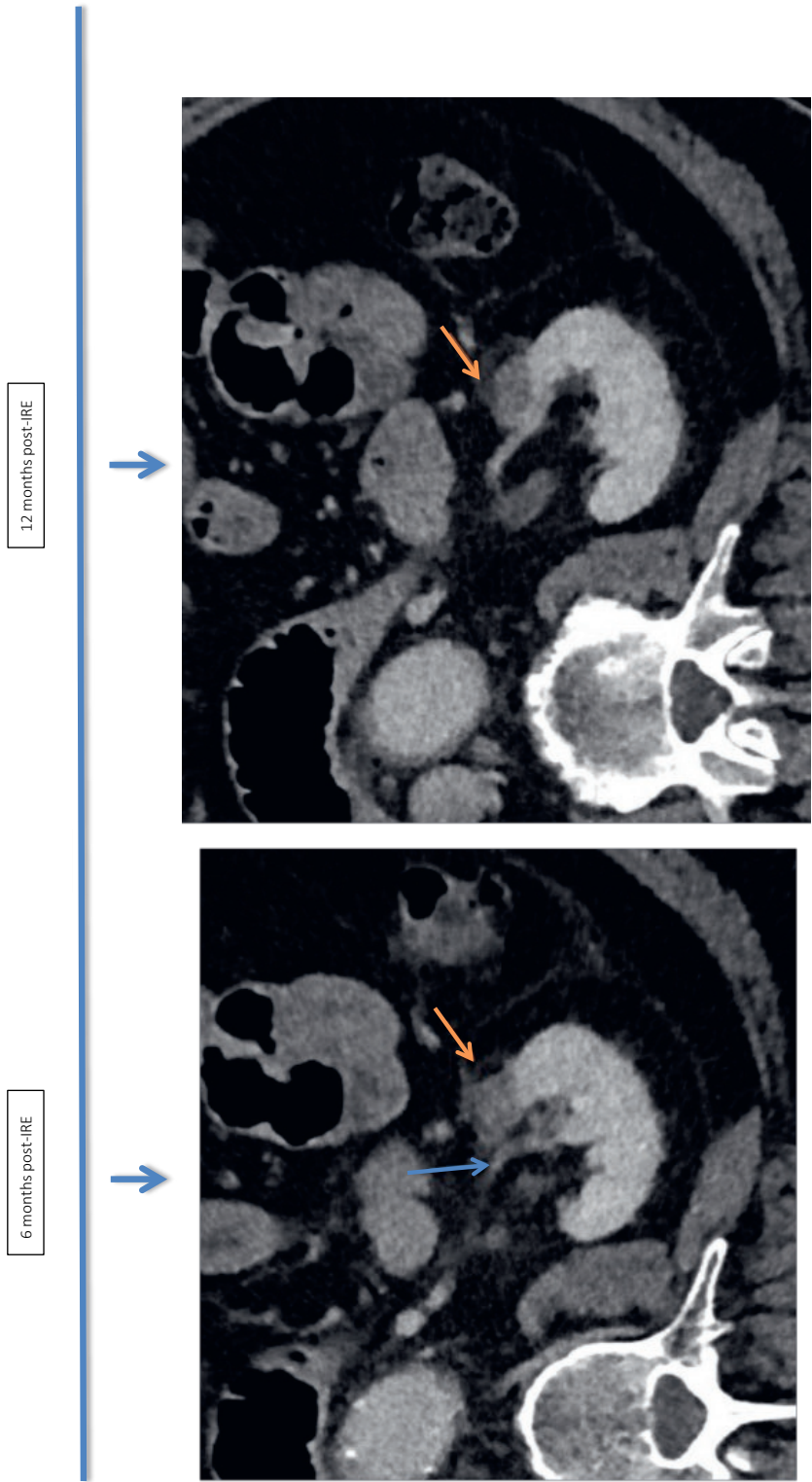


Fig. 1b: Evolution through time of CT ablation zone. From left to right: Tumour pre-IRE (4.5 cm³); Perioperative ablation zone immediately after ablation (14.8 cm³); 3 months post-IRE ablation zone (4.4 cm³); 6 months post-IRE ablation zone (3.9 cm³); 12 months post-IRE ablation zone (2.5 cm³). Notice the proximity of the tumour pre-IRE (green arrow) and the ablation zone post-IRE (orange arrow) to the ureter (yellow arrow) and the renal vasculature in the hilum (blue arrow).

Ablation zone enhancement and characteristics

Pre-IRE, median tumour enhancement was 92 HU (IQR 62-193 HU). The perioperative AZ showed a median decrease in enhancement to 44 HU (IQR 37-54 HU). At 3 months post-IRE, the median AZ enhancement was 37 HU (IQR 35-52 HU), at 6 months post-IRE the median AZ enhancement was 42 HU (IQR 39-67 HU) and at 12 months was 44 HU (IQR 37-45 HU). Enhancement data are depicted in Fig. 2.

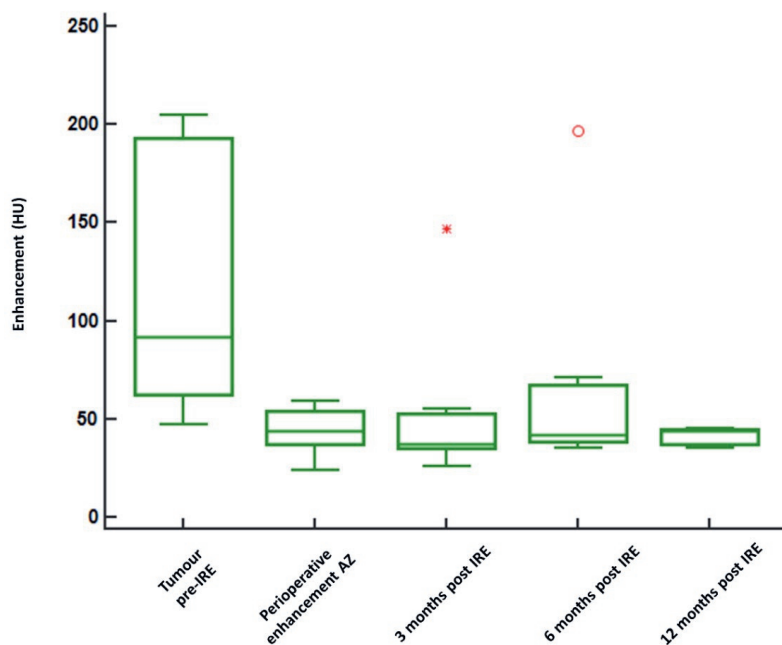


Fig. 2: CT enhancement in Hounsfield Units (HU) over time (median, 25th-75th percentile). On X-axis from left to right: Tumour enhancement pre-IRE 92 HU (IQR 62-193 HU); perioperative enhancement of ablation zone immediately after ablation (perioperative enhancement AZ) 44 HU (IQR 37-54 HU); 3 months post-IRE enhancement 37 HU (IQR 35-52) HU; 6 months post-IRE enhancement 42 HU (IQR 39-67 HU); 12 months post-IRE enhancement 44 HU (IQR 37-45 HU). The outlier at 3 months post-IRE and 6 months post-IRE is the residual tumour of SRM 7.

In the perioperative AZ we observed 'gas bubbles' in proximity of, and within, the ablation zone in all cases (10/10) (Fig. 3). On the contrast-enhanced, perioperative CT-scan performed directly after ablation, there was clearly an ablated tumour visible, which could be distinguished from the edema/inflammation surrounding the ablated tumour in majority of cases (6/10) (Fig. 4). Perinephric stranding developed immediately after ablation which persisted and gradually reduced during the follow-up of 12 months (10/10) (Fig. 3 and fig. 4).

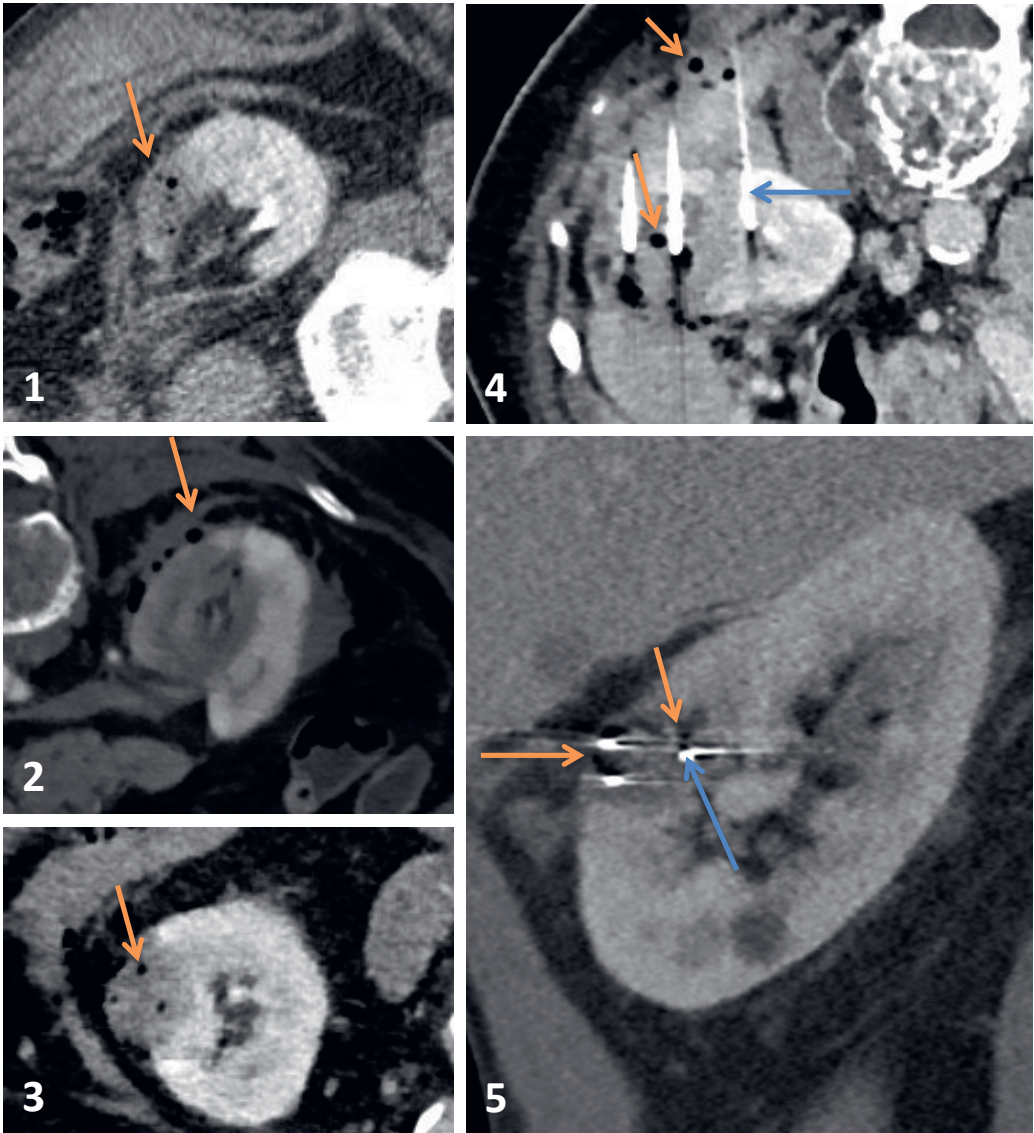


Fig. 3: CT effects of IRE perioperatively (immediately after ablation): Notice the gas bubbles (orange arrows) in and around the hypodense ablation zone. Blue arrows point out the IRE electrodes punctured in the border of the the tumour.

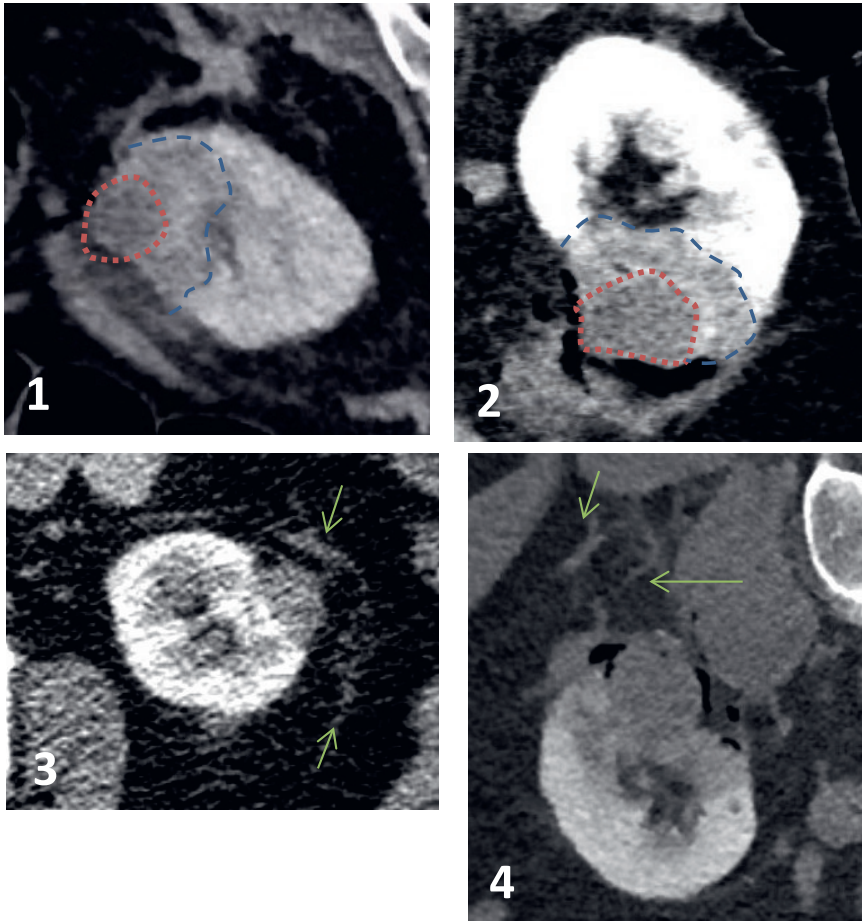


Fig. 4: CT effects of IRE perioperatively. 1 en 2: CT scan performed perioperatively in SRM 10 and 6 respectively. Red lining indicates the hypodense ablated tumour. Blue lining indicates the oedematous and inflammation tissue surrounding it, also hypodense but less grey. 3: CT scan performed 3 months post-IRE in SRM 8. Green arrows indicate the perinephric stranding. 4: CT scan performed perioperatively in SRM 5. Green arrows outlining the perinephric stranding.

MRI for the evaluation of IRE

Tumour- and ablation zone volume

ICC was 0.92 (95% CI 0.86-0.96). The median TV on MRI pre-IRE was 7.1 cm³ (IQR 2.6-11.4 cm³). The median NCV is 4.8 cm³ (IQR 3.6-9.4 cm³). The median volume post-IRE at 1 week was 14.5 cm³ (IQR 12.0-30.4 cm³) and 3 times larger when compared to the NCV. At 3 months post-IRE the median volume was 4.6 cm³ (IQR 2.6-12.8 cm³), at 6 months post-IRE 3.0 cm³ (IQR 1.5-6.8 cm³), and at 12 months post-IRE 1.1 cm³ (IQR 0.9-4.5 cm³). Volume outcomes are described in Fig. 5 and Table 3 respectively.

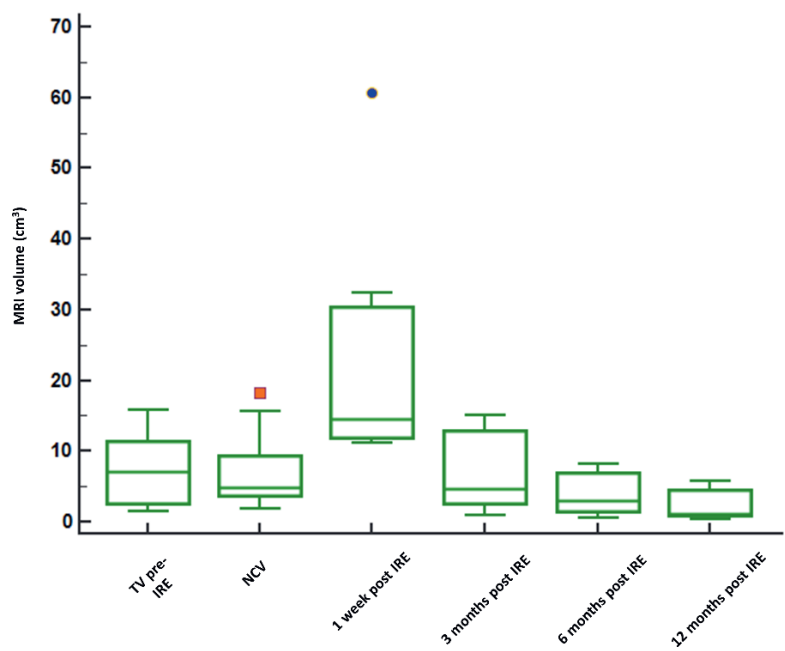


Fig. 5a: MRI volumes in cm³ over time (median, 25th-75th percentile). On X-axis from left to right: Tumour volume (TV) pre-IRE 7.1 cm³ (IQR 2.6-11.4 cm³); needle configuration volume (NCV) 4.8 cm³ (IQR 3.6-9.4 cm³); 1 week post-IRE volume 14.5 cm³ (IQR 12.0-30.4 cm³); 3 months post-IRE volume 4.6 cm³ (IQR 2.6-12.8 cm³); 6 months post-IRE volume 3.0 cm³ (IQR 1.5-6.8 cm³); 12 months post-IRE volume 1.1 cm³ (IQR 0.9-4.5 cm³). One outlier resembles SRM 7 with an initial tumour size of 3.9x3.9x3.7 cm and was the residual tumour diagnosed at 3 months

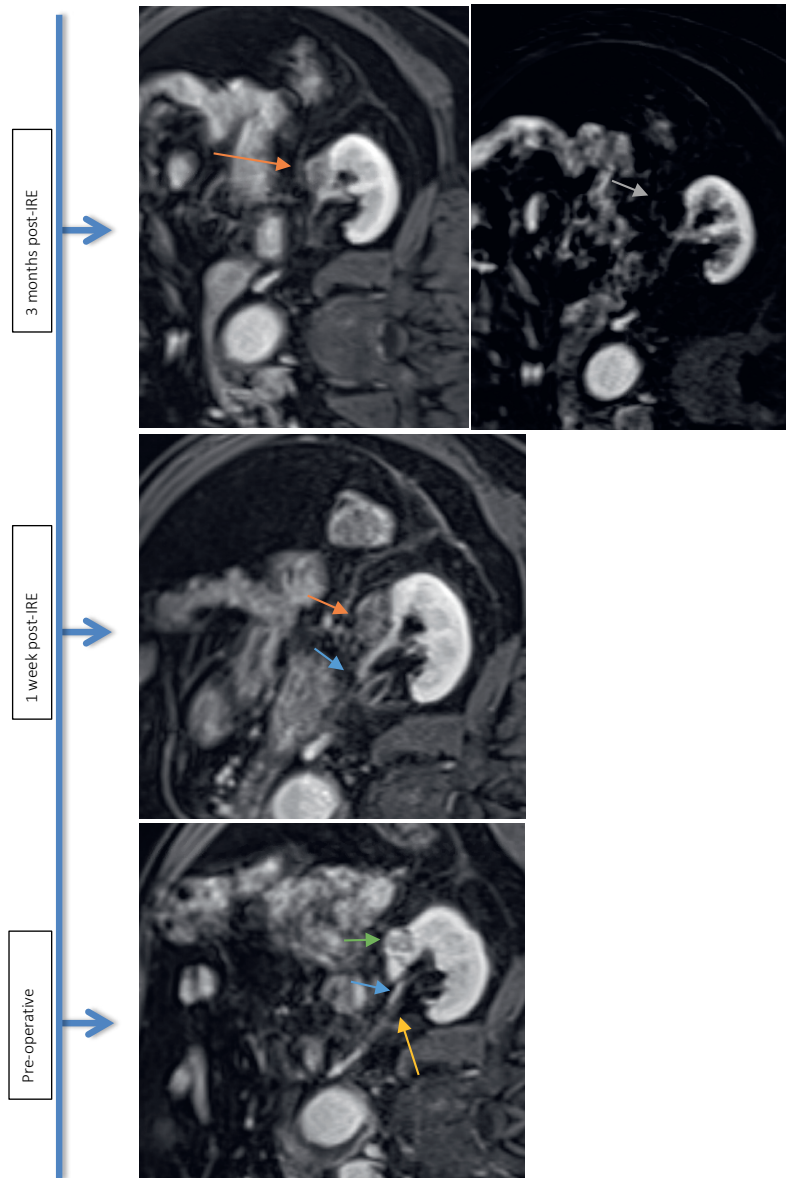


Fig. 5b: Evolution through time of MRI ablation zone. The lower row of images resemble subtraction images to clarify possible enhancement of the ablation zone seen on post-contrast dynamic images (upper row). From left to right: Tumour pre-IRE (PA: clear cell RCC, volume 3.4 cm³). Notice the proximity of the tumour (green arrow) and the ablation zone post-IRE (orange arrow) to the ureter (yellow arrow) and the renal vasculature of the hilum (blue arrow). 1 week post-IRE ablation zone (volume 11,3 cm³). 3 months post-IRE ablation zone (volume 4,3 cm³). 6 months post-IRE ablation zone (volume 3,6 cm³). 12 months post-IRE ablation zone (volume 1,3 cm³).

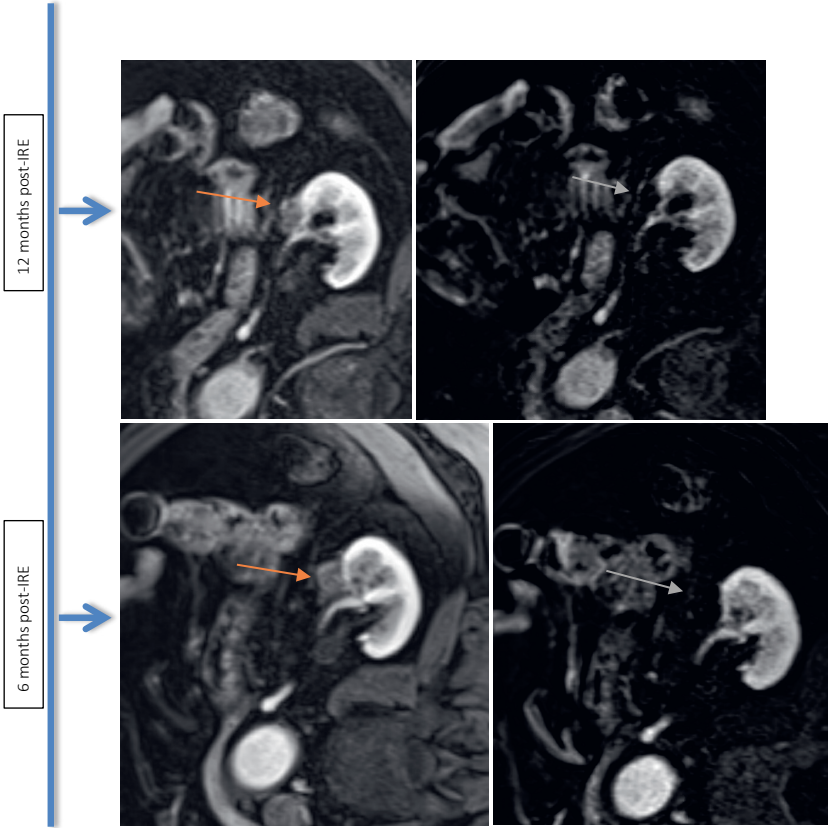


Fig. 5b: Evolution through time of MRI ablation zone. The lower row of images resemble subtraction images to clarify possible enhancement of the ablation zone seen on post-contrast dynamic images (upper row). From left to right: Tumour pre-IRE (PA: clear cell RCC, volume 3,4 cm³). Notice the proximity of the tumour (green arrow) and the ablation zone post-IRE (orange arrow) to the ureter (yellow arrow) and the renal vasculature of the hilum (blue arrow). 1 week post-IRE ablation zone (volume 11,3 cm³). 3 months post-IRE ablation zone (volume 4,3 cm³). 6 months post-IRE ablation zone (volume 3,6 cm³). 12 months post-IRE ablation zone (volume 1,3 cm³).

Table 3. Comparison of volumes between timepoints.

| Timepoint | Median (IQR) in cm ³ |
|--|---------------------------------|
| CT Tumour volume (TV) | 9.5 (7.1-14.4) |
| Needle configuration volume (NCV) | 4.8 (3.6-9.4) |
| CT Perioperative ablation zone volume (peri-AZV) | 16.8 (14.3-19.6) |
| CT 3-months post-IRE ablation zone volume (3-AZV) | 6.2 (4.4-9.4) |
| CT 6-months post-IRE ablation zone volume (6-AZV) | 4.8 (3.9-7.4) |
| CT 12-months post-IRE ablation zone volume (12-AZV) | 4.2 (2.2-5.5) |
| MRI Tumour volume (TV) | 7.1 (2.6-11.4) |
| Needle configuration volume (NCV) | 4.8 (3.6-9.4) |
| MRI 1-week post-IRE ablation zone volume (1w-AZV) | 14.5 (12.0-30.4) |
| MRI 3-months post-IRE ablation zone volume (3-AZV) | 4.6 (2.6-12.8) |
| MRI 6-months post-IRE ablation zone volume (6-AZV) | 3.0 (1.5-6.8) |
| MRI 12-months post-IRE ablation zone volume (12-AZV) | 1.1 (0.9-4.5) |

Imaging characteristics

Pre-IRE:

Seven SRMs showed enhancement in the arterial phase on T1volumetric interpolated breath-hold examination (VIBE) (7/8), which was confirmed by subtraction images (7/8). Three SRMs showed presence of focal DR (3/8). For the non-contrast-enhanced phase, 4 SRMs were isointense, 2 SRMs were hypo-intense, and 2 SRMs were hyperintense. For the T2 weighted, 2 SRMs were isointense, 3 SRMs were hypointense, 3 SRMs were hyperintense.

Post-IRE:

Non-contrast-enhanced phase: After ablation, most AZ's developed to hyperintensity through the follow-up of 12 months (6/9). Other AZ's developed hyperintensity but resolved after 1 week- 3 months and became isointense (3/9).

T1 VIBE: All AZ's were non-enhanced post-IRE, with the exception of the residual tumour. Eight SRMs showed non-enhancement 1 week after ablation in the arterial phase and remained like this until the end of the study (8/9). In three out of those eight non-enhancing Subtraction images confirmed the non-enhancement in all nine SRMs. One SRM contained residual tumour (SRM 7) (1/9) showing heterogeneous signal at 1 week and persisting enhancement from 3 months on.

Diffusion weighted images: In the majority of the SRMs there was no presence of focal DR post-IRE. In the minority of cases presence of focal DR was seen at one time point but was transient. In seven SRMs there was no DR during the entire follow-up of 1 year post-IRE (7/9). In 3 SRMs, there was presence of focal DR at 1 week-3 months but resolved after this follow-up visit.

T2 weighted imaging: The majority of masses were hypointense after ablation (7/9). In the minority there was heterogeneous signal, which evolved to hypointensity in time (2/9).

Comparison planned volumes, AZVs- MRI and AZVs- CT

Regression analyses of MRI and CT plotted against the NCV showed a moderate to strong positive correlation for both CT and MRI, with larger intercepts for CT than for MRI in every time point (Fig. 6). Bland-Altman plots of CT and MRI per time point showed a mean difference (estimated bias) of -0.7 cm³ for the tumour volume prior to ablation, -0.7 cm³ at 3 months post-IRE, -0.18 cm³ at 6 months post-IRE and 0.52 cm³ at 12 months post-IRE (Fig.7).

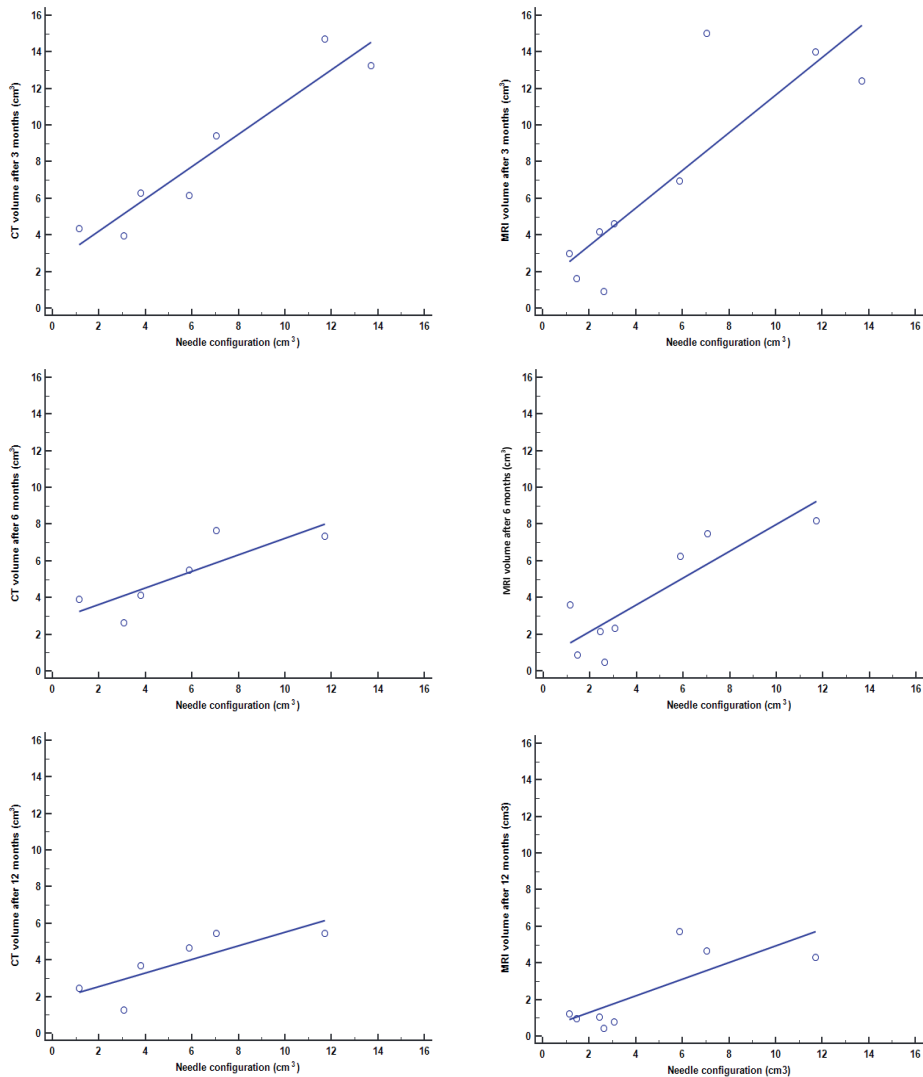


Fig. 6: Fig. 6: Scatterplots of 3-months, 6-months, and 12-months post-IRE for CT volumes and MRI volumes correlated to the needle configuration volume (NCV).

A: $r=0.9$ with a slope 0.88 and an intercept of 2.5 , resulting in $y= 2.5 + 0.88x$
B: $r=0.69$ with a slope 0.45 and an intercept of 2.8 , resulting in $y= 2.8 + 0.45x$

C: $r=0.65$ with a slope 0.37 and an intercept of 1.8, resulting in $y = 1.8 + 0.37x$
 D: $r=0.74$ with a slope 1.03 and an intercept of 1.4, resulting in $y = 1.4 + 1.03x$
 E: $r=0.75$ with a slope 0.73 and an intercept of 0.71, resulting in $y = 0.71 + 0.73x$
 F: $r=0.60$ with a slope 0.46 and an intercept of 0.39, resulting in $y = 0.39 + 0.46x$

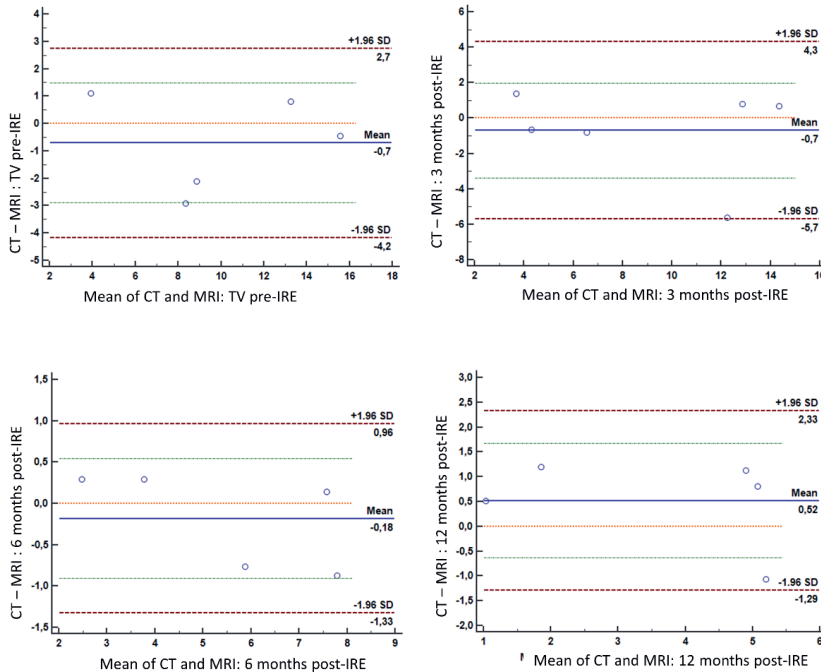


Fig. 7: Bland-Altman plot per time point of CT vs MRI. From left to right: A mean difference (estimated bias) of -0.7 cm^3 of the tumour volume prior to ablation, -0.7 cm^3 at 3 months post-IRE, -0.18 cm^3 at 6 months post-IRE, and 0.52 cm^3 at 12 months post-IRE.

Discussion

This prospective study assessed MRI and CT imaging pre- and post-IRE treatment for SRMs. There was no loss to follow-up and the follow-up visits were planned according to regularly scheduled timepoints, as in clinical practice. Expertise on pre- and post-IRE MRI and CT images is an unmet need for planning renal IRE ablation, and for determination of the ablation response and treatment effect [20].

We reported an increase of the AZV on respectively CT and MRI immediately after ablation until 1 week post-IRE and 3 months post-IRE. At 6 months, the AZV started to decrease in comparison to the perioperative AZV, 1-week and 3 months post-IRE AZV. This decrease continued until the end of the study at 12 months. The increase of the ablation zone can be clarified by possible edema, reactive inflammation tissue and transient hyperaemia. The increase is consistent with previous articles: Trimmer et al reported this increase in a retrospective patient series [8]. Other authors demonstrated an increase and subsequently

a decrease of lesion size after renal ablation, although these observations were in pigs [21,22]. In other organs, such as pancreas and prostate, this is in human investigated and similarly reported the increase [13,14].

Second, all SRMs appeared non-enhanced 1 week after ablation until the end of the study on MRI and CT, except for one patient with a residual tumour. In case of unclear tumour enhancement (3/9), subtraction images were especially helpful confirming (non-)enhancement (Fig 5b). One patient (SRM 7) had a residual tumour, diagnosed at 3 months post-IRE and biopsy confirmed during her salvage cryoablation (clear cell renal Cell carcinoma Fuhrman grade 3). This patient resembles an outlier in volumes and enhancement post-IRE. The tumour size was 3.9cm x 3.9cm x 3.7 cm, hence this was the largest in our cohort. Literature has shown that tumours of 4cm or larger decreases the effectiveness of IRE [23], emphasizing that we should be cautious in future with ablating large tumours since the produced electrical field is more difficult to control. Another possibility is that the residual disease may be the result of a malposition of one of the IRE electrodes.

Several other MRI sequences like the non-contrast enhanced-, diffusion weighted-, and T2-weighted images were analysed but did not appear to have an additional value. Obviously, the sample size of our pilot study is small, therefore these conclusions should be interpreted with caution.

We attempted to compare CT with MRI to evaluate if both imaging techniques deviate from each other and therefore may be more suitable for IRE follow-up. The Bland-Altman plots demonstrated that after renal IRE the MRI volumes were slightly larger than the CT volumes. The regression analysis showed a strong correlation between the needle configuration volume (the planned volume) and the post-treatment volumes for most of the timepoints. According to these regression analyses, CT volumes appeared slightly larger than MRI volumes. Again, our sample size is small hence reliable conclusions are not yet to be drawn based on this cohort. When looking at the evaluation of visual characteristics after renal IRE, MRI had an advantage over CT. When there were doubts about recurrences or residual tumour due to unclear enhancement, which is more than often the case after ablation due to reactive edema or inflammation tissue, the subtraction images of MRI were able to differentiate between the latter.

On both MRI and CT, the TV appears larger than the NCV. Based on previous experiments in porcine kidney, we assumed that the eventual ablation zone exceeds the NCV with approximately 5 mm in every direction [24]. This has never been properly investigated for renal IRE in humans, hence those calculations were not taken into account for our NCV. However, in prostatic IRE studies in humans this has been confirmed with histopathology correlation [13].

Although we had a vulnerable study population including 3 solitary kidneys, IRE was well-tolerated. Two patients had a grade 3 adverse event according to the Common Terminology Criteria for Adverse Events (CTCAE). One patient with a solitary kidney experienced pain and had an impaired renal function due to a blood clot which partially obstructed the ureter postoperative. After a double J ureteral stent was inserted his renal function returned to preoperative levels (CTCAE grade 3). One patient had a pyelonephritis 17 days after the ablation requiring admission for 2 nights and IV antibiotics (CTCAE grade 3). Three patients had a CTCAE grade 1 adverse event (macroscopic hematuria, painful micturition, perinephric hematoma). The renal functions of all patients returned to pre-operative levels. All patients recovered from their minor or major complication without any lasting symptoms.

Our study is limited by a small sample size as the primary objective of the study was to assess technical feasibility and safety. The second objective was to evaluate the use of several imaging modalities, including CT and MRI, on the visualization of the ablation zone in the follow-up after renal IRE. For determining AZVs in imaging after IRE, several studies have demonstrated that correlation is excellent in a small number of cases [13,25].

Another limitation is the comparison of multiple types of NCVs (2-6 needle configurations). For uniformity of the ablation zones, ideally the same number of needles should be used in every patient. As IRE was used as a curative treatment in our trial and differently sized tumours were included, it was considered unethical to use the same NCV for every tumour.

At last, our study is limited by a lack of histopathologic confirmation during follow-up. Generally, guidelines recommend renal mass biopsies only in case of suspicion on cross-sectional imaging [18]. Ideally, for optimal correlation of CT and MR images with histopathology, this would have required a nephrectomy or at least routine biopsies. Considering that this population was extremely vulnerable, we decided not to obtain histopathology.

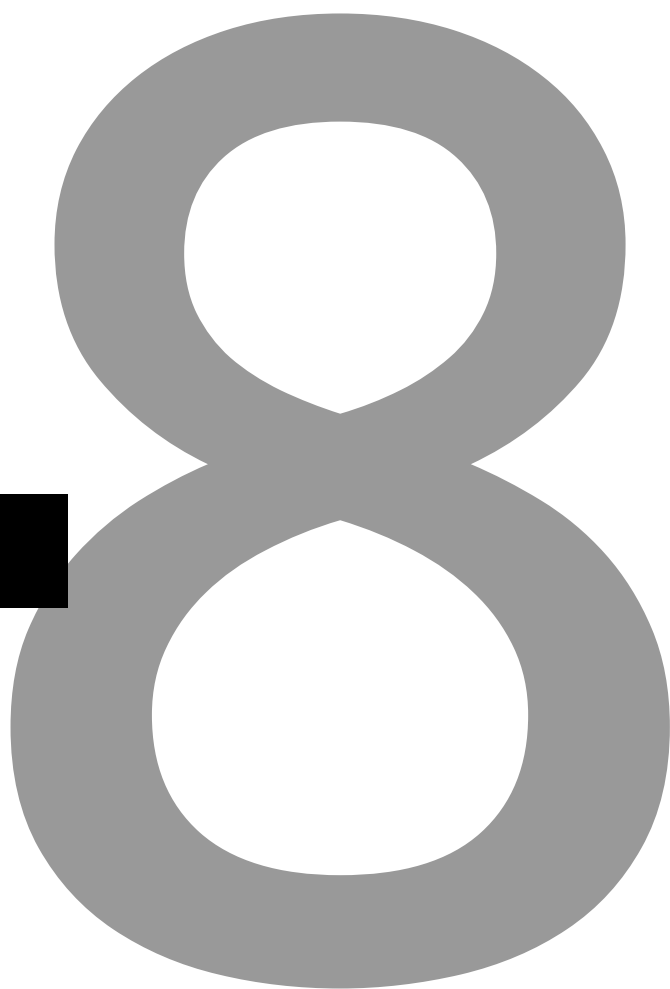
We have quantified the ablation zone post-IRE in SRMs. With this, we are providing a foundation for larger trials to further investigate follow-up imaging after renal IRE, and providing guidance to clinicians for planning IRE ablation and monitoring response. In conclusion, the AZV increases after renal IRE ablation. At 6 months the decrease of the AZV starts gradually until 12 months. Enhancement was absent post-IRE, except for one patient showing residual tumour. On MRI, subtraction images can be used to confirm (non-)enhancement accurately and hence may be applied as a predictor for residual disease or early recurrences. Gas bubbles, perinephric stranding and edema are normal findings on CT and MRI after renal IRE.

References

- Pillai,K., Akhter,J., Chua,T.C., et al. (2015) Heat sink effect on tumour ablation characteristics as observed in monopolar radiofrequency, bipolar radiofrequency, and microwave, using ex vivo calf liver model. *Medicine*; 2015: 94.
- Chu,K.F. and Dupuy,D.E. (2014) Thermal ablation of tumours: biological mechanisms and advances in therapy. *Nature Reviews Cancer*; 2014: 14.
- Ringe,K.I., Lutat,C., Rieder,C., Schenk,A., Wacker,F. and Raatschen,H.-J. (2015) Experimental evaluation of the heat sink effect in hepatic microwave ablation. *PLoS One*, **10**, e0134301.
- Park,B.K. and Kim,C.K. (2009) Complications of image-guided radiofrequency ablation of renal cell carcinoma: Causes, imaging features and prevention methods. *Eur. Radiol.*, **19**, 2180–2190. <https://doi.org/http://dx.doi.org/10.1007/s00330-009-1399-1> <http://www.ncbi.nlm.nih.gov/pubmed/2009420726>
- Gervais,D.A., Arellano,R.S., McGovern,F.J., McDougal,W.S. and Mueller,P.R. (2005) Radiofrequency ablation of renal cell carcinoma: part 2, Lessons learned with ablation of 100 tumours. *AJR Am J Roentgenol*, **185**, 72–80. <https://doi.org/10.2214/ajr.185.1.01850072> <http://www.ncbi.nlm.nih.gov/pubmed/15972401>
- Wendler,J.J., Pech,M., Friebe, B., et al. (2017) Upper-Urinary-Tract Effects After Irreversible Electroporation (IRE) of Human Localised Renal-Cell Carcinoma (RCC) in the IRENE Pilot Phase 2a Ablate-and-Resect Study. *Cardiovasc Interv. Radiol.*, 10.1007/s00270-017-1795-x. <https://doi.org/10.1007/s00270-017-1795-x>
- Rubinsky,B., Onik,G. and Mikus,P. (2007) Irreversible electroporation: A new ablation modality - Clinical implications. *Technol. Cancer Res. Treat.*, **6**, 37–48. <https://doi.org/10.1177/153303460700600106> <http://www.ncbi.nlm.nih.gov/pubmed/17241099>
- Trimmer,C.K., Khosla,A., Morgan,M., Stephenson,S.L., Ozayar,A. and Cadeddu,J.A. (2015) Minimally Invasive Percutaneous Treatment of Small Renal Tumours with Irreversible Electroporation: A Single-Center Experience. *J Vasc Interv Radiol*, **26**, 1465–1471. <https://doi.org/10.1016/j.jvir.2015.06.028> <http://www.ncbi.nlm.nih.gov/pubmed/26250855>
- Tracy,C.R., Kabbani,W. and Cadeddu,J.A. (2011) Irreversible electroporation (IRE): A novel method for renal tissue ablation. *BJU Int.*, **107**, 1982–1987. <https://doi.org/10.1111/j.1464-410X.2010.09797.x> <http://www.ncbi.nlm.nih.gov/pubmed/21044244>
- Thomson,K.R., Cheung,W., Ellis,S.J., Federman,D., Kavnoudias,H., Loader-Oliver,D., et al. (2011) Investigation of the safety of irreversible electroporation in humans. *J. Vasc. Interv. Radiol.*, **22**, 611–621. <https://doi.org/10.1016/j.jvir.2010.12.014> <http://www.ncbi.nlm.nih.gov/pubmed/21439847>
- Wendler,J.J., Ricke,J., Pech,M., Fischbach,F., Jürgens,J., Porsch,M., et al. (2017) Initial assessment of clinical feasibility, safety and efficacy of NanoKnife irreversible electroporation (IRE) in the focal treatment of localised renal cell carcinoma (RCC) with delayed interval tumour resection (IRENE trial). *Eur. Urol. Suppl.*, **16**, e102–e103. [https://doi.org/10.1016/S1569-9056\(17\)30129-X](https://doi.org/10.1016/S1569-9056(17)30129-X)
- Buijs,M., Zondervan,P.J., de Bruin,D.M., van Lienden,K.P., Bex,A. and van Delden,O.M. (2019) Feasibility and safety of irreversible electroporation (IRE) in patients with small renal masses: Results of a prospective study. *Urol. Oncol. Semin. Orig. Investig.*, **37**, 183.e1-183.e8. <https://doi.org/10.1016/j.urolonc.2018.11.008>
- van Den Bos,W., de Bruin,D.M., van Randen,A., Engelbrecht,M.R.W., Postema,A.W., Muller,B.G., et al. (2015) MRI and contrast-enhanced ultrasound imaging for evaluation of focal irreversible electroporation treatment: results from a phase I-II study in patients undergoing IRE followed by radical prostatectomy. *Eur. Radiol.*, 10.1007/s00330-015-4042-3. <https://doi.org/10.1007/s00330-015-4042-3> <http://www.ncbi.nlm.nih.gov/pubmed/26449559>
- Vroomen,L.G.P.H., Scheffer,H.J., Melenhorst,M.C.A.M., de Jong,M.C., van Den Bergh,J.E., van Kuijk,C., et al. (2016) MR and CT imaging characteristics and ablation zone volumetry of locally advanced pancreatic cancer treated with irreversible electroporation. *Eur. Radiol.*, 10.1007/s00330-016-4581-2. <https://doi.org/10.1007/s00330-016-4581-2> <http://www.ncbi.nlm.nih.gov/pubmed/27659702>
- Barabasch,A., Distelmaier,M., Heil,P., Krämer,N.A., Kuhl,C.K. and Bruners,P. (2016) Magnetic Resonance Imaging Findings After Percutaneous Irreversible Electroporation of Liver Metastases: A Systematic Longitudinal Study. *Invest. Radiol.*, **52**, 1. <https://doi.org/10.1097/RLI.0000000000000301> <http://www.ncbi.nlm.nih.gov/pubmed/27379698>

16. Buijs,M., van Lienden,K.P., Wagstaff,P.G., Scheltema,M.J., de Bruin,D.M., Zondervan,P.J., et al. (2017) Irreversible Electroporation for the Ablation of Renal Cell Carcinoma: A Prospective, Human, In Vivo Study Protocol (IDEAL Phase 2b). *JMIR Res. Protoc.*, **6**, e21. <https://doi.org/10.2196/resprot.6725> <http://www.ncbi.nlm.nih.gov/pubmed/28209559>
17. Nielsen,K., Scheffer,H.J., Vieveen,J.M., van Tilborg,A.A.J.M., Meijer,S., van Kuijk,C., et al. (2014) Anaesthetic management during open and percutaneous irreversible electroporation. *Br. J. Anaesth.*, **113**, 985–992. <https://doi.org/10.1093/bja/aeu256> <http://www.ncbi.nlm.nih.gov/pubmed/25173767>
18. Ljungberg,B., Albiges,L., Bensalah,K., Bex,A., Giles,R., Hora,M., et al. (2018) EAU Guidelines on Renal Cell Carcinoma 2018. *Euro Urol*, **29**, 451–458. <http://www.ncbi.nlm.nih.gov/pubmed/1064520>
19. Monsky,W.L., Raptopoulos,V., Keogan,M.T., Doty,D., Kamel,I., Yam,C.S. et al. (2004) Reproducibility of linear tumour measurements using PACS: Comparison of caliper method with edge-tracing method. *Eur. Radiol.*, **14**, 519–525. <https://doi.org/10.1007/s00330-003-2027-0> <http://www.ncbi.nlm.nih.gov/pubmed/14658000>
20. McGraw,K.O. and Wong,S.P. (1996) Forming inferences about some intraclass correlation coefficients. *Psychol. Methods*, **1**, 30.
21. Koo,T.K. and Li,M.Y. (2016) A Guideline of Selecting and Reporting Intraclass Correlation Coefficients for Reliability Research. *J. Chiropr. Med.*, **15**, 155–163. <https://doi.org/10.1016/j.jcm.2016.02.012> <http://www.ncbi.nlm.nih.gov/pubmed/27330520>
22. Solomon,S.B. and Silverman,S.G. (2010) Imaging in interventional oncology. *Radiology*, **257**, 624–640. <https://doi.org/10.1148/radiol.10081490> <http://www.ncbi.nlm.nih.gov/pubmed/21084414>
23. Wendler,J.J., Porsch,M., Hühne,S., Baumunk,D., Buhtz,P., Fischbach,F., et al. (2013) Short- and mid-term effects of irreversible electroporation on normal renal tissue: An animal model. *Cardiovasc. Intervent. Radiol.*, **36**, 512–520. <https://doi.org/10.1007/s00270-012-0452-7> <http://www.ncbi.nlm.nih.gov/pubmed/22893419>
24. Deodhar,A., Monette,S., Single,G.W., Hamilton,W.C., Thornton,R., Maybody,M., et al. (2011) Renal tissue ablation with irreversible electroporation: Preliminary results in a porcine model. *Urology*, **77**, 754–760. <https://doi.org/10.1016/j.urol.2010.08.036> <http://www.ncbi.nlm.nih.gov/pubmed/21111458>
25. Kingham,T.P., Karkar,A.M., D’Angelica,M.I., Allen,P.J., Dematteo,R.P., Getrajdman,G.I., et al. S(2012) Ablation of perivascular hepatic malignant tumours with irreversible electroporation. *J. Am. Coll. Surg.*, **215**, 379–387. <https://doi.org/10.1016/j.jamcollsurg.2012.04.029> <http://www.ncbi.nlm.nih.gov/pubmed/22704820>
26. Wagstaff,P.G.K., de Bruin,D.M., van den Bos,W., Ingels,A., van Gemert,M.J.C., Zondervan,P.J., et al. (2014) Irreversible electroporation of the porcine kidney: Temperature development and distribution. *Urol. Oncol.*, **10.1016/j.urolonc.2014.11.019**. <https://doi.org/10.1016/j.urolonc.2014.11.019> <http://www.ncbi.nlm.nih.gov/pubmed/25557146>
27. Scheltema,M.J., Postema,A.W., de Bruin,D.M., Buijs,M., Engelbrecht,M.R., Laguna,M.P., et al. (2017) Irreversible electroporation for the treatment of localised prostate cancer: A summary of imaging findings and treatment feedback. *Diagnostic Interv. Radiol.*, **23**. <https://doi.org/10.5152/dir.2017.16608>
28. Perzyna,B. and Stolzmann,W. (2018) EAU Guidelines on Renal Cell Carcinoma 2018. **29**, 451–458. <http://www.ncbi.nlm.nih.gov/pubmed/1064520>

CHAPTER 8



Concluding remarks and future perspectives

Optical coherence tomography (OCT)

In this thesis, we investigated the diagnostic value of percutaneous, needle-based, optical coherence tomography (OCT) for the diagnosis of renal cell carcinoma (RCC), filling the gap between cross-sectional imaging and histopathologic diagnosis. We assessed the diagnostic accuracy, defined as the sensitivity, specificity, negative predictive value (NPV), and positive predictive value (PPV), and the diagnostic yield of OCT in a patient cohort of 95 patients with a renal mass (RM). This was compared with the pathology of their renal mass biopsy (RMB). The OCT data were analysed using quantitative analysis by measuring the μOCT of the RMs. We utilized this to develop μOCT cut-off values for diagnosing RCC, paving the way for diagnosing kidney cancer through OCT.

Accuracy of OCT was high (sensitivity 92%; specificity 67%; PPV 95%; NPV 55%), indicating the potential of OCT for diagnosing kidney cancer. The NPV and specificity of RMB remain higher than OCT (OCT 55% and 67% vs RMB 89% and 100%). Although these diagnostic accuracy measures are in favour of RMB, the accuracy calculations typically exclude all the non-diagnostic results. These were higher for RMB than for OCT, translating into a diagnostic yield of 99% for OCT and 79% for RMB. This thesis supports the usefulness of OCT in patients with renal masses and yields a promising balance between accuracy and diagnostic yield.

A beneficial feature of OCT is the real-time visualization and the option for direct adjustment. This means that during an OCT scan, the operator is able to notice that the OCT probe is not (entirely) located in the tumour and therefore has the possibility to reposition the probe. Subsequently, the operator repeatedly performs an OCT scan and re-evaluates the new position of the probe. When properly positioned, the scan can be used for diagnosis. This is also demonstrated by the high diagnostic yield in our study of 99%. In the future, when the proposed cut-off values of μOCT are validated in a larger cohort, they can provide a foundation for automated analysis of the OCT data. This model aims at performing and analyzing the OCT scan 'on the spot', resulting in a real-time diagnosis within minutes. This may even lead to the concept of diagnosis and treatment in one visit: Real-time diagnosis of RCC based on automated, quantitative OCT analysis, and consecutive a percutaneous ablative therapy in the same session. The patient enters the hospital with a renal mass and leaves with a RCC diagnosis and eradication of the tumour on the same day.

An important drawback of OCT during our study is that analysis of the data was not yet optimized: The used 'manual' analysis leaves out a very large portion of all the cross-sectional data (B-scans) that are harvested along the total OCT trajectory of the tumour. With that, a lot of valuable diagnostic information is left out and the μOCT that leads to the

OCT-diagnosis is only based on 5 individual B-scans of suspected lesion within the total data set (\approx 300-500 B-scans). This problem might contribute to the relatively high percentage of false-negative and false-positive OCT scans in our cohort, rendering the low NPV and specificity. This may be solved by a fully automated μ OCT analysis of the complete dataset.

RCC is a heterogeneous malignancy including various subtypes with diverse morphologies and molecular characteristics. Additionally, the intratumour heterogeneity of RCC poses a challenge for a correct sampling of the tumour as well. If the sample, in this case of OCT, is very small this inherently leads to a large margin of error. Future research should focus on including all, or at least the majority of the B-scans of the tumour in the analysis of the OCT data and in this way on contributing to a more representative μ OCT of the tumour. As a result, this may lead to a higher specificity and NPV of OCT.

The success of implementation of a new diagnostic tool into daily clinical practice depends on multiple factors such as costs, practical use, availability of the materials, and of course clinical data such as the accuracy, diagnostic yield, and complication rate or adverse events. All of these characteristics should be compared with the currently used reference test or gold standard. As stated earlier, the accuracy of OCT is proved to be high and may improve as the technology further evolves. Since the quantitative parameter μ OCT can be used for renal mass differentiation, the outcome of OCT is objectified as it is based on numerical cut-off values. Such an analysis is by nature insensitive to interobserver variation, which is a known difficulty in regular pathology analysis.

The OCT procedure itself has a steep learning curve. Additionally, it is well-tolerated by patients owing to the low complication rate. The availability and costs should be further investigated before OCT can be used as a routine test in clinical practice.

Whether OCT will be used as a stand-alone differentiating technique or in combination with other diagnostic tools and/or treatments remains uncertain. Recent research has demonstrated that for the intra-operative assessment of margins of resected renal tumours OCT may be valuable [1], as it can differentiate malignant from benign tissue on a near-microscopic level and potentially prevent residual disease as a result of positive margins. Additionally, in a different scenario, OCT may function as an aid to renal mass biopsies. Since the main disadvantage of renal mass biopsies is the non-diagnostic outcomes, OCT can contribute to the solution of this problem. The non-diagnostic outcomes may be reduced if the OCT probe can be incorporated in a renal mass biopsy needle. In this way, OCT can guide the biopsy needle on a near-microscopic level and locate it precisely into the solid tumour tissue, and avoid sampling necrotic or inflamed tissue.

Irreversible electroporation (IRE)

We prospectively assessed the feasibility and safety of renal IRE in humans in a phase 2 IDEAL study (development phase). The prospect of safely treating renal masses in the proximity to vital structures like the ureter or the collecting system is a unique advantage compared to other ablative techniques with a thermal mechanism. We determined the feasibility of IRE by evaluating the technical success of the IRE ablation itself assessed by a contrast-enhanced CT scan immediately after IRE. Technical success was achieved when the procedure was able to ablate the tumour according to the protocol, and when the ablation zone covered the whole tumour as seen on cross-sectional imaging [2]. The safety of IRE was determined by evaluating the device and procedural adverse events (AEs) within one month after the procedure. We demonstrated a high immediate technical success rate and a low AE rate based on our pilot study of 10 SRMs. Hence, we concluded that IRE was safe and feasible for the treatment of small renal masses (SRMs).

Our study population was a fragile population with multiple comorbidities and an average age-adjusted Charlson comorbidity index (ACCI) of 7, which is not uncommon for patients that qualify for renal ablation. Out of the ten small renal masses (SRMs) that received IRE ablation, 3 were in a solitary functioning kidney (SFK). All patients retained preoperative renal function within 3 weeks after the ablation, demonstrating that IRE did not affect the renal function.

Centrally located renal masses, meaning in the vicinity of the renal hilum, the ureter, and/or the collecting system, remain a challenge among renal mass management. IRE is thought to preserve vital structures like ducts and vessels and is, therefore, able to treat RMs that are centrally located. When evaluating this potential of IRE we treated a group of patients in which 7 out of 9 patients had tumours located close to vital structures. As our complication rate was low, we concluded that in our population IRE was safe. There were two serious adverse events in our study: Acute kidney failure as a result of a partially obstructed ureter due to a blood clot 1 day after IRE ablation, and a pyelonephritis 3 weeks after IRE ablation. The acute kidney failure due to the obstructed ureter was probably the result of an unintended puncture of the urinary tract by one of the IRE electrodes during the procedure that caused an intra-ureteral blood clot, requiring a temporary JJ-stent. This puncture is a risk that is accompanied by any needle-based, percutaneous procedure and would not have been less if cryoablation or RFA was applied. Both patients did not require dialysis and recovered without any lasting symptoms from the complication.

The postulation that IRE can safely ablate in proximity to vital structures is in line with Wendler et al, who demonstrated this on a pathohistological level: They showed preservation and regeneration of the collecting system after renal IRE in swine [3]. This

implies that the demonstrated rise in temperature within the IRE needle configuration by Wagstaff et al [4] does not seem to cause significant damage to the vital structures to the extent that it causes severe, short-term complications or limits the ablation effect. Future research, preferably following the recommendations of the IDEAL collaboration, should confirm this potential advantage.

Limitations of renal IRE are the need of anesthesia and the long procedural time: Mean anesthesia time was 3.7 hours (range 3–5 hours), mean procedural time was 2.1 hours (range 1 hour 45 minutes–2 hours 30 minutes) and mean ablation time was 50 minutes (range 20 minutes–1 hour 45 minutes). The placement of the needles prior to the ablation was complex, as a consequence IRE requires an experienced interventional radiologist. Additionally, the general anesthesia, in particular, the deep muscle relaxation to prevent muscle contractions, may also be time-consuming as it takes time to induce deep sleep and to wake up from this.

A major target for improvement in renal IRE is the optimization of the electric parameters needed to induce an adequate IRE ablation. The amount of Voltage used for the amplitude is entered by the operator into the IRE console. This produces an electrical current of a certain amount of Ampere. The desired height of the Voltage and the Ampere used to achieve adequate RCC destruction is still unknown. The same goes for the pulse length and the number of pulses applied per session. Most of the settings are copied from treatment plans of other tumours (i.e. pancreas carcinoma or colorectal liver metastases). Renal masses have many different pathophysiologically subtypes exhibiting different biological behaviours and therefore display a variable risk of progression and metastasis. Ideally, these electric parameters of IRE should be evaluated per tissue type and tumour type. Electroporation properties may vary amongst different cell types and therefore the clinical effect of IRE may differ. Hence, for optimal tumour destruction, those properties should be evaluated and stratified accordingly. In practice, this means that based on the histopathological results of a RMB, an IRE operator should adapt the amount of Voltage applied, the desired electrical current outcome (Ampere), and the number of pulses and the pulse length.

The electrical parameters are closely related to another underexposed subject around IRE, specifically the planning of the ablation zone. Ideally, a pre-treatment model should be developed that can simulate the 3D-volume and shape of the ablation zone for every kind of needle configuration (i.e. the number of IRE needles used). This model should also anticipate the tissue type of the ablation target and the physical mechanism of electrical field-tissue interaction. Currently, the planning model that is used on the IRE operator is a 2D, schematic visualization of the planned ablation that only considers the length of the needles, the distance between needles, and the number of needles (Fig. 1). Ideally, the

future model should include the planned 3D volume and visualize this within the CT scan of the patient. In this way, the interventional radiologist can precisely plan and treat different kinds of tumours and shapes.

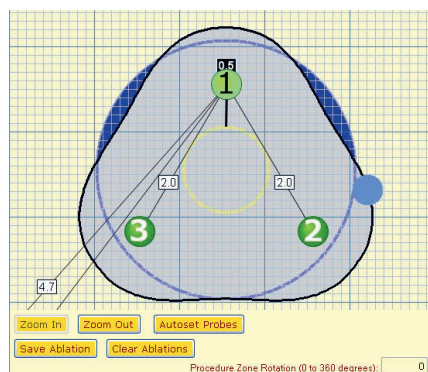


Figure 1. Schematic 2D ablation zone. 1, 2, and 3 represent the IRE probes. The grey area represents the ablation zone that is shaped around the IRE probes. The blue area represents the schematic view of the tumour.

Lastly, imaging in the follow-up after renal IRE should be further investigated. We assessed CT and MRI in the follow-up after renal IRE and found that the volume of the ablation zone increases directly after IRE ablation until 3 months after on both CT and MRI. The volume of the ablated tumour decreases from 6 months on. We demonstrated that the detection of residual- or recurrent disease is characterised by enhancement of the ablation zone after ablation. Subtraction images in MRI were especially helpful in differentiating residual tumour from edema and other post-interventional reactive tissue. Our study has a small sample size of 10 SRMs because it was developed with the intent to prospectively investigate the safety and feasibility of renal IRE (development & exploration IDEAL phase). Therefore, we used only descriptive imaging reports in the follow-up after renal IRE. Research in larger study cohorts has to demonstrate which imaging modality is more suitable in characterizing the ablation zone after IRE. However, in our cohort, MRI appeared to be the best visualization modality because of the ability to accurately detect residual tumours/recurrences with the help of subtraction images. MRI has the advantage that it does not expose the patient to radiation damage and it is feasible for patients with $eGFR < 30$. The disadvantages are that an MRI scan is costly, time-consuming and unsuitable for pacemakers. To date, CT remains the first-line modality for detecting and staging renal tumours. However, since the 'renal ablation population' is in general medically inoperable and in need of nephron-sparing management, MRI can be more valuable in this specific niche.

The assessment of ablation response remains challenging, as in thermal ablation. In most ablation responses there is an increase in the size of the ablation zone followed by a

subsequent decrease, as in our study. But at what point in time after the ablation this decrease will take place and in what scenario the growth of the ablation zone should be noted as suspicious remains unknown. Therefore, in ablation response, the pattern of enhancement within the ablated tumour is thought to be of more diagnostic value. The combination of evolution of the ablation zone volume and enhancement pattern should be deciding whether a patient should undergo a biopsy.

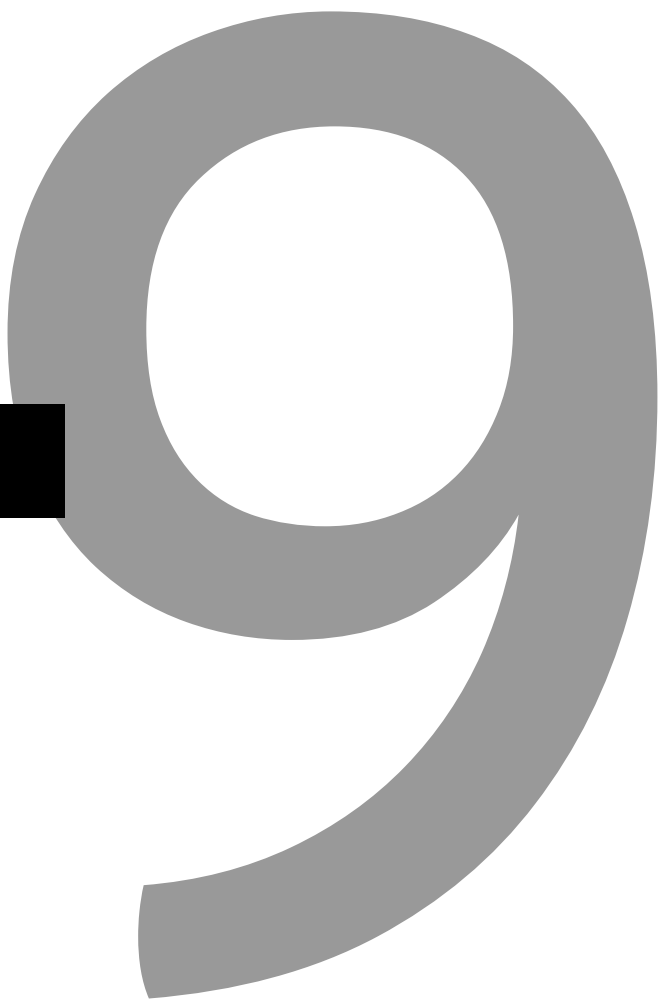
Whether renal IRE will obtain a place in the standard practice is still undetermined and will mainly depend on the research that is needed on the earlier mentioned fronts. In the present situation, renal IRE should be applied in a research setting or registry. Phase 3 research should further assess and validate the clinical evaluation and, if possible, compare IRE with thermal ablation in a randomized setting. Thermal ablation, in particular RFA and cryoablation, is widely investigated, contributing to excellent oncological outcomes of thermal ablation for the treatment of cT1a RCCs (4cm or smaller). The particular niche in which renal IRE can be of additional value is particularly the group of centrally located RMs amongst the ablation population, defined as the non-operable patient or the patient with a need for maximum conservation of renal parenchyma.

In the face of an aging population, it might be profitable to tailor management to minimize overtreatment as the competing risk of death increases with age. The implementation of shared decision making will generate a more personalized approach in oncology. Patients will face complex decisions regarding management options, and more studies should be performed to guide patients within these options. It is imperative that as clinicians we should be able to explain the gain of treating a tumour but also to elaborate on the advantages of no treatment (active surveillance). The majority of small renal masses grow slowly (around 3-5mm per year) and therefore the need for treatment is not always urgent, especially not in patients with significant comorbidity or/and of advanced age. However, around 20% of patients with SRMs show an aggressive growth pattern [5, 6]. This emphasizes that the clinical behaviour of 'the group' SRMs is diverse, implicating that there is a variable potential to cause harm to a patient. Every treatment modality is accompanied by a potential risk of complications and a recovery period which can have significant consequences for a fragile patient. As a result, active surveillance with the option to a delayed intervention will, besides ablative therapies, gain ground in the management of SRMs.

References

1. Ludwig,W.W., Wobker,S.E., Ball,M.W., Zysk,A.M., Yemul,K.S., Pierorazio,P.M., Gorin,M.A. and Allaf,M.E. (2018) Margin assessment in renal surgery using a handheld optical coherence tomography probe. *Urology*, **113**, 241–245.
2. Ahmed,M., Solbiati,L., Brace,C.L., Breen,D.J., Callstrom,M.R., Charboneau,J.W., Chen,M.-H., Choi,B.I., de Baere,T., Dodd,G.D. 3rd, *et al.* (2014) Image-guided tumor ablation: standardization of terminology and reporting criteria--a 10-year update. *Radiology*, **273**, 241–260. <https://doi.org/10.1148/radiol.14132958> <http://www.ncbi.nlm.nih.gov/pubmed/24927329>
3. Wendler,J.J. *et al.* (2017) Upper-Urinary-Tract Effects After Irreversible Electroporation (IRE) of Human Localised Renal-Cell Carcinoma (RCC) in the IRENE Pilot Phase 2a Ablate-and-Resect Study. *Cardiovasc Interv. Radiol.*, 10.1007/s00270-017-1795-x. <https://doi.org/10.1007/s00270-017-1795-x>
4. Wagstaff,P.G.K., de Bruin,D.M., van den Bos,W., Ingels,A., van Gemert,M.J.C., Zondervan,P.J., Verdaasdonk,R.M., van Lienden,K.P., van Leeuwen,T.G., de la Rosette,J.J.M.C.H., *et al.* (2014) Irreversible electroporation of the porcine kidney: Temperature development and distribution. *Urol. Oncol. Semin. Orig. Investig.*, **33**, 168.e1-168.e7. <https://doi.org/10.1016/j.urolonc.2014.11.019> <http://www.ncbi.nlm.nih.gov/pubmed/25557146>
5. Frank I, Blute ML, Cheville JC, Lohse CM, Weaver AL, Zincke H. Solid renal tumors: an analysis of pathological features related to tumor size. *J Urol.* 2003 Dec;170(6 Pt 1):2217-20. doi: 10.1097/01.ju.0000095475.12515.5e. PMID: 14634382.
6. Reuter, V. E., Kurta, J. M., Nogueira, L., Kundu, S., Kaag, M., Russo, P., Tickoo, S. K. (2009). Tumour Size is Associated With Malignant Potential in Renal Cell Carcinoma Cases. *Journal of Urology*, *181*(5), 2033–2036. <https://doi.org/10.1016/j.juro.2009.01.027>

CHAPTER 9



English & Dutch summary

English summary

Chapter 1 describes the rationale of this thesis by elaborating on the principles and drawbacks of the diagnosis and treatment of renal masses. The incidence of localised renal cancer in an early stage is increasing, whilst mortality appears to be stabilizing. Obtaining a pre-operative histopathologic diagnosis is desirable to avoid overtreatment. Renal mass biopsies are restricted by high non-diagnostic rates and are reported in up to 22% in small renal masses (SRMs, $\leq 4\text{cm}$). This emphasizes the need for a tool that distinguishes the aggressive RCC from the indolent or even benign renal mass. Optical coherence tomography (OCT) refers to a group of optical technologies that uses light to image and differentiate tissue without the need for excision. In renal mass treatment, a trend is observed towards minimal invasive management, like thermal ablation (cryoablation, radiofrequency ablation, and microwave ablation), stereotactic ablative radiotherapy, and even active surveillance. Irreversible electroporation (IRE), a relatively new ablation technique, is proposed to potentially overcome the hurdles of thermal ablation as it preserves vital structures. The aim of this thesis is to investigate the diagnostic value of optical coherence tomography (OCT) for the differentiation of renal masses and to assess the feasibility and safety of irreversible electroporation (IRE) for the treatment of small renal masses (SRMs).

In **Chapter 2**, the diagnostic accuracy and diagnostic yield of percutaneous OCT and renal mass biopsy are assessed in 95 patients. The diagnostic accuracy is defined as the sensitivity, specificity, positive predictive value (PPV), and negative predictive value, and the diagnostic yield is defined as the percentage of biopsies that lead to a diagnosis. Both techniques are compared with each other and in their potential to differentiate between renal masses. Two groups were evaluated: all malignant renal masses versus all benign renal masses, and oncocytomas (the most prevalent benign renal mass) versus renal cell carcinoma (the most prevalent malignant renal mass). OCT reveals high accuracy for both groups, although still slightly lower than renal mass biopsy. As a counterpart, the diagnostic yield of OCT is higher than of renal mass biopsy.

Chapter 3 evaluates the novel ablation technologies microwave (MWA), irreversible electroporation (IRE), and stereotactic ablative radiotherapy (SABR) for the treatment of localised renal cell cancer. Advantages and disadvantages are compared to the currently used ablation technologies cryoablation (CA), and radiofrequency ablation (RFA). A literature search was conducted to identify original articles on the novel ablation technologies. The majority of the articles are level 3 of evidence and retrospective of nature. Generally, for ablation, the percutaneous approach is preferred over the laparoscopic because of fewer complications and its minimal invasiveness. MWA may have potential advantages in ablating larger lesions with short procedure times compared to

radiofrequency ablation or cryoablation. IRE shows promising results in centrally located tumours, although the need for general anesthesia with deep muscle relaxation and long procedure times is a potential concern. SABR shows excellent local control and is not limited by location or size of the tumour. An additional advantage is that there is no need for general anesthesia. Overall, the type of treatment chosen for renal mass management depends mainly on the expertise of the operating center, the condition of the patient, and the location and size of the tumour.

Chapter 4 provides an overview of in vivo IRE research performed in the liver, pancreas, kidney, and prostate. Additionally, this chapter describes the procedure and the principle of IRE. The prospect of treating tumours in the vicinity of vital structures gives IRE a potential edge over conventional ablation techniques. Most of the IRE research is performed in the liver and pancreas, showing promising results on different fronts, namely early efficacy and safety and feasibility. Prostate and kidney IRE research is limited and mainly retrospective of nature. For IRE to evolve into a clinically accepted ablation technique, further improvement is needed on tissue-specific device settings/protocols, ablation monitoring, follow-up imaging, and long-term oncological outcomes. At this stage, it is imperative to perform IRE only in the setting of a clinical trial and with this providing a stepwise, safe, and scientifically valid evaluation of IRE. Organ-specific evaluation of IRE should be carried out preferably adhering to standardized guidelines.

Chapter 5 presents a prospective, human, in-vivo study protocol, aiming at feasibility, safety, and clinical efficacy of IRE ablation in small renal masses (SRMs). Renal ablation is increasingly used due to its nephron-sparing properties, low complication rate, and the short postoperative recovery. IRE is not influenced by the heat sink effect and is suitable for tumours in proximity to vital structures, extending the ablation indication to centrally located tumours. For IRE to evolve into a clinically accepted technique, clinical outcomes should be investigated in a small patient population to provide prospective data (IDEAL phase 2) before embarking on a larger trial (IDEAL phase 3). Hence, the objectives of this study are feasibility, safety, and clinical efficacy of IRE in small renal masses with a specific focus on several cross-sectional imaging modalities (MRI, CT, and contrast-enhanced ultrasound) for the visualization of the IRE ablation zone in the follow-up. Lastly, perioperative outcomes like quality of life, renal function, and postoperative pain will be recorded. This study will provide prospective information regarding the safety and feasibility of renal IRE ablation, with an extensive description of the radiological evolution of the ablated lesion along time as well as mid-term oncological outcomes.

Chapter 6 demonstrates the results of the feasibility and safety of percutaneous IRE for the treatment of small renal masses (SRMs). Both commonly used grading systems the Clavien-Dindo (CD) and the common terminology criteria for adverse events (CTCAE) were

used to assess safety. In total, ten SRMs in nine patients were included. Renal mass biopsy demonstrated seven clear cell RCCs, one papillary RCC, and two non-diagnostic biopsies. Technical success was achieved in nine out of ten cases. Seven out of ten SRMs were in proximity to vital structures. One patient had a grade 3b Clavien-Dindo complication (CTCAE grade 3): an impaired renal function due to a partially blocked ureter because of a blood clot. Mean anesthesia time was 3.7 hours and mean ablation time was 50 minutes. Renal function 1-month post-IRE was unaffected by IRE. Postoperative pain was rare and usually mild. Based on this pilot study, we concluded that renal IRE ablation in SRMs is safe and feasible, and well-tolerated in centrally located tumours. A limitation is that the IRE procedure is relatively complex and time-consuming in this stage.

Ablation is guided by cross-sectional imaging and the success of the procedure is also assessed by cross-sectional imaging. However, prospective imaging studies on renal IRE are absent. **Chapter 7** reports on the imaging modalities MRI and CT for the visualization of the ablation zone after IRE in patients with SRMs. The volumes of the ablation zone and the imaging characteristics, including enhancement of the ablation zone, after IRE in SRMs were evaluated. The volume of the ablated tumour increases directly after IRE until 3 months after IRE. After this, a decrease in volume takes place. All SRMs appeared non-enhanced immediately after ablation, except for one residual (1/10). MRI was particularly helpful in distinguishing post-interventional edema from the residual tumour by the use of subtraction images. Gas bubbles, perinephric stranding, and ablation zone edema are normal findings directly post-IRE.

Nederlandse Samenvatting

In **hoofdstuk 1** wordt de diagnostiek naar en de behandeling van nierkanker beschreven, alsmede de nieuwe ontwikkelingen hierin. Het vóórkomen van kleine niertumoren neemt toe door onder andere toevalsbevindingen bij toenemend gebruik van beeldvormende technieken. Het opsporen van nierkanker binnen deze groep wordt momenteel door de uitslag van het nierbiopt bepaald, met als nadeel een hoog percentage van zogenaamde niet-diagnostische biopten, maximaal 22% in kleine niertumoren. Een niet-diagnostisch of een niet-conclusief biopt is een biopt dat geen diagnostische uitslag oplevert, doordat er bijvoorbeeld te weinig weefsel of alleen nierweefsel zonder tumorweefsel in het biopt zit. Het diagnostisch vermogen van de nierbiopten kan hierdoor beperkt zijn.

Optische coherentie tomografie (OCT) is een optische techniek waarmee onder andere verschillende soorten weefsels van elkaar te onderscheiden zijn. Het voordeel is dat met behulp van deze minimaal-invasieve en hoge resolutie techniek potentieel direct een diagnose kan gesteld kan worden. Een tweede voordeel is dat het een 'real-time' techniek is, wat onder andere betekent dat de OCT meting 'real-time' aan te passen is bij een niet-conclusieve uitslag. Dit zou moeten bijdragen om het percentage niet-diagnostische uitslagen te verminderen.

Bij de behandeling van niertumoren staat van oudsher de nieroperatie centraal. Tegenwoordig is er een trend ontstaan richting de minimaal-invasieve behandelingen. Voorbeelden hiervan zijn thermale ablatie zoals radiofrequente ablatie en cryoablatie, stereotactische radiotherapie en zelfs 'active surveillance', oftewel het actief volgen van niertumoren zonder te behandelen. Irreversibele elektroporatie (IRE) is een nieuwe ablatie techniek waarbij de nadelen van thermale ablatie potentieel te voorkomen zijn omdat het werkingsmechanisme van IRE gebaseerd is op elektriciteit en niet afhankelijk is van temperatuur, in tegenstelling tot thermale ablatie. Dit heeft als gevolg dat IRE de vitale structuren minder lijkt aan te tasten. Het doel van dit proefschrift is om de diagnostische waarde te onderzoeken van optische coherentie tomografie (OCT) voor het diagnosticeren van nierkanker. Daarnaast is het doel de haalbaarheid en veiligheid van IRE te onderzoeken voor de behandeling van kleine niertumoren.

In **hoofdstuk 2** wordt de accuratesse (sensitiviteit, specificiteit, negatief voorspellende waarde en positief voorspellende waarde) en het diagnostisch vermogen (het percentage diagnostische uitslagen) van zowel OCT als de conventionele nierbiopten beoordeeld en met elkaar vergeleken in 95 patiënten. Er wordt in het bijzonder gekeken naar hun potentie om te differentiëren tussen kwaadaardige en goedaardige niertumoren. Er zijn hierbij twee groepen geëvalueerd: alle kwaadaardige niertumoren versus alle goedaardige niertumoren, en meer specifiek de oncocytomen (de meestvoorkomende goedaardige

niertumor) versus de renaal cel carcinomen (de meest voorkomende kwaadaardige niertumor). OCT toont hoge accuratesse in beide groepen, alhoewel iets lager dan het conventionele nierbiopt. Aan de andere kant is het diagnostische vermogen van OCT hoger dan dat van de nierbiopten. Dit artikel ondersteunt de bruikbaarheid van OCT in niertumoren en laat een gunstige balans zien tussen accuratesse en het diagnostische vermogen. Indien deze data worden gevalideerd door toekomstige studies, zal de praktische en klinische implementatie van OCT uiteindelijk, niet alleen afhangen van de accuratesse en het diagnostisch vermogen, maar ook van de benodigde expertise, de beschikbare apparatuur en de kosteneffectiviteit.

Hoofdstuk 3 evalueert de nieuwe ablatietechnieken microwave ablatie (MWA), irreversibele elektroporatie (IRE) en van stereotactische radiotherapie (SABR) voor behandeling van gelokaliseerde nierkanker en beoordeelt hun potentie in vergelijking met de momenteel meest gebruikte technieken, zoals radiofrequente ablatie (RFA) en cryoablatie (CA). Een literatuuronderzoek is opgezet om originele artikelen op te sporen die de uitkomsten van deze nieuwe ablatietechnieken onderzoeken. Het grootste deel van de huidige literatuur is level of evidence 3 en retrospectief van aard. Over het algemeen wordt de percutane benadering van de ablatietechnieken geprefereerd boven de laparoscopische benadering bij RFA, MWA en CA. MWA heeft mogelijk voordelen in het ableren van grote tumoren en de proceduredtijd is kort in vergelijking met RFA en CA. IRE laat veelbelovende resultaten zien bij centraal gelegen tumoren (dwz dichtbij bloedvaten of het verzamelsysteem van de nier), alhoewel de lange proceduredtijd een potentieel nadeel is. SABR laat hoge locale controle zien en wordt niet beperkt door locatie of grootte van tumoren, bovendien is er geen (algehele) narcose nodig. Het bepalen van het type behandeling dat geschikt is voor niertumoren hangt over het geheel genomen af van de expertise van het behandelend centrum, de conditie van de patient, en de locatie danwel grootte van de niertumor.

Hoofdstuk 4 biedt een overzicht van alle in-vivo IRE onderzoeken uitgevoerd tot op heden in de lever, pancreas, nier en prostaat. Daarnaast beschrijft dit hoofdstuk de IRE procedure en het principe waarop IRE is gebaseerd. De eerste onderzoeksresultaten in IRE voor de lever, pancreas, nier en prostaat lijken veelbelovend. Het grootste gedeelte van het onderzoek is uitgevoerd in lever en pancreas wat veelbelovende resultaten laat zien met name op het gebied van effectiviteit, veiligheid en haalbaarheid. De mogelijkheid van het behandelen van tumoren die dichtbij vitale structuren liggen geeft IRE een potentieel voordeel ten opzichte van conventionele ablatietechnieken als CA en RFA. Echter zal IRE, voordat het naar een klinisch geaccepteerde techniek kan worden vertaald, zich eerst verder moeten ontwikkelen op verschillende fronten. Daarbij gaat het met name om weefselspecifieke apparaatinstellingen danwel protocollen, het monitoren van de ablatie en de follow-up beelden en tot slot de lange termijn oncologische resultaten. Het

onderzoek naar IRE in verschillende organen is snel aan het uitbreiden, maar de meeste resultaten zijn gebaseerd op laag-kwaliteit onderzoek, te kwalificeren als level of evidence 4. Daarom is het in dit stadium essentieel om IRE alleen uit te voeren in onderzoeksverband en om het per orgaan stapsgewijs te evalueren.

Hoofdstuk 5 presenteert een prospectief, in-vivo studieprotocol gericht op de uitvoerbaarheid, veiligheid en klinische effectiviteit van IRE ablatie in patiënten met kleine niertumoren. IRE is een opkomende ablatietechniek met het potentiële voordeel vitale structuren rondom de tumor minder te beschadigen dan de huidige thermale ablatietechnieken, zoals cryoablatie en radiofrequente ablatie. Met deze studie richten wij ons op een gestandaardiseerde en stapsgewijze evaluatie van IRE in niertumoren, door met een kleine prospectieve studie (IDEAL fase 2 onderzoek) te starten die de basis kan vormen voor grotere studies (IDEAL fase 3 onderzoek). De uitvoerbaarheid zal worden beoordeeld door het technische succes van de procedures bij te houden. De veiligheid wordt beoordeeld door het aantal ongewenste voorvallen bij te houden. Naast het bepalen van de haalbaarheid, veiligheid en klinische effectiviteit zal deze studie ook verschillende beeldvormende technieken, namelijk CT, MRI en contrast echografie (CEUS), in de follow-up na IRE evalueren. Tot slot zullen perioperatieve parameters zoals kwaliteit van leven, nierfunctie en postoperatieve pijn worden bijgehouden.

Hoofdstuk 6 toont de resultaten van onderzoek naar de uitvoerbaarheid en veiligheid van percutane IRE voor de behandeling van kleine niertumoren. Twee graderingssystemen, de Clavien-Dindo (CD) en de common terminology criteria for adverse events (CTCAE), zijn gebruikt om de veiligheid te beoordelen. In totaal zijn er tien kleine niertumoren in negen patiënten geïnccludeerd en behandeld met IRE. De nierbiopsen lieten in totaal zeven heldercellige renaal cel carcinomen zien, een papillair renaal cel carcinoom en twee niet-diagnostische uitslagen. In totaal lagen zeven van de tien tumoren in de buurt van een vitale structuur. Technisch succes was behaald in negen van de tien tumoren. Een patiënt had een graad 3b Clavien-Dindo complicatie (CTCAE graad 3). De gemiddelde anesthesie tijd was 3.7 uur en de gemiddelde ablatie tijd was 50 minuten. Over het algemeen was de nierfunctie onaangetast door IRE. Postoperatieve pijn was zeldzaam en indien het voorkwam mild van aard. Concluderend kan gesteld worden dat IRE ablatie in niertumoren uitvoerbaar, veilig en goed te verdragen is in tumoren dichtbij vitale structuren. Een beperking is dat de IRE procedure van niertumoren in dit stadium tijdrovend is en relatief complex.

Ablatie begint een steeds grotere rol te spelen binnen de behandeling van kleine niertumoren gezien het niersparende en minimaal invasieve karakter. Ablaties worden beeld-gestuurd uitgevoerd en het succes hiervan wordt ook door beeldvorming

gecontroleerd en gemonitord in de follow-up. Echter, studies waarin beeldvorming wordt onderzocht in IRE ge-ableerde niertumoren zijn zeldzaam.

Hoofdstuk 7 beschrijft de beeldvorming van MRI en CT na IRE in kleine niertumoren. De volumes van de ablatie zone, oftewel de ge-ableerde tumoren, en de beeldvormende karakteristieken zijn beoordeeld. De volumes van CT en MRI zijn vergeleken met elkaar en met het geplande ablatievolume. De ablatievolumes correleren goed met het geplande ablatievolume. Het volume van de ge-ableerde tumoren neemt direct toe na ablatie en houdt aan tot 3 maanden na IRE. Hierna vindt er een afname van ablatievolume plaats. Alle ge-ableerde tumoren lieten geen aankleuring meer zien op CT en MRI, behalve de enige resttumor. Gas bubbels, perinefrische 'draderigheid' en oedeem in en rondom de ge-ableerde tumoren zijn normale bevindingen direct na IRE.

Author contributions

Author's initials

| | | | |
|-----------------|----|---------------------|----|
| M Buijs | MB | TG van Leeuwen | TL |
| DM de Bruin | DB | KP van Lienden | KL |
| W van den Bos | WB | RJA van Moorselaar | RM |
| OM van Delden | OD | JJMCH de la Rosette | JR |
| MRW Engelbrecht | ME | CD Savci Heijink | CS |
| Scheltema MJV | MS | PGK Wagstaff | PW |
| Axel Bex | AB | PJ Zondervan | PZ |
| MP Laguna Pes | PL | | |

Chapter 2

An In-vivo Prospective Study of the Diagnostic Yield and Accuracy of Optical Biopsy Compared with Conventional Renal Mass Biopsy for the Diagnosis of Renal Cell Carcinoma: The Interim Analysis

M Buijs, DM de Bruin, PJ Zondervan, CD Savci-Heijink, OM van Delden, TG van Leeuwen, RJA van Moorselaar, JJMCH de la Rosette, MP Laguna Pes.

Conception and design: MB, DB, PW, RM, PL, TL, JR

Data/literature acquisition: MB, PW, OD, PZ, CS, PL

Data/literature analysis and interpretation: MB, DB, PL, OM

Drafting the manuscript: MB, PW, PL, DB

Critical revision of the manuscript: PW, PZ, OD, JR, PL, RM, TL

Supervision: PL, OD, JR, PW, RM

Chapter 3

Available ablation energies to treat cT1 renal cell cancer: emerging technologies

PJ Zondervan, M Buijs, DM de Bruin, OM van Delden, KP van Lienden.

Conception and design: PZ, OD, KL

Data/literature acquisition: PZ, MB, DB, KL

Data/literature analysis and interpretation: PZ, OD, MB, KL, DB

Drafting the manuscript: PW, MB, DB, OD

Critical revision of the manuscript: OD, MB, DB, PL

Supervision: OD, KL, DB

Chapter 4

Irreversible electroporation: state of the art

PGK Wagstaff, M Buijs, W van den Bos, DM de Bruin, PJ Zondervan, JJMCH de la Rosette, MP Laguna Pes

Conception and design: PW, MB, PL, JR, DB

Data/literature acquisition: MB, PW, WB, DB

Data/literature analysis and interpretation: MB, PW, WB

Drafting the manuscript: MB, PW, PJ, JR, PL

Critical revision of the manuscript: JR, PL, PZ, WB

Supervision: JR, PL, DB

Chapter 5

Irreversible electroporation for the ablation of renal cell carcinoma: a prospective, human, in vivo study protocol

M Buijs, KP van Lienden, PGK Wagstaff, MJV Scheltema, DM de Bruin, PJ Zondervan, OM van Delden, TG van Leeuwen, JJMCH de la Rosette, MP Laguna Pes.

Conception and design: MB, KL, PW, PL, JR

Data/literature acquisition: MB, PW, PL, PZ

Data/literature analysis and interpretation: MB, PW, MS, DB

Drafting the manuscript: MB, PW, MS, DB

Critical revision of the manuscript: JR, PL, OD, TL

Supervision: PL, OD, JR, TL, KL

Chapter 6

Feasibility and safety of irreversible electroporation (IRE) in patients with small renal masses: Results of a prospective study

M Buijs, PJ Zondervan, DM de Bruin, KP van Lienden, A Bex, OM. van Delden

Conception and design: MB, DB, KL, OM, PL

Data/literature acquisition: MB, PL, KL, OD

Data/literature analysis and interpretation: MB, DB, KL, AB

Drafting the manuscript: MB, OD, AB, KL

Critical revision of the manuscript: JR, PL, OD, AB

Supervision: PL, OD, JR

Chapter 7

MRI and CT in the follow up after irreversible electroporation (IRE) for the treatment of small renal masses in humans

M Buijs, DM de Bruin, PGK Wagstaff, PJ Zondervan, MJV Scheltema, MW Engelbrecht, MP Laguna, KP van Lienden

Conception and design: MB, KL, OM, PL

Data/literature acquisition: MB, KL, ME, PJ

Data/literature analysis and interpretation: MB, DB, KL, OD, MS

Drafting the manuscript: MB, MS, KL, PW

Critical revision of the manuscript: DB, PW, PJ, MS, ME, PL, KL

Supervision: PL, OD, KL

Curriculum Vitae

Mara Buijs was born in Driehuizen, The Netherlands on January the 24th 1989. She was raised together with her sister Jorie in a happy and supportive family. When she was 10, Mara, her sister, and both her parents went on a travel to India for 6 weeks. She went to high school and graduated from the Jan Arentsz in Alkmaar in 2007. In this year she also started her medical school at the University of Leiden. During the course of her studies, she performed two clinical internships abroad (Melbourne, Australia and Paramaribo, Suriname) and did a clinical research project abroad regarding chronic pain (Adelaide, Australia). She obtained her medical degree in 2015. In 2015 she also started working as a research physician at the department of Urology at the Academic Medical Center, Amsterdam.



She worked under the supervision of prof. dr. MP Laguna Pes, prof. dr. OM van Delden, and later on under the supervision of prof. dr. HP Beerlage. During her PhD program, she investigated the value of OCT for detecting kidney cancer and she set up and coordinated a novel study on IRE for the treatment of kidney cancer. Besides her clinical and research work, Mara was an active board member for the Young AMC Board. Within this framework, she organized multiple symposiums, hospital-wide masterclasses, and social events. Mara started her training to become an oncologic radiotherapist in May 2019 at the Dutch Cancer Hospital (the Antoni van Leeuwenhoek Ziekenhuis) in Amsterdam.

Dankwoord

Dankbaar ben ik voor alle mensen die gedurende mijn promotieproject mij hebben gesteund. Er zijn velen die hebben bijgedragen aan de totstandkoming van dit proefschrift: In de inhoudelijke zin van het woord, maar ook door aanmoediging, inspiratie en ondersteuning.

Professor van Delden, beste Otto. Ik wil je hartelijk bedanken voor de supervisie van dit promotieproject, je waardevolle input en de prettige samenwerking met een goede dosis humor. Ik heb ontzettend veel geleerd bij de interventieradiologie, een afdeling waar ik met plezier mijn onderzoek uitvoerde. Bedankt voor het creëren van deze fijne leeromgeving en het mogelijk maken van dit promotietraject.

Professor Beerlage, beste Harrie. Dank voor het begeleiden van het afronden van mijn proefschrift. Ik waardeer de inspanning en toewijding die je in dit proefschrift hebt gestoken. Ik kon met vragen altijd bij je terecht. De rust die je uitstraalde had een goed effect op onze samenwerking!

Beste professor Laguna, ik wil u bedanken voor uw inzet en alle moeite die u in mijn proefschrift hebt gestoken. Uw passie voor het vak was bewonderenswaardig en ik heb veel geleerd tijdens de periode dat u mij begeleidde waarvoor ik u dankbaar ben.

Dr van Lienden, beste Krijn. Ontzettend bedankt voor jouw toewijding als copromotor en alle leerzame momenten die daarbij horen, maar ook voor je enthousiasme, humor en fijne samenwerking. Dank voor het altijd klaar staan met een integere en sympathieke houding, zelfs in de perioden dat je niet meer in het AMC werkte. Jouw bijdrage aan dit proefschrift was essentieel, zonder jou was dit proefschrift er niet geweest!

Dr de Bruin, del Brunos, Martino! Wat een bijzondere tijd hebben we meegemaakt en wat hebben we veel avonturen beleefd. Super bedankt voor jouw immense bijdrage op wetenschappelijk gebied aan dit proefschrift, voor zowel het OCT als het IRE-onderzoek, maar ook voor jouw gezellige ‘analyse middagen’ waarbij we kilo’s snoep en liters koffie nuttigden. Jij zorgde voor pertinente support, een plezierige samenwerking en de fundamentele basis van mijn onderzoek!

Graag wil ik alle leden van mijn promotiecommissie bedanken voor het beoordelen van mijn proefschrift en de bereidheid zitting te nemen in mijn commissie. In het bijzonder wil ik dr Axel Bex bedanken voor het (tijdelijk) superviseren van mijn proefschrift in het laatste gedeelte van het traject, ik heb hier veel aan gehad! Verder wil ik professor Frederique Bemelmans graag bedanken voor de bijdrage die zij heeft geleverd in de totstandkoming van mijn IRE-protocol. Professor Martijn Meijerink wil ik bedanken voor zijn waardevolle IRE-input gedurende mijn traject, de leerzame regionale Nanoknife vergaderingen en de onvergetelijke interventie-oncologie congressen in Miami. Professor Anema wil ik

bedanken voor de leerzame meekijk dagen bij de optische biopten van de lymfeklieren op de longafdeling.

Mijn paranimfen, Olivia en Jorie.

Olivia: Wat ben ik blij dat ik jou heb leren kennen in het AMC en dat je ben uitgegroeid tot een goede vriendin. Samen op kamertje G4-263 (ook wel de gangkast genoemd gezien de beperkte oppervlakte van circa 2,5m²) bracht veel hilarische, gelukkige, maar soms ook ellendige momenten met zich mee die ik onvoorwaardelijk met jou kon delen. Broodjes bapao en ham-kaas croissantjes gingen er voor 10 uur 's ochtends ongelimiteerd in. Ik kan jou niet genoeg bedanken voor alle mooie momenten die wij samen hebben meegemaakt in deze bijzondere periode.

Jorie: Paranimf, mijn grote zus en natuurlijk ook collega! Bedankt voor alle momenten dat jij er voor mij bent geweest en me van wijze adviezen, lekkere dropjes of goede kaasplankjes hebt voorzien. Op alle fronten van mijn geneeskundige carrière heb jij altijd voor mij klaar gestaan, enorm bedankt hiervoor!

Mijn oud-collega onderzoekers uit het AMC:

Peter Wagstaff, de steun en toeverlaat rondom alle nier-gerelateerde onderwerpen en natuurlijk een maatje. Jouw bijdrage aan mijn proefschrift is essentieel: Jij leerde mij het ontwerpen van fancy congres posters, hoe ik m'n artikelen moest schrijven, maar ook hoe ik logistieke afspraken van mijn onderzoek het beste kon plannen (lees: collega's omkopen met stroopwafels). Arnoud, Matthijs en Willemien, wat was het leuk om jullie als collega's te hebben en dagelijks op G4 met jullie te zijn. Onvergetelijke tijden hebben we door dik en dun meegemaakt en ik hoop deze band met jullie nog jaren te kunnen voortzetten.

Alle overige (oud)onderzoekers: Rob, Jaap, Esmee, Christophe en Jan-Erik onwijs bedankt voor de leuke tijd en fijne samenwerkingen, gezelligheid op de congressen en andere borrels buiten werk!

Alle urologie-collega's uit het AMC, Martine, Natasha, Alice, Laura, Sonja en Alette, bedankt voor jullie altijd luisterende oor, gezellig koffie momenten en wijze woorden. Alle urologie stafleden: Bedankt voor jullie bijdrage aan mijn promotie, voor alle kansen en leerzame momenten.

Alle collega's van de Biomedical Engineering en Physics, bedankt voor jullie ondersteuning op inhoudelijk OCT vlak en voor het creëren van een fijne sfeer op de afdeling. Dank aan al het ondersteunend personeel van de Radiologie, in het bijzonder Peggy, Marjolein en Roos, die ervoor zorgden dat ik mijn onderzoek afspraken er altijd tussen kon krijgen met als resultaat dat mijn inclusie goed liep en dat het onderzoek patiëntvriendelijk bleef.

Mijn ouders, Kees en Yvonne, veel dank voor het vangnet dat jullie voor mij hebben klaar staan. Het is een warm bad waar ik altijd naar kan terug keren, betere ouders had ik me niet kunnen wensen. Jullie geven me rust, vertrouwen en support in moeilijke tijden maar

ook in mooie tijden met gezellige etentjes of lange wandelingen. Ik hoop nog veel mooie momenten met jullie te mogen doorbrengen en wie weet zelfs nog een reisje naar Nepal te mogen maken! En in het bijzonder bedankt voor het grondig nalezen en corrigeren van mijn boekje.

Pieter, en natuurlijk Pim en Bente, bedankt voor het vormen van een tweede thuis voor mij in Rotterdam. Erg fijn dat ik altijd mijn toevlucht bij jullie kan zoeken als ik O2O even zat was!

Al mijn andere familieleden, Liesbeth en Arie, Jelmer en Natasha, de oma's in gereïncarneerde versie, Hank en Tracey, Felix, Angela, en tot slot mijn nichtjes Sanne, Kirsten en Samara: Bedankt!

Alle vriendinnen:

Nancy, Kitty, Lesley, Amber, Anoes, Suus en Josje: Bijzonder is de vriendschap die wij afgelopen 12 jaar zo hecht hebben opgebouwd met elkaar. Vanuit jullie heb ik steun mogen ontvangen in alle tijden van dit promotietraject die enorm waardevol was. Jullie vriendschap betekent veel voor mij en zonder jullie had ik dit klusje niet kunnen klaren.

Annieke, onze vriendschap begon tijdens ons coschap in Suriname maar is uitgegroeid tot een soort lineair pad dat we samen hebben afgelegd: Wonen in Amsterdam, promotieonderzoek in het AMC, samen jong AMC bestuurslid en nu allebei in opleiding. Wat een mooie vriendschap heb ik aan die stage in Suriname overgehouden!

Susan, op de eerste plaats vriendin maar ook collega! Na een eerste en laatste seizoen hockey met jou te hebben gespeeld (met een eindstand waarbij ons puntenaantal in het negatief eindigde) hebben we onze vriendschap opgepakt buiten de hockey. Jij kwam me stevast opzoeken als ik in het buitenland zat voor een stage, onderzoek of congres, met als resultaat dat we samen prachtige reizen en avonturen hebben beleefd. Bedankt voor het opvangen van mijn promotie-buien, de after-hours support en het opkalefateren van mijn stemming als het even tegen zat. Op nog vele jaren vriendschap!

Mijn collega AIOS van de radiotherapie: Bedankt voor het leveren van morele support in de afrondende fase van mijn onderzoek en natuurlijk bedankt voor het verdragen van mijn promotie-gerelateerde activiteiten op de AIOS kamer ;-).

Tot slot wil ik alle patiënten bedanken die deel hebben genomen aan mijn studie. Zonder de input van patiënten is het wetenschappelijk onderzoek nergens. Enorm bedankt voor jullie deelname, jullie vertrouwen in mij en voor jullie bijdrage aan de wetenschap!



ACADEMISCH PROEFSCHRIFT

Mara Buijs